YUNIBESITI YA BOKONE-BOPHIRIMA
NORTH-WEST UNIVERSITY
NOORDWES-UNIVERSITEIT

EVALUATION OF ALTERNATIVE SANITARY WATER HEATING CONFIGURATIONS FOR DEMAND SIDE MANAGEMENT

G. du Plessis, B.Eng.

Dissertation submitted in partial fulfilment of the degree
Master of Engineering
in the
School of Mechanical and Materials Engineering,
Faculty of Engineering
at the
North-West University, Potchefstroom Campus

Promoter: Prof. P.G. Rousseau
Potchefstroom
2005

ACKNOWLEDGEMENTS

I thank God for the opportunities he has given me as well as the strength and guidance to make the most of them.

I would like to thank Prof. P.G. Rousseau for his outstanding motivation, guidance and support. With his motivation, few things seem impossible.

Last but not least, many thanks to my mother, brother and Sàdie for their understanding, support and love during my years of study.

ABSTRACT

Title	:	Evaluation of alternative sanitary water heating configurations for Demand Side Management.
Author	:	G. du Plessis
Promoter	:	Prof. P.G. Rousseau
School	:	Mechanical and Materials Engineering
Degree	:	Master of Engineering

The largest percentage of sanitary hot water used in South Africa is heated by means of electrical resistance heaters. This is one of the major contributing factors to the undesirable high morning and afternoon peaks imposed on the national electricity supply grid. Water heating therefore continues to be of concern to Eskom, currently South Africa's only electrical utility company. New water heating technologies have been developed for large-scale sanitary water heating in the form of the so-called in-line heater (ILH) and stratified in-tank (SIT) configurations. The purpose of this study was to evaluate the performance of these newly developed water heating technologies under load shedding conditions.

The performance of the ILH and SIT water heating technologies was evaluated via an existing simulation model under load shedding conditions. Furthermore, an extensive empirical investigation was conducted on a number of real-world water heating plants in order to evaluate the actual performance of the ILH-configuration. The results obtained via the empirical investigation were also employed to further verify the existing simulation model.

A new model simulating the standing heat losses suffered by water heating systems was developed. The model can be used to simulate the standing heat losses suffered by a typical centralised water heating facility with good accuracy.

It was found that the ILH-technology performs excellent under load shedding conditions. The ILH-plants under investigation were able to shed their entire load during peak demand periods while still supplying the occupants with sufficient hot water throughout the day. The SIT-technology proved to be a good alternative where the ILH-technology is not economically viable, realising the maximum load shedding potential in under-utilised water heating systems.

It was also found that the implementation of these water heating systems on a national scale would provide the utility with substantial load shedding potential. The facilities at which the systems are installed would also benefit greatly with annual savings potential on electricity cost ranging from 8.5% to 24%.

OPSOMMING

Titel	:	Evaluasie van alternatiewe sanitêre waterverhitting-konfigurasies vir elektriese aanvraagbestuur.
Outeur	:	G. du Plessis
Promotor	:	Prof. P.G. Rousseau
Skool	:	Meganiese en Materiaal-ingenieurswese
Graad	:	Magister in Ingenieurswese

Die meeste warm water wat aangewend word vir sanitêre gebruik in Suid-Afrika word verhit deur elektriese weerstandsverhitters. Hierdie verhitting lewer `n groot bydrae tot die ongewensde hoë pieke gedurende die oggende en aande op die nasionale elektrisiteitsverspreidingsnetwerk. Om hierdie rede is Eskom, huidiglik Suid-Afrika se enigste elektrisiteitsverskaffer, besorg oor waterverhitting. Nuwe waterverhittingstegnologieë is ontwikkel in die vorm van die sogenaamde inlyn-verhitter en gestratifiseerde tenk-konfigurasies. Die doel van hierdie studie was om die vertoning van hierdie nuut ontwikkelde tegnologieë te evalueer onder lasvergietingstoestande.

Die werkverrigting van die inlyn-verhitter en gestratifiseerde tenk waterverhittingstelsels is geëvalueer deur gebruik te maak van `n bestaande simulasie model onder lasvergietings-toestande. Verder is 'n uitgebreide empiriese ondersoek gedoen op 'n aantal werklike waterverhittingstelsels om sodoende die werklike vertoning van die inlyn-verhitter konfigurasie te bepaal. Die empiriese resultate is ook aangewend om die bestaande simulasie model verder te verifieer.

'n Nuwe model wat die hitte verliese gelei deur waterverhittingstelsels simuleer, is ontwikkel. Die model kan aangewend word om die hitte verliese wat deur 'n tipiese sentrale waterverhittingstelsel gelei word met goeie akkuraatheid te simuleer.

Daar is gevind dat die inlyn-verhitter tegnologie uitstekend onder lasvergietingstoestande vertoon. Die inlyn-verhitter aanlegte wat ondersoek is, was instaat om die totale las te vergiet gedurende spitstye sonder om onvoldoende warm water aan die bewoners te verskaf. Dit is ook bewys dat die gestratifiseerde tenk tegnologie 'n goeie alternatief bied in gevalle waar die inlyn-tegnologie nie ekonomies lewensvatbaar is nie. In hierdie gevalle word die maksimum lasvergietingspotensiaal verwerklik in ondergebruikte waterverhittingstelsels.

Daar is verder gevind dat implementering van hierdie waterverhittingstelsels, op `n nasionale skaal, substansiële lasvergietingspotensiaal vir die elektrisiteitsverskaffer sal inhou. Die fasiliteite waarby die stelsels geïmplementeer word, sal ook baat vind daarby in die vorm van `n jaarlikse besparing op elektrisiteitskoste van 8.5% tot 24%.

NOMENCLATURE

A_{ci}	:	Average heat transfer area of cladding wall at node i	m^2
A_{ii}	:	Reservoir inside surface area at node i	m^2
A_{li}	:	Average heat transfer area of lagging at node i	m^2
A_{oi}	:	Reservoir outside surface area at node i	m^2
A_{wi}	:	Average heat transfer area of reservoir wall at node i	m^2
$Baseline_{adj}$	:	Adjusted baseline load	kWh
$Baseline_{norm}$	:	Normalised baseline load	-
$Cost_{hour}$	:	Electricity cost per hour	R
c_p	:	Specific heat capacity	kJ/kg.K
dt	:	Time-step	s
E_{elec}	:	Electricity consumption	kWh
E_{in}	:	Energy input	MJ
$E_{in,exp}$	:	Energy consumed by in-line heater as measured	kJ
$E_{in,sim}$	:	Energy consumed by in-line heater as simulated	kJ
E_{out}	:	Energy output	MJ
E_{tot}	:	Total daily energy consumed by water heating plant	kWh
h_i	:	Internal convective heat transfer coefficient at node i	$W/m^2.K$
h_o	:	External convective heat transfer coefficient at node i	$W/m^2.K$
k_c	:	Thermal conductivity of cladding	W/m.K
k_{eff}	:	Effective heat loss factor	$W/m^2.K$
k_i	:	Thermal conductivity of effective reservoir shell	W/m.K
k_l	:	Thermal conductivity of lagging	W/m.K
k_w	:	Thermal conductivity of reservoir wall	W/m.K
$\dot{m}_{del}$	:	Mass flow rate of delivered hot water	kg/s
$\dot{m}_{heat}$	:	Mass flow rate of water through in-line heater	kg/s
$\dot{m}_{ri}$	:	Return flow rate at node i	kg/s
m_w	:	Water mass	kg
P	:	Power consumed by in-line heater	kW
QD	:	Performance number concerning delivered water	-
$Q_{del,exp}$	:	Energy delivered by the system as measured	kJ
$Q_{del,sim}$	:	Energy delivered by the system as simulated	kJ

QE	:	Performance number for in-line heater energy consumption	-
QI	:	Performance number concerning in-line heater temperature	-
$Q_{in,exp}$	:	Energy consumed by in-line heater as measured	kJ
$Q_{in,sim}$	:	Energy consumed by in-line heater as simulated	kJ
Q_{losses}	:	Heat loss at node i	W
R_{eff}	:	Effective resistance at node i	K/W
R_{ii}	:	Inside convective resistance at node i	K/W
R_{li}	:	Wall, lagging and cladding material resistance at node i	K/W
R_{oi}	:	Outside convective resistance at node i	K/W
R_{ri}	:	Return flow resistance at node i	K/W
t_c	:	Temperature of cold-water feed from supply mains	°C
t_i	:	Water temperature entering in-line heater	°C
T_i	:	Temperature inside the reservoir at node i	°C
T_{in}	:	Average inlet temperature	°C
T_o	:	Ambient temperature	°C
T_{out}	:	Average outlet temperature	°C
T_r	:	Temperature of return flow	°C
t_s	:	Temperature of water supplied to occupants	°C
t_w	:	Water temperature leaving in-line heater	°C
x_c	:	Thickness of cladding	m
x_i	:	Effective thickness of reservoir shell	m
x_l	:	Thickness of lagging	m
x_w	:	Reservoir wall thickness	m

ABBREVIATIONS

CIT	:	Conventional in-tank
c/kWh	:	Cent per kilo-watt-hour
CSIR	:	Council for Scientific and Industrial Research
DLC	:	Direct load control
DSM	:	Demand Side Management
ILH	:	In-line heater
I/O	:	Input/Output
kW	:	Kilowatt
kWh	:	Kilo-watt-hour
MD	:	Maximum Demand
min	:	Minutes
MW	:	Megawatt
PC	:	Personal computer
PLC	:	Programmable logic controller
PT-100	:	Platinum thermometer for 0-100 °C
R	:	South African Rand
RTP	:	Real-time-pricing
SIT	:	Stratified in-tank
TOU	:	Time-of-use
US	:	United States
USA	:	United States of America
W	:	Watt

TABLE OF CONTENTS

PAGE

LIST OF FIGURES

LIST OF TABLES

Chapter 1

INTRODUCTION

1.1 Background

Unlike the United States of America (USA) and most European countries, South Africa has very few accessible commercial supply networks of natural gas. Therefore, at present most hot water in buildings such as hostels, hospitals, prisons, and residences at universities and schools are heated by means of direct electrical resistance heaters. This is one of the major contributing factors to the undesirable high morning and afternoon peaks imposed on the national electricity supply grid. Water heating, therefore continues to be of concern to Eskom, currently the country's only electrical utility company (Rousseau *et al.*, 2001).

On the other hand, water heaters have energy storage capability and can easily be controlled by switching the resistance heaters on or off during specific times of the day. Therefore, they are ideal candidates for Demand Side Management (DSM) applications to shift part of the utility power demand from peak periods to off-peak periods. For this reason electric water heaters have been the focus of many DSM-studies (Lacroix, 1999; Lemmer & Delport, 1999; Van Tonder & Lane, 1996; Rousseau *et al.*, 2001).

Conventional DSM-strategies focus on block by block or random on-off control of water heaters. In these control strategies certain water heaters are turned off during certain time-periods through a direct load control (DLC) strategy (La Meres *et al.*, 1999; Nehrir & LaMeres, 2000; Van Harmelen & Van Tonder, 1998; Van Tonder & Lane, 1996). However, considering the energy storage capability of water heaters, they may not have to heat water at their full-rated power when hot water is being used during peak demand periods. In industrial applications, where more than one heating element is installed, the power consumption can be controlled by dividing the resistance elements into groups. Each group represents a stage which is controlled separately, allowing a control algorithm to control the number of stages switched on or off during certain periods of the day. In a time-of-use (TOU) environment, customers can benefit by controlling their water heaters not to heat water at their full capacity during peak demand hours, if the temperature of the water is higher than a certain minimum value.

In South Africa, the largest percentage of resistance heaters consists of in-tank heaters. The in-tank configuration has electrical resistance elements and a control thermostat installed inside the reservoir, usually close to the bottom (Rousseau *et al.*, 2001). In the in-tank configuration the water is actually heated gradually at the bottom of the reservoir and the supply water is drawn from the top. This means that whenever water is drawn from a fully heated reservoir, the cold water entering at the bottom of the reservoir will lower the temperature at the thermostat. The thermostat will then call for the full heating capacity to be activated.

If the heating load is shed during peak demand periods, the hot water will accumulate at the top of the reservoirs and the cold water at the bottom, which is very useful. However, once the heaters are switched on, the little hot water available at the top of the reservoirs will almost instantly be mixed with the colder water at the bottom. Now practically all the water in the reservoirs must be reheated before any of it is available to the occupants at the desired temperature. Therefore, in this configuration there is very little opportunity to correct the situation if cold water reaches the top of the reservoirs during the load shedding period. The overall result will be that cold water may be supplied to the occupants during the peak demand period as well as for an extended period after load shedding has taken place.

New water heating configurations have been developed to address the problems presented by the conventional in-tank configuration under load shedding conditions. This study focuses on evaluating the performance of two of these newly developed configurations, namely: the in-line heater (ILH) configuration as well as the stratified in-tank (SIT) configuration.

1.2 Problem statement

The conventional in-tank design philosophy is not ideally suited for load shedding applications. Furthermore, the conventional DLC-strategies used for sanitary water heaters do not take customer satisfaction into account.

The performance of the new ILH-configuration as well as the SIT water heating configuration under load shedding conditions has not been investigated extensively.

1.3 Research objectives

- Evaluate the performance of the newly developed ILH and SIT water heating configurations under load shedding conditions in a real-world industrial application. This will be done by using water heating simulation software as well as measurements obtained from actual applications.

- Determine the impact of the alternative water heating configurations on the peak electricity demand by doing an impact assessment.

1.4 Research methodology

In order to achieve the objectives mentioned in the previous paragraph, the following steps are taken:

- A complete literature survey is presented in order to evaluate existing water heating configurations together with existing control strategies. A brief description of the water heating simulation model developed by Rousseau *et al.* (2001) together with its verification is also presented to provide confidence in the simulation results that follow.

- The performance of the newly developed water heating configurations is investigated using the existing software for the simulation of water heating plants.

- In order to evaluate the accuracy of the simulation model and the performance of the new ILH-configuration, an empirical investigation is performed on a number of real-world water heating plants. Using the empirical results, the simulation model is verified and calibrated in order to generate satisfactory results.

- The impact of the alternative water heating configurations on the peak electricity demand is determined by comparing the electrical loads before and after the change in configuration.

Chapter 2

LITERATURE SURVEY

2.1 Introduction

From Chapter 1 it is clear that an extensive literature survey is needed to gather information on existing water heating configurations as well as existing Demand Side Management control strategies for conventional sanitary water heaters. Therefore, this chapter investigates the following:

- Demand Side Management (DSM) as a method of energy management.
- The contribution of sanitary water heating to the electricity peak demand.
- The most common water heating installations used.
- Existing demand side management control strategies for large-scale sanitary water heaters.
- The simulation model used to simulate the thermal performance of water heating systems.

2.2 Demand Side Management

The term, Demand Side Management, is used to describe the planning (scheduling) and implementation of activities to influence the time, pattern and amount of electricity usage. This is done in such a way that it produces a change on the load profile of industry, while still maintaining customer satisfaction (Eskom, 2004). This will assist the utility, such as Eskom, to reduce or shift electricity peaks.

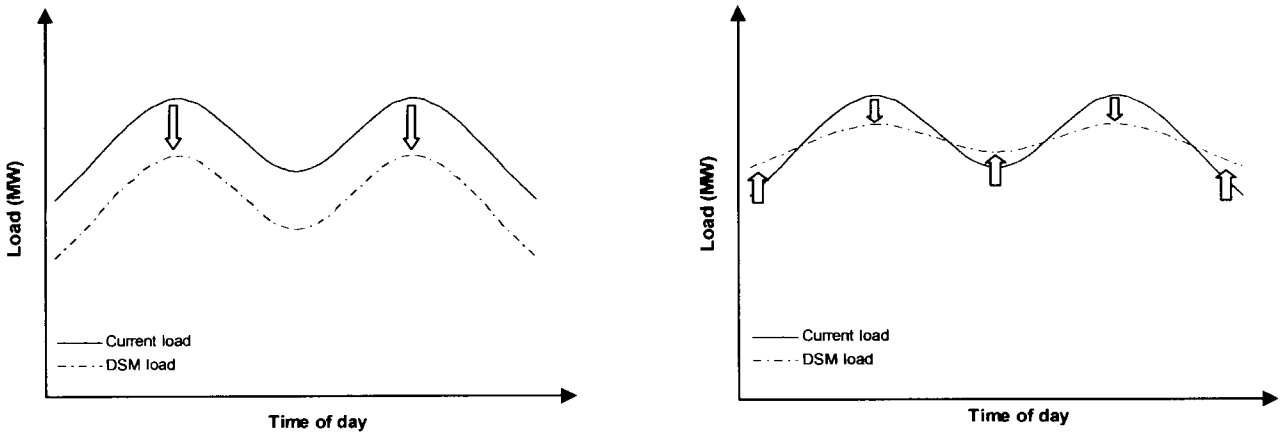

Figure 2.1: DSM through (a) energy efficiency and (b) load management.

Figure 2.1 shows the typical methods of DSM. Figure 2.1(a) shows DSM through improved energy efficiency. This implies that less energy is consumed, accompanied by a reduction in peak load and a decreasing area beneath the load curve. Figure 2.1(b) depicts DSM through load shifting. This implies that moving the load to lower demand periods will decrease the peak demand, but the area beneath the profile remains the same. An ideal DSM-project will satisfy both of these DSM-types (Els, 2002).

2.3 Effect of water heating on electricity demand

The effect of water heating on the national electricity demand experienced in South Africa will be discussed in the following paragraphs. Most of the data that will be used is applicable to the residential sector as well as the commercial sector. Although this study focuses on large-scale industrial water heating installations within communal living environments such as mine residences, the data obtained from the residential and commercial sectors gives a good reflection of large-scale industrial water heating characteristics.

According to Lane and Beute (1996) sanitary water heating in the domestic sector is responsible for a very large percentage (30% to 50%) of the total domestic energy load. Thus, controlling sanitary water heaters during peak hours can substantially reduce the electricity cost of the consumer as well as reduce the electrical peak demand experienced by the utility.

Rousseau and Greyvenstein (2000) report that the major types of water heating installations currently found in the commercial sector in South Africa are central coal- or diesel fired

boiler plants, central gas fired boiler plants, resistance heaters and central electricity driven heat pump plants. Figure 2.2 shows the distribution of occupants among the different types of installations. By far the largest portion of the total sanitary hot-water consumption in South African commercial buildings is heated by means of resistance heaters.

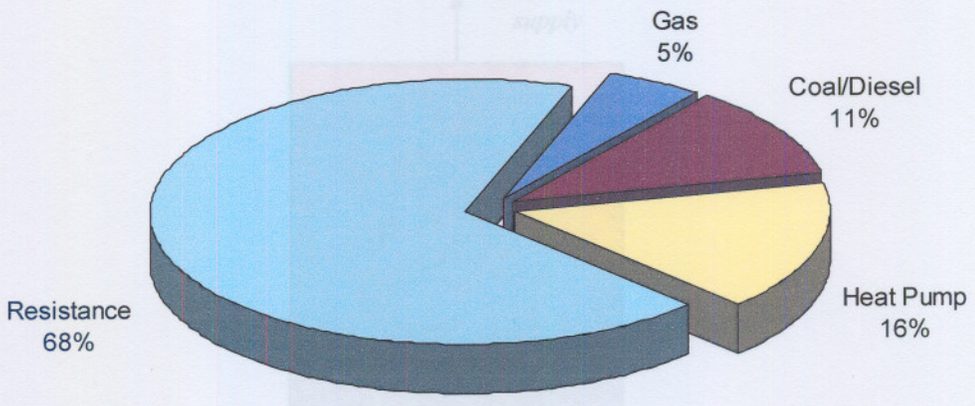

Figure 2.2: Distribution of occupants among the different types of heating installations in commercial buildings (Rousseau & Greyvenstein, 2000).

According to Forlee (1997) residential water heating load is one of the largest contributors, if not the largest to household demand during peak hours. Wilken and Delport (2000) state that with water heating control on its own, it is possible to defer and remove the need for an additional generating plant to be built. The major advantage of water heating load control to the utility is that the load can be shifted without a reduction in energy sales.

2.4 Sanitary water heating installation design

The next section discusses the most commonly found water heating installations used for large-scale sanitary water heating in South Africa.

2.4.1 Conventional design philosophy

According to Rousseau and Greyvenstein (2000) the largest portion of the total sanitary hot-water consumption in South African commercial buildings is heated by means of resistance heaters. Resistance heaters, almost exclusively in-tank heaters, account for 68% of the total number of residents served (Strauss, 1999).

The in-tank configuration has electrical resistance elements and a control thermostat installed inside the reservoir, usually close to the bottom. This is shown schematically in Figure 2.3 (Rousseau *et al.*, 2001).

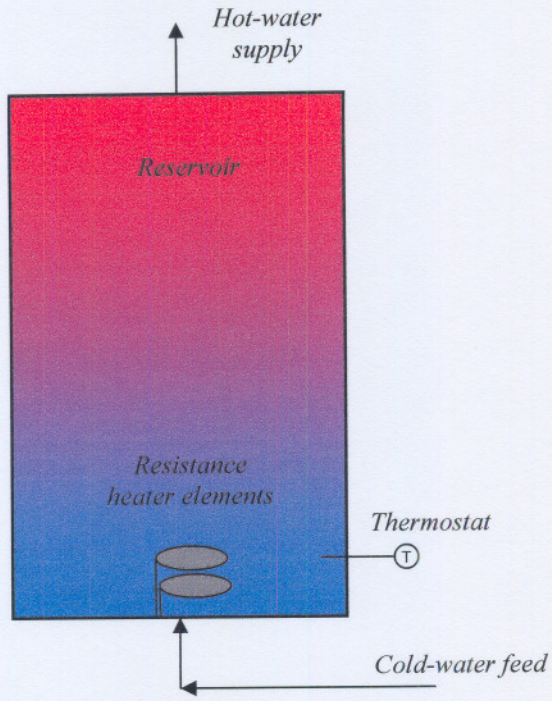

Figure 2.3: Schematic of conventional in-tank water heating configuration.

In the in-tank configuration the water is actually heated gradually at the bottom of the reservoir and the supply water is drawn from the top. This means that whenever water is drawn from a fully loaded reservoir, the cold water entering at the bottom of the reservoir will lower the temperature at the thermostat. The thermostat will then call for the full heating capacity to be activated. This results in the high morning and afternoon peaks that make such an undesirable impact to the national peak demand profile (Rousseau *et al.*, 2001).

2.4.2 Dual-tank water heating installation

Kar and Al-Dossary (1995) compare the performance of a single-tank water heater and a dual-tank water heater with tanks connected in series. It is to be determined which configuration provides the greater amount of daily hot water without the outlet temperature dropping below 60 °C. Both configurations are subject to the US domestic average hourly hot-water use profile (Becker & Stogsdill, 1990).

The single-tank water heater has a volume of 150 litres and power rating of 4 500 W. It was found that this single-tank water heater can provide 1 219 litres of hot water daily with a

temperature between 60 °C and 65 °C. This configuration requires 182.67 kJ of electrical energy per litre of hot water.

The dual-tank water heater used in this study has the same volume as the single-tank water heater. However, the distribution of the total volume as well as the power rating between the first and the second tank have been varied to find the optimal capacity and power rating for each tank. The volume and power rating of each tank are varied without the outlet hot-water temperature dropping below 60 °C or exceeding 65 °C. However, no temperature minimum is enforced for the first tank. Results indicate that, when the second tank has 10%-30% of the total tank volume and 70%-80% of the total power rating, the dual-tank water heater provides about 10% more hot water for a day than the single-tank water heater. Furthermore, the dual-tank heater requires 4.5% less energy input per litre of hot-water withdrawal.

It is concluded in this study, that a dual-tank water heater, where the tanks are connected in series and the second tank has 10%-30% of the total tank volume and 70%-80% of the total power rating, provides more hot water while requiring less energy per litre of hot water. A disadvantage of this configuration is that two tanks and two heaters are required.

From this study it can be seen that two tanks in series with the same total volume and power rating as a single tank are more energy efficient. This configuration may be used in a DSM-program in order to reduce energy consumption and to reduce peak electricity load.

In a study conducted by Minquez (1987) two methods of providing hot water are compared: one with a single tank and another with two equal-size tanks connected in series. The temperature of the hot water at the exit point, in each case, is computed as a function of time for two cases: (i) a single water heater; (ii) two water heaters in series, each with half of the capacity and power rating of the single tank. The study shows that the outlet temperature is higher in case (ii) until the inversion time, which ranges from 11 to 13 min, is reached. It is concluded, that it is unlikely that water would be drawn for as long as the inversion time. In a real application, there will be a high proportion of low volume draws from the heater. It is stated that two tanks in series, with the same total volume and total power rating as a single-tank heater, are more energy efficient.

Kar and Kar (1996) investigated a dual-tank water heater with tanks connected in series for more efficient energy use. Single-tank and dual-tank electric water heaters are optimised

and compared to facilitate the selection of the one with better energy conservation. The US average hourly hot-water use profile is utilised to determine the hourly hot-water load distribution for a given daily hot-water consumption (Becker & Stogsdill, 1990).

Parametric optimisation is performed on single-tank water heaters to obtain the maximum amount of daily hot water producible for different values of tank volume and power rating. It was found that the amount of hot water provided by single-tank water heaters does not vary with tank size, but does vary with power rating. However, the energy consumption increases with increasing tank volume.

Parametric optimisation of dual-tank water heaters must include parameters such as the relative proportion of each tank and the relative power input to each tank, as well as the total volume and power rating of the heaters. The volume and power rating of each tank are varied without the outlet hot-water temperature dropping below 60 °C or exceeding 65 °C. However, no temperature minimum is enforced for the first tank. Results indicate that, when the first tank has 75% of the total tank volume and 25% of the total power, the dual-tank water heater provides about 22% more hot water for a day than the single-tank water heater. Furthermore, it requires 9.4% less energy input per litre of hot-water withdrawal, as compared to a single-tank water heater. It was also found that the hot-water output of the dual-tank water heater with constant power rating increases with the volume of the heater. Furthermore, the energy consumption per litre of hot-water output decreases for larger tanks as well as for larger power ratings. These two variations are in contrast to the behaviour of single-tank water heaters. In order to determine the reason for this discrepancy, temperature profiles of both heaters with the same total volume and total power rating were examined. Since the temperature of the single-tank water heater is controlled by a thermostat and is constrained to be above 60 °C, it stays between 60 °C and 65 °C. However, no lower limit was set on the temperature of the first tank in the dual-tank heater, and when the power was not enough, its temperature dropped down to 27 °C while the temperature of the second tank remained between 60 °C and 65 °C. This may be the reason why the dual-tank water heater can provide more hot water at lower energy per litre hot water.

From the discussion above it seems that two tanks in series with the same total volume and in-tank power rating as a single tank is more energy efficient. This configuration may be used in a DSM-program in order to reduce energy consumption and to reduce peak

electricity load. Therefore, more attention will be given to the control of such water heating systems as a possible DSM-option.

2.4.3 In-line water heating installation

Another water heating installation, illustrated in Figure 2.4 is the so-called in-line water heater with resistance heating elements installed outside the reservoir (Strauss, 1999).

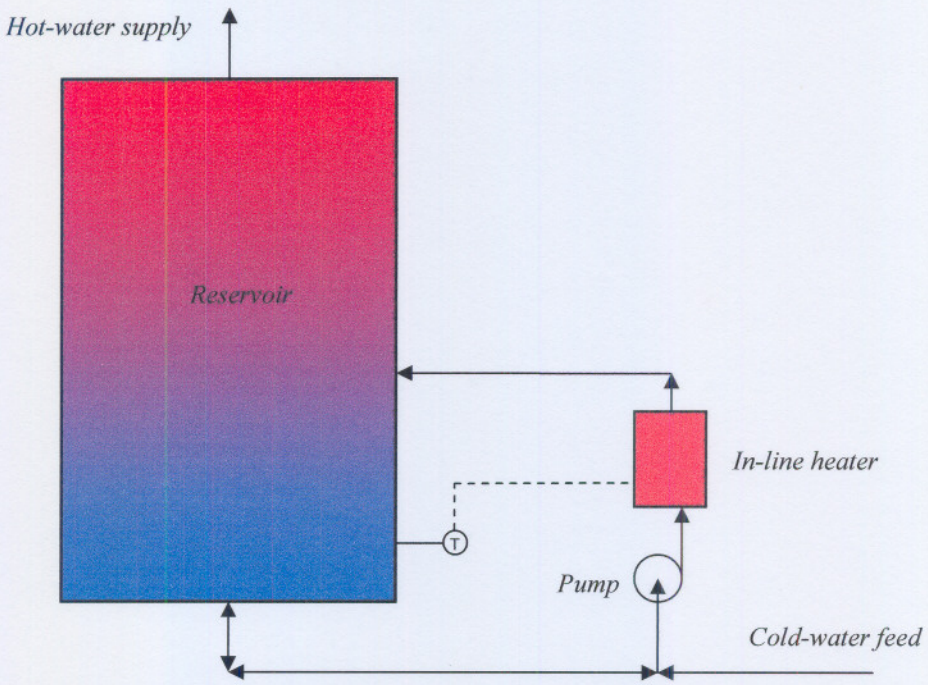

Figure 2.4: Schematic of in-line water heating concept.

In this configuration the water is supplied at the bottom of the reservoir and the supply water is taken from the top. This implies that if the reservoir is filled with colder water after a period of high take-off, practically all the water in the reservoir has to be reheated to approximately 65 °C before any water is available at that temperature.

2.4.4 Heat pump water heater

Heat pumps are commonly used as an alternative to electrical resistance heaters for heating of sanitary hot water. The heat pump system is implemented in the same manner than the in-line heater, with the heat pump installed outside of the storage tank combined with a circulation system to the storage tank, illustrated in Figure 2.5. The main advantage of a heat pump is that for every one unit of electrical energy supplied to the heat pump, two units of energy is extracted from the outside air, thus supplying three units of energy to the hot water. This is in contrast to the electrical heating element where less than one unit of energy is

supplied to the water for every one unit of electrical energy. The heat pump is therefore typically three times more efficient than the electrical resistance element (Rousseau & Greyvenstein, 2000).

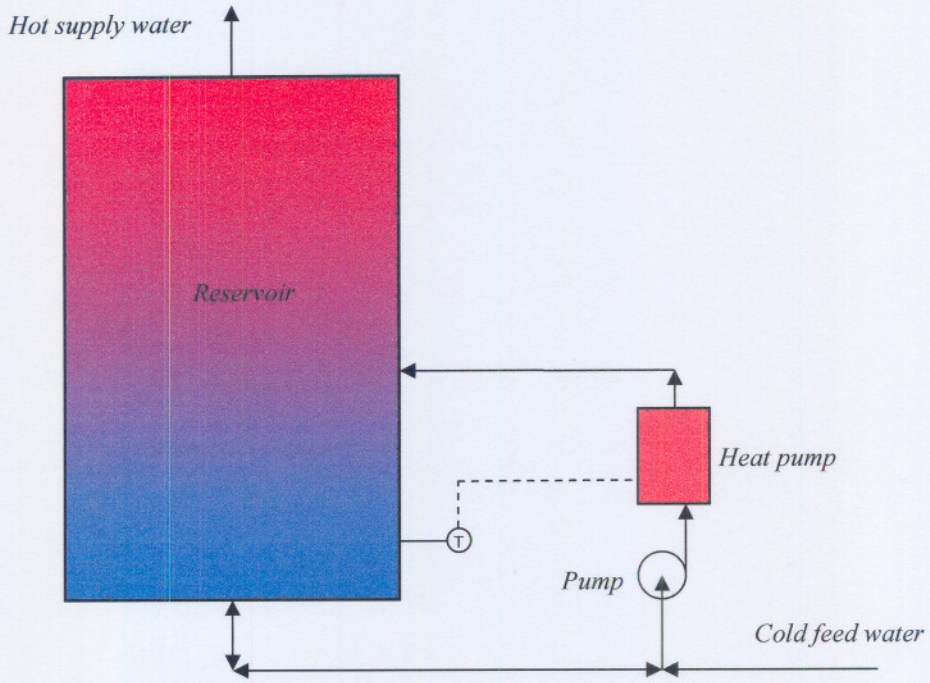

Figure 2.5: Schematic of heat pump water heater.

The reason why heat pumps are not employed in each and every heating installation is due to the relatively high initial cost, which makes it unattractive to most consumers. Installing heat pumps as a DSM-option increases the efficiency of the water heater by decreasing the energy consumption. Thus, the water heating load is reduced rather than shifted, causing energy sales to be lost, which is not ideal for the utility.

2.5 Existing DSM control strategies

Various control strategies are currently used to improve the energy efficiency and to lower the peak demand of electrical sanitary water heaters. This survey is conducted in order to evaluate the different control strategies. Valuable information is gathered from the literature on the control of conventional water heating systems for DSM-applications. The information is used to evaluate the performance of alternative water heating configurations in relation to the current DSM control strategies of conventional water heaters. This section discusses the different control strategies found in the literature in descending order of relevance.

Lemmer and Delport (1999) suggest a concept which uses a variable volume storage tank with in-tank resistance elements in order to decrease the peak electrical demand. The variable volume of the storage tank is established, due to the fact that the inlet and outlet mass flow may not be the same. The control strategy depicts two set-points for the storage tank. Set-point 1 keeps the volume of the water in the storage tank at the highest volume. Set-point 2 keeps the volume of the water above the lowest acceptable volume. During peak hours set-point 2 is used and the volume of stored water is able to decrease by not letting any cold water into the storage tank. This causes the water in the tank to remain hot without switching on the resistance elements. During off-peak hours set-point 1 is used and the water level is kept above the higher set-point, with cold water allowed to enter the reservoir. This concept could only be effective as long as the water extracted during peak hours does not reach the lowest volume setting. In such a case, cold water enters the reservoir and causes the resistance elements to be switched on fully during peak hours. This results in an undesirable load during peak hours.

In a further study (Lemmer *et al.*, 1998) the authors present a comparative real-time-pricing (RTP) case study with the same variable volume water heater concept. The same control algorithm as described above is used under different electricity tariff structures. The potential savings under each tariff structure is compared. It is recommended that a RTP-structure is used for the variable volume heater. The electricity tariff determines when the cold water will be let into the storage tank. The cold water must always be let into the tank during the lowest electricity cost. High real-time prices signal load reduction and low real-time prices signal load increase. It is found that a RTP tariff structure results in the lowest electricity cost compared to the other tariff structures. The conclusion is drawn that the savings achieved by the variable volume heater are dependant on the particular tariff structure imposed onto the control system.

The multi-objective controller proposed by Rautenbach and Lane (1996) provides a new method of controlling the domestic hot-water load. It aims to reduce the peak electrical demand while minimizing discomfort to the end-user and reducing the user's monthly electricity cost. The multi-objective controller is a centralised control strategy for the domestic hot-water load, which can be applied from town or city electricity control rooms on conventional in-tank water heaters. The control strategy distinguishes itself by incorporating a pro-active rather than a reactive control method. By increasing the thermostat setting of a hot-water heater, more energy can be stored inside the storage tanks. The load is controlled

to allow maximum storage of energy prior to peak load periods, and the hot-water load is shed during peak load periods. The multi-objective control strategy is primarily suited for use under a TOU tariff structure. A TOU tariff structure would decrease the price of electricity during off-peak periods and increase the price of electricity during peak load periods. The domestic end-users are classified in groups according to their different electricity usage. Each of these end-user groups are controlled uniquely. The multi-objective control strategy optimises the load switching schedule for each end-user group, given certain constraints and implements the optimised switching schedule on each end-user group. The optimisation is carried out via simulation on a digital computer. The aggregate cost is minimised iteratively to find the optimal load switching times for each end-user group. This strategy still has to be tested thoroughly in the field to prove its worth.

LaMeres *et al.* (1999) investigate a fuzzy logic-based variable power control strategy for shifting the average power demand of residential electric water heaters. The power consumed by the water heater is controlled, based on the information available from the water heating system. It includes the current temperature of the water, the maximum and minimum temperatures of the water allowed and distribution level power demand. Based on the status of the above variables, the fuzzy controller will determine the percentage of the maximum allowable power that the water heater should consume. Based on this information, a control signal is generated to control the voltage applied to the water heater. The proposed control strategy shifts the average residential electric water heater demand curve in such a way that the peak demand occurs during the periods where the total utility power demand is low and vice versa. The fuzzy logic controller uses four inputs namely: hot-water temperature, distribution level demand, and maximum and minimum allowed temperature to generate output signals which control the magnitude of the input voltage to the water heater. This control strategy reduces peak demand using a customer-interactive DSM-strategy, where the customer determines the minimum allowable hot-water supply temperature. However, the strategy uses a reactive strategy which can be improved by using a pro-active strategy where the load schedule is optimised.

In another study conducted by Nehrir and LaMeres (2000) it is stated that considering the energy storage capability of water heaters, they may not have to heat water at their full-rated power, when hot water is being used during peak demand periods. A water heater's power consumption can be controlled to be anywhere between zero and its full capacity by controlling the voltage applied to its heating elements. In a RTP-environment, some

customers may choose to control their water heaters not to heat water at their full capacity during peak demand periods. The control method discussed here, uses a multiple-block fuzzy logic-based water heater DSM-strategy. In this strategy electric water heaters are divided into several blocks and the peak demand of each block is shifted to a different time-period throughout the day, where the demand is low. The strategy uses the same fuzzy logic-based methodology to control the water heaters as discussed in the previous paragraph (LaMeres *et al.*, 1999). The only difference is that the peak demand of the different blocks of water heaters are shifted to a different time-period throughout the day. In the previous paragraph the peak demand of all the heaters are shifted simultaneously. This may cause a new peak demand during a once off-peak period. This control strategy reduces peak demand using a customer-interactive DSM-strategy and shifts the peak load of blocks of water heaters to different time-periods. This ensures that the creation of a new peak during once off-peak periods is avoided. However, the strategy still uses a reactive strategy which can be improved by using a pro-active strategy where the load schedule is optimised.

Horn and De Kock (2004) conducted a water heating system case study, in which a new control strategy is implemented on an existing in-line water heater. The proposed control strategy uses predetermined rules to switch the resistance elements on/off in stages. At certain times during the day, only a fraction of the total heating capacity is activated according to the peak demand periods and the average water temperature. The peak demand period in this case, lasts only two hours, but the objective was to store enough hot water for the period from 08:00 to 14:00. If the average water temperature drops below 40 °C in this peak demand period only two-thirds of the heating capacity is switched on. During off-peak periods the controller allows the resistance elements to be switched on fully. This methodology proves to be very effective. It has a definite advantage over DLC, due to the fact that only two-thirds of the heating capacity is switched during peak periods where insufficient hot water is supplied. A direct load control strategy does not switch on at all during peak demand periods causing insufficient hot water supplied to the consumer. The disadvantage of this strategy is that it is limited to a specific case where the water consumption profile is a fixed variable. This strategy could be improved by formulating a more generic algorithm in order to implement it more widely. The switching schedule could also be optimised by considering different possibilities for the control schedule set-points in order to minimise the electricity cost.

Van Tonder and Lane (1996) state that the general approach to controlling water heaters linked to a certain point of supply is to divide them into groups of equal size. All the water heaters in a certain group are controlled simultaneously. The control strategy becomes more flexible as the number of control blocks increases. The maximum number of blocks may however be limited by the control equipment since each block needs its own control signal. The basic principle followed by the control strategy is to switch off a block of water heaters when the total load gets close to a preset target. When the load has decreased enough to allow a block to be switched on again, the water heaters are reactivated on a first-off first-on basis. A block will also be switched on when it has been off for the maximum allowable time. In this case one or more other blocks will be switched off to allow the recovery of the block switched on. This strategy utilises a DLC-strategy under certain constraints. This strategy will reduce the peak demand, but customer complaints are inevitable. The strategy is reactive and could be improved using a more pro-active control strategy in order to optimise the load schedule of the water heating systems and to minimise customer dissatisfaction.

El-Amin *et al.* (1999) propose a control strategy that, unlike most existing control strategies, gives the consumer the privilege to share in the load shedding policy. The system hardware consists of a personal computer (PC) at the utility site and a programmable logic controller (PLC) at the consumer location. The PC is used as a control centre that initiates the commands to the PLC. The PLC is used to energize or de-energize the loads at the consumer side. After receiving a warning alarm generated by the PLC, initiated by the PC at the utility control centre, the consumer has the chance to switch off any desired load. If he does not act within a predefined period, the PLC will take the required action based on the scenario decided by the utility. Since this control strategy is based on customer interaction and discomfort the success depends largely on customer acceptance.

Lacroix (1999) examines the performance of three electric water heater designs for electric load management and control of bacterial contamination. The thermal behaviour of the water heaters is simulated numerically using the TRNSYS computer program. The TRNSYS computer program simulates the dynamic behaviour of complex thermal systems. The first design consists of a standard water heater to which various minor modifications were made. The results of the simulations reveal a benefit in large capacity water heaters (350 and 540 litre) equipped with a vertical heating element and a time-clock. The second design consists of a high temperature water heater equipped with a heat exchanger or a mixing valve. Although capable of storing more heat and better able to impede bacterial

growth, these water heaters consume more electricity, are more prone to scaling and often have a limited service life. The third design consists of connecting two 175 litre or two 270 litre water heaters, equipped with a time-clock, in series. The results indicate that such a system is capable of meeting load management requirements and eliminating bacterial contamination. Enough heat can be stored overnight so that the heating elements need not be operated during the day, and in addition, the temperature of the water in the service tank remains high, thus preventing the growth of bacteria. This design is most attractive for Canadian manufacturers, since it only requires minor modifications to be made to existing water-heater systems. It is estimated that such a system could save the five Canadian electric utilities considered in this study up to 1 819 MW in power. This strategy uses a DLC-strategy with water heaters connected in series. The entire load is shed during peak hours resulting in a reduction in peak demand.

Akridge and Keeburgh (1990) investigate the load management potential of a conventional in-tank water heater with a group of resistance elements situated at the bottom of the reservoir and another group situated at the top. The lower heating elements are controlled by a timer to operate only between the hours of 23:00 and 7:00. The upper heater elements are controlled via a thermostat and are permitted to operate whenever needed. The system's performance is investigated with different element wattages and different hot-water load profiles. Timer control of the lower heating elements not only shifts a significant portion of the hot-water heating load to off-peak periods, it also causes the tanks to become highly stratified, with large thermal gradients over relative short distances within the tank. Stratification allows the tank to provide hot water at 50 °C at times when the average tank temperatures were below 50 °C. Empirical results obtained from the study shows that the tank maintains good stratification as long as the lower resistance elements are not permitted to come on. The tank is only heated from the top during peak hours and does not mix the water to a significant degree. Stratification disappears almost entirely as soon as the lower elements are switched on. It is concluded by the authors that a relatively simple timer control system can be used to effectively shift hot-water heating load to off-peak hours. Unfortunately most in-tank water heaters found in South Africa only have one group of resistance elements situated at the bottom. The cost of modifying water heaters to incorporate a group of resistance elements at the top of the tank off-sets the peak demand savings potential, making this a less attractive option.

Bzuru (1989) investigates a radio control strategy for remotely controlling residential electric water heaters during peak demand hours. The electricity company concerned has in the past controlled residential water heaters by using built-in timers and relays. This particular combination has no back-up energy source, so it falls behind schedule after every outage. Another drawback is that the timer only has a 24-hour capability; weekends and holidays are treated identically as weekdays. Another disadvantage is that one schedule cannot cover both winter peak hours and summer peak hours. For these reasons a radio controller will be investigated. The primary benefit of load control with a remote radio controller is flexible control hours for different seasons. Elimination of control during weekends and holidays and the ability to quickly shed the load of all water heaters as desired. From results obtained via an empirical study, it is concluded that although the demand reduction was less than anticipated, the radio controller had definite advantages over the conventional timer-switches.

Wilken and Delport (2000) suggest a centralised DLC-strategy for residential water heating. Each residential customer will be placed in a group with similar hot-water needs and behaviour. A different control algorithm based on a DLC-strategy is used to control the different groups individually. This is an improvement on the conventional direct load control strategy where all the water heaters are controlled in the same way. This strategy improves customer satisfaction and creates trust in the load management scheme.

Van Harmelen and Van Tonder (1998) suggest a DLC-strategy for residential water heaters by using a RTP tariff structure. RTP-based load control is aimed at controlling the load to obtain optimal financial benefit (for both supplier and consumer) by dropping load at times when the energy is high and allowing the load to recover when the energy price is lower. Once again control parameters had to be set within reasonable limits. The control algorithm is therefore programmed only to control the water heating load during three hours in the morning and three hours in the evening when energy prices are the highest.

Calmeyer and Delport (1999) propose a control strategy which controls the hot-water load of large water heaters in groups. The heaters are simulated and controlled according to the simulation. The simulation uses the hot-water consumption and determines the temperature inside the water heater. The temperature is kept above a certain level in order to minimise customer dissatisfaction. The strategy has to be tested in order to verify its applicability. A disadvantage is the fact that the strategy is without any compensation. No monitoring is

done on the system in order to evaluate the performance. In cases of a water demand profile deviating from the original demand profile, the system will not be able to compensate and the consumer may be supplied with insufficient hot water.

According to Forlee (1999) conventional hot-water load management systems have traditionally been used in such a manner as to effectively manage load during peak periods with little or no regard for customer comfort. The objective of this study is to implement a water heating load management system, which would be loosely based on conventional water heater load management systems (radio/ripple). The system proposed would, however be of a far more intelligent and flexible nature than the existing systems. Complex control algorithms, developed using data from notch testing will be implemented. The objective is to maximise the amount of deferrable load during peak periods whilst still ensuring that customers seldom/never experience cold water. The flexibility lies in the fact that the customer has a choice as to how their hot-water cylinder is controlled. The load management system implemented, allows each geyser relay to be addressed individually. This means that it is possible to customise the manner in which each customer's water heater is controlled. Four different control algorithms, each with a lesser or greater degree of control will be available. Customers will be allocated a control algorithm by answering a short questionnaire. A 24-hour customer care centre will be available. Based on the customer complaints they will be dynamically allocated to different control algorithm.

Bhattacharyya and Crow (1996) propose a methodology to optimise both customer satisfaction and utility peak demand savings, based on a fuzzy logic load model for direct load control of appliances. A new approach to DLC is proposed in which customer preferences are accommodated while concurrently maximising the savings of the utility. This new approach to DLC is based on fuzzy logic techniques which optimise the trade-off between customer preference, utility resources and uncertainties in the load. DLC is accomplished by switching appliances on or off according to a set of fuzzy logic rules. Different schedules are imposed onto different groups of water heaters in order to find the optimum reduction in peak demand.

In a study by Roman and Wilson (1995) a customer driven control strategy is proposed. Customers give the utility the permission to readily control appliances such as heat pumps, air-conditioners or water heaters during peak production hours. The customer in return receives a rate reduction based on their monthly power consumption. The success of any

load management program is directly proportional to the satisfaction of the customer with the program. Customers are given a warning alarm one hour prior to the control period. The customer acknowledges the alarm and his appliances can be controlled by the utility. The utility uses a DLC-strategy to switch appliances on or off using one-way radio switches as communication medium. The appliances of the customers can be controlled for a period of not longer than three hours, thereafter the appliances are switched back on. This strategy depends on customer co-operation and is a reactive control approach. The strategy may be successful in regions where the customer is willing to interact with the utility in order to save on their monthly electricity cost.

In a study by Lane and Beute (1996) a model of the domestic hot-water load is derived in order to use this model to predict the effects of load control on a water heating system. The authors state that much needs to be done to encourage the consumer to control and reduce his hot-water load. The authors further suggest ways to achieve more efficient hot-water systems by:

- Improving thermal insulation of storage tanks and pipes.
- Motivation of the public to use hot water more wisely.
- Automation to control the time of day when water is heated. The controller needs to sense when hot water is needed, and it needs to be aware of the off-peak times in the electrical demand, when water should be heated.
- The supplier of electricity needs to price electricity in such a way that gives the consumer cost-savings when water is not heated in peak demand periods.

The above-mentioned guidelines for achieving more efficient hot-water systems are very useful. Some of the guidelines are implemented during the evaluation of new alternative water heating configurations suited for DSM.

Laurent *et al.* (1995) proposes a column generation method for optimal load management of in-tank water heaters. The model assumes a fully mixed storage tank. The proposed control strategy uses DLC to switch water heaters on or off during peak demand hours. A column generation approach for maximum electric load peak reduction is used.

This section discussed existing control strategies for conventional water heater installations. From the literature it can be seen that there exists a need for alternative water heating

configurations which lend themselves more towards DSM without having to be controlled in such complex manners.

2.6 Water heating simulation model

In order to evaluate the performance of alternative water heating configurations, a simulation model is needed to simulate the thermal behaviour of a water heating system. A comprehensive simulation model exists in the literature (Rousseau *et al.*, 2001) which is used to simulate the thermal performance of different water heating configurations. The simulation model mentioned in the literature is expanded to accommodate multi-reservoir systems with reservoirs connected in series or in parallel. The simulation model can accommodate a system configuration with the heater in parallel outside the reservoirs as well as a system configuration with the heaters situated inside the reservoirs. In a study by Rousseau and Greyvenstein (2000) a description of the simulation model together with its verification is discussed.

The simulation model provides as output the temperatures and electrical energy consumption associated with different water heating configurations, control strategies and set-point temperatures. The inputs to the simulation are the daily consumption profile, the geometry of the system, the climatic conditions and the heating capacity of the resistance heaters.

The reservoir is divided into a number of horizontal control volume layers each represented by a single node similar to the so-called stratified multimode model of Kleinbach *et al.* (1993). The mass of water contained in each control volume is assumed to be perfectly mixed. The heat storage as well as the conduction and forced convection heat transfer rates between the nodes and between each node and the outside of the reservoir are modelled via an electrical analogue network, thereby ensuring conservation of energy. The resistances accounting for the forced convection heat transfer take into account the direction of flow through the reservoir, either up or down, between each pair of adjacent nodes. The thermal storage, due to the mass of water in each node, is represented by appropriate capacitors. The resulting partial differential equations are discretised in a fully implicit manner and the resulting algebraic equations are solved explicitly at each time-step with the aid of the well-known tri-diagonal matrix algorithm. The model does not account for conduction inside the shell material of the reservoir.

The stratification, due to natural convection, is accounted for with a mixing model superimposed onto the solution of the electrical analogue model at the end of each time-step. The model applies complete mixing between adjacent nodes, starting from the top, at each pair of nodes where a temperature inversion occurs. The mixing rule ensures conservation of both mass and energy. Mixing between adjacent layers continues in the appropriate manner until a positive temperature gradient exists from the bottom to the top throughout the reservoir. The assumption of perfect stratification between adjacent layers is off-course not physically realistic since in practice some dilution of the temperature gradient is always encountered. This can effectively be accounted for by reducing the number of nodes employed in the simulation.

The flow rates through the reservoir and the in-line heater are obtained by applying conservation of mass and incorporating the prescribed controller algorithm. The controller algorithm takes into account the different set-point and dead-bands for each of the thermostats, the set-point of the water flow regulating valve as well as the load shedding period that may be specified.

In order to verify the accuracy of the simulation model a detailed laboratory validation study was conducted by Strauss (1999) on a scaled-down storage reservoir. A low-pressure, 114 litre, copper storage reservoir with a representative height to diameter ratio was used in the experiments. The reservoir was fitted with both an in-tank and in-line resistance heater with a water pump and flow control valve. The inlet and outlet temperatures were monitored with accurate resistance thermometer devices. Inside the reservoir thermocouples were evenly spaced from top to bottom to monitor the temperature distribution through the reservoir.

A flow meter and solenoid valve were placed in series with the outlet water pipe. All the different temperature sensors, the flow meter and solenoid valve were monitored and controlled from a central computer via intelligent sensor-to-PC remote data acquisition modules. Built-in microprocessors independently provided intelligent signal conditioning, analogue input/output (I/O), and digital I/O through a two-wire RS-485 communication network.

Two tests were used as benchmarks for both the in-tank and in-line configuration. The first was to simply heat up the whole reservoir that was initially filled with cold water until the heater was switched off by the thermostat. The second was to apply a typical water consumption profile for a number of days to obtain a quasi-steady state situation. When

comparing the measured and simulated results for verification, the performance numbers of Kleinbach *et al.* (1993) were employed and the current results were also compared with those reported in the reference.

It was found that the new storage vessel model could predict the supply temperature within 2% for a system configuration with the heater in parallel outside the reservoir and within 12% for a configuration with the heater situated inside the reservoir. This compares favourably with existing models found in the literature provided by Rousseau and Greyvenstein (2000).

2.7 Summary

In this chapter an extensive literature survey was provided. The survey showed that sanitary water heating forms a critical part of the peak demand imposed on the national electricity supply grid. By far the largest portion of the total sanitary hot-water consumption in South Africa is heated by means of resistance heaters. Resistance heaters, almost exclusively in-tank heaters, account for 68% of the total number of residents served. These in-tank resistance heaters are not ideally suited for DSM-applications. A lot of research has been done on DSM on sanitary water heaters. Most DSM control strategies for in-tank water heaters use a reactive, direct load control strategy switching water heaters on or off during peak demand periods without taking into account customer satisfaction. There exists a need for alternative water heating configurations which lend themselves better towards DSM. These alternative water heating configurations must reduce the peak demand imposed on the national electricity supply grid while minimising customer discomfort due to insufficient hot water being supplied.

The next chapter presents alternative water heating configurations which lend themselves better towards DSM. The operation of these alternative water heating configurations is evaluated via simulation and compared to the thermal behaviour of the conventional in-tank water heating configuration under load shedding conditions.

Chapter 3

EVALUATION OF ALTERNATIVE WATER HEATING CONFIGURATIONS

3.1 Introduction

In the previous chapter an extensive literature survey was provided. It was found that sanitary water heating forms a critical part of the peak demand imposed on the national electricity supply grid. Furthermore, the largest percentage of water heaters found in South Africa comprises of in-tank water heaters which are not ideally suited for DSM-applications. A need therefore exists for alternative water heater technologies which lend themselves better towards DSM.

This chapter presents various new water heating configurations developed by Enerflow Technologies CC that allow the realisation of the maximum DSM-potential under different operating conditions. The operation of each of these new alternative water heating configurations is evaluated via simulation and compared to the thermal behaviour of the conventional in-tank water heating configuration.

3.2 Conventional heater design philosophy

Conventional design philosophy for large scale multi-reservoir water heating plants is to connect two or more reservoirs in parallel as shown in Figure 3.1. The water in the reservoirs is heated by independently controlled in-tank heaters consisting of electrical resistance elements at the bottom of each reservoir. The cold water is therefore heated gradually from the bottom while the hot supply water is drawn from the top. This means that whenever hot water is drawn from the fully heated reservoirs, the cold water entering at the bottom will lower the temperature of the water at the thermostats. The thermostats will then call for the full heating capacity of the resistance elements to be activated. This contributes to the high morning and evening electricity peak demand suffered by the electrical utility.

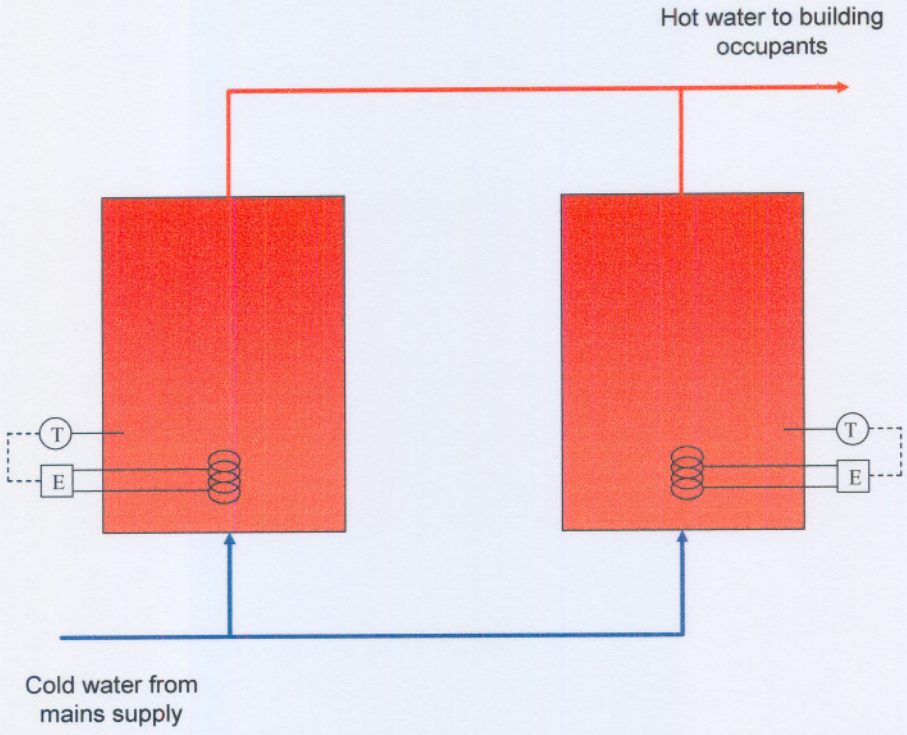

Figure 3.1: Conventional design for large scale multi-reservoir water heating plants.

The fact that the heating is done at the bottom of the reservoir implies that when the heaters are operating, the water in the reservoir is usually very well-mixed. This is due to natural convection phenomena that cause the hot water at the bottom to rise and mix with the rest of the water in the reservoir. Therefore, the water's average temperature at the top of the reservoir is lower than the desired set-point value for most of the day.

If the heating load is shed during peak demand periods, the hot water will accumulate at the top of the reservoirs and the cold water at the bottom, which is very useful. However, once the heaters are switched on, the little amount of hot water available at the top of the reservoirs will almost instantly be mixed with the colder water at the bottom. Now practically all the water in the reservoir must be reheated before any of it is available to the occupants at the desired temperature. Therefore, in this configuration there is very little opportunity to correct the situation if cold water reaches the top of the reservoir while load shedding is activated. The overall result will be that cold water may be supplied to the occupants during the peak demand period as well as for an extended period after load shedding has taken place.

A detail simulation model has been developed by Rousseau *et al.* (2001) for the simulation of both in-tank and in-line configurations which are investigated in this study. The simulation model allows the specification of various plant geometries, heating capacities,

control algorithms, set-points, etc. This simulation model is used to compare the thermal performance of different water heating configurations under load shedding conditions. In order to compare the thermal performance of the different water heating configurations, the simulated plants need to be subjected to the exact same operating conditions. All of the simulated plants are subjected to a typical water demand profile for the application in which the plants are being used. Figure 3.2 shows the normalised hourly water demand profile used as input to the simulations. This normalised water consumption profile is used for all of the simulations that are done in the remainder of this chapter.

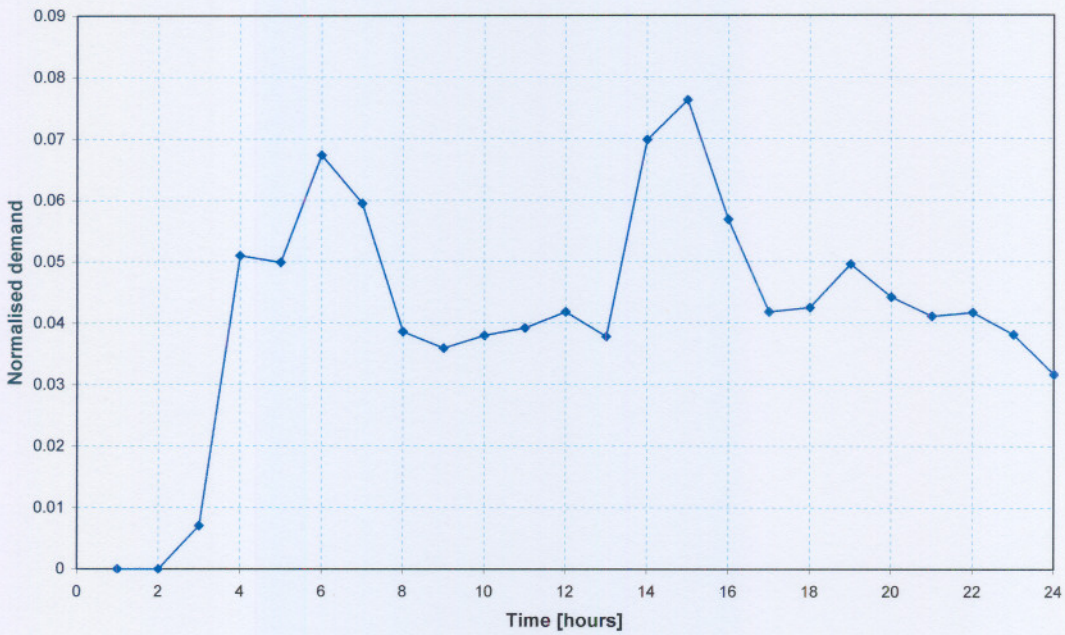

Figure 3.2: Typical normalised hot-water consumption profile.

Figure 3.3 to Figure 3.5 present the results obtained by using the simulation model to investigate the thermal behaviour of a conventional in-tank water heating plant. The plant consists of two reservoirs connected in parallel with in-tank resistance heaters in each tank. The simulation is conducted for a typical winter's day, in the Johannesburg region. The weather data is obtained from the widely used "Council for Scientific and Industrial Research" (CSIR) climate database. Table 3.1 provides a summary of the simulated plant specifications and operating conditions.

Table 3.1: Summary of conventional in-tank plant specifications.

Heating capacity	240 kW
Heating equipment	In-tank resistance elements
Storage capacity	2 x 10 000 litre (Parallel connected)
Occupancy	1 150 residents
Hot-water consumption	75 litres per person per day
Temperature set-point	60 °C for both tanks

Figure 3.3 shows the simulated electrical demand profile during a typical winter's day with load shedding during the peak demand period (18:00 to 20:00).

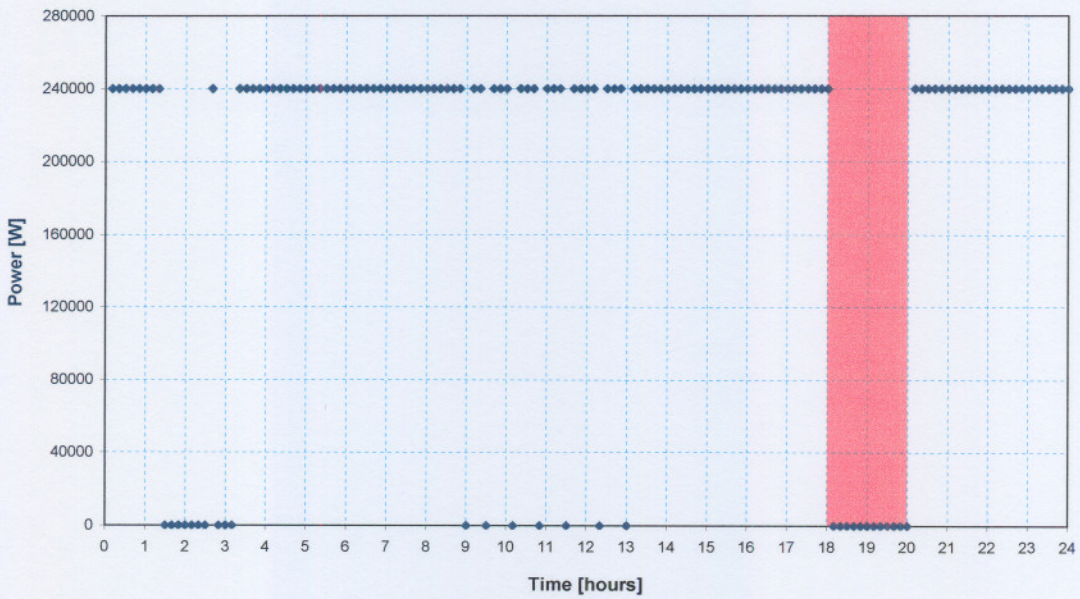

Figure 3.3: Simulated electrical demand profile for a typical winter's day.

The simulated hot-water supply temperatures are shown in Figure 3.4. From this figure it can be seen that the hot-water supply temperature does not drop extensively during the load shedding period. This is due to the fact that the hot water accumulates at the top of the reservoirs and the cold water at the bottom. However, after the load shedding period the hot-water supply temperature drops rapidly to a temperature below the minimum allowable temperature of 40 °C. This is the result of the mixing of the cold water at the bottom with the hot water at the top of the reservoir which occurs as soon as the in-tank resistance elements are switched back on. It can also be seen that the hot-water supply temperature stays below the set-point temperature of 60 °C for an extended period after load shedding has occurred, due to the fact that almost all the water in the reservoir must be reheated. The overall result is that sufficient hot water is supplied to the occupants during the peak

demand period, however insufficient hot water is supplied for an extended period after load shedding has taken place.

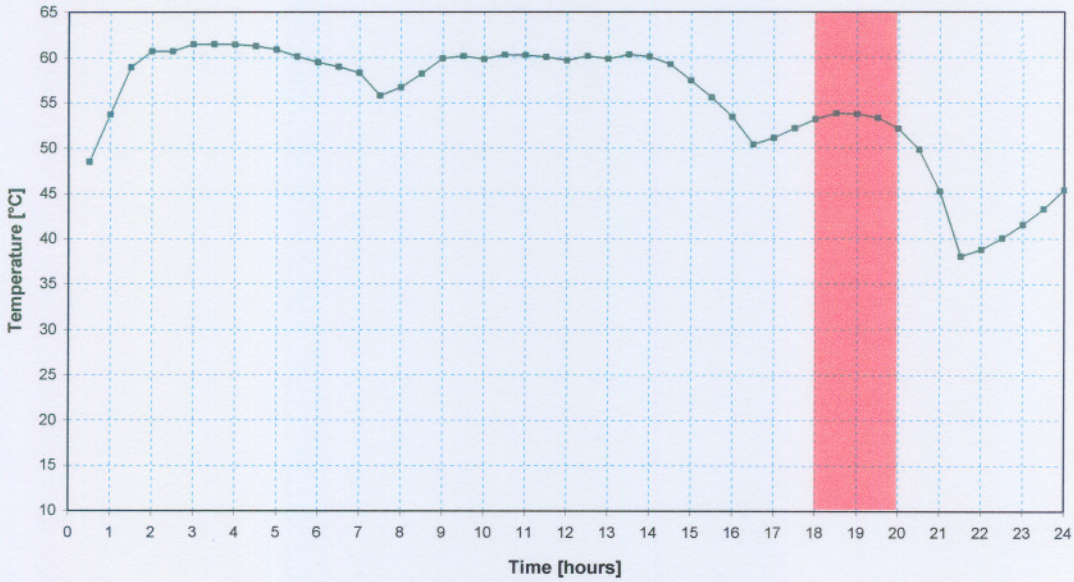

Figure 3.4: Simulated hot-water supply temperature for a typical winter's day.

Figure 3.5 shows the vertical temperature distribution through both reservoirs. The stratification effect can be seen during the load shedding period (18:00 to 20:00) in which the temperature of the water at the top is much higher than the temperature at the bottom. After the load shedding period, the temperature gradient disappears completely, resulting in a fully mixed tank only one hour after the load shedding period.

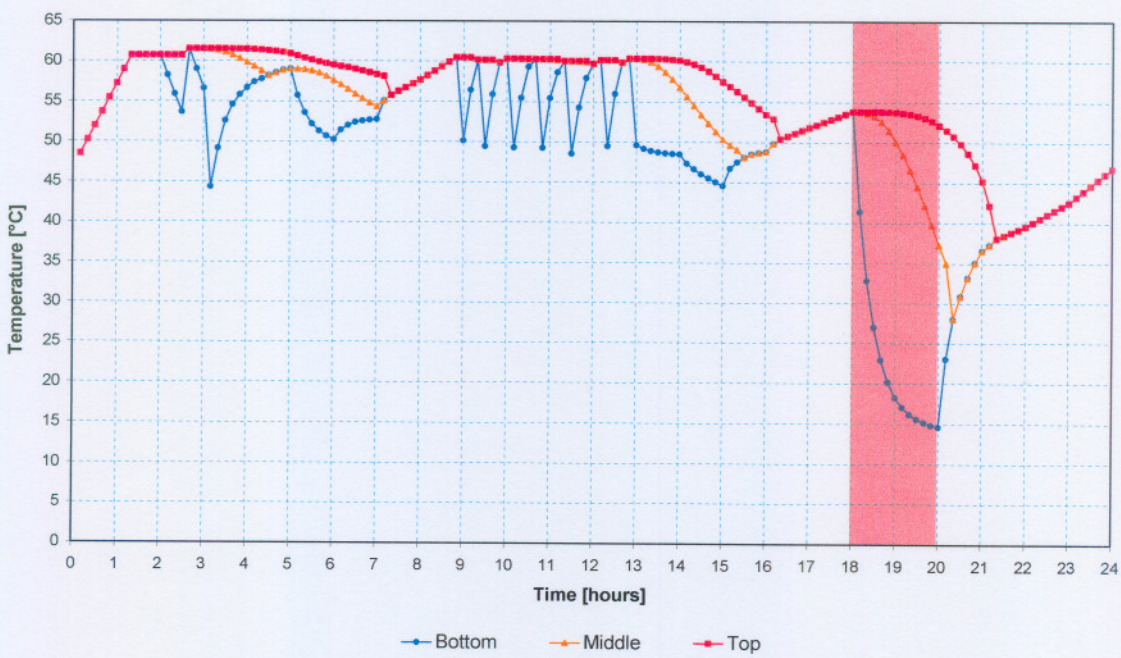

Figure 3.5: Simulated vertical temperature distribution through reservoirs.

Two different technologies have been developed to address the problems associated with the conventional heater design philosophy while still realising the maximum DSM-potential. These technologies are the ILH- and the SIT-systems.

3.3 In-line heater (ILH) system

In the in-line heater configuration the reservoir connections are altered so that they are connected in series rather than parallel. An in-line resistance heating device is also installed outside the reservoir and connected to the top of the last reservoir as shown schematically in Figure 3.6.

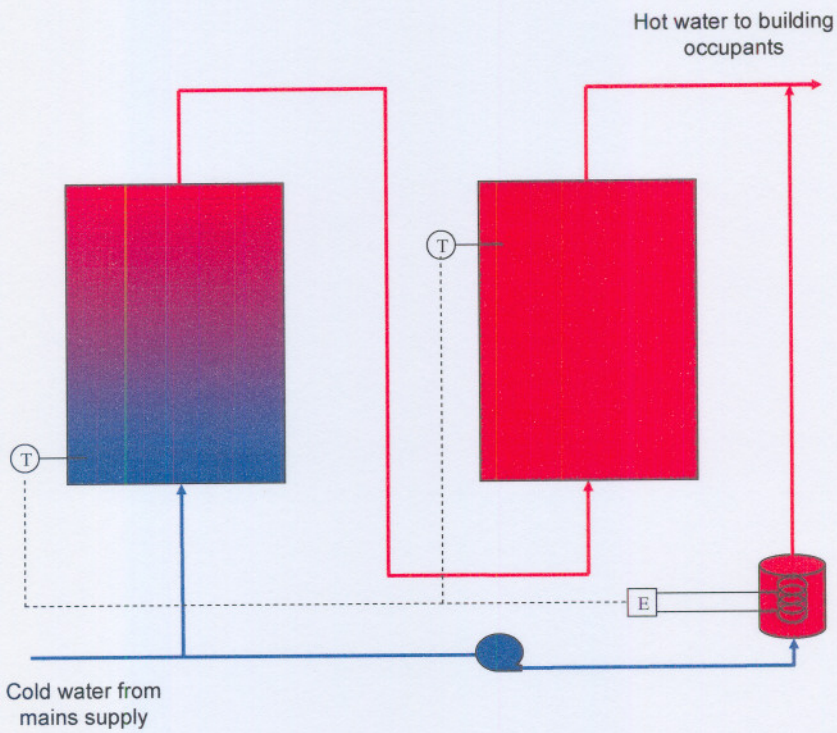

Figure 3.6: Schematic of the new in-line electrical heater layout.

In the in-line configuration the hot water produced by the heater is returned to the top of the reservoir instead of to the bottom. The circulation system includes a pump and a control valve that regulates the flow rate through the heater in such a way that the temperature of the water leaving the heater is maintained at the set-point temperature. If the reservoir is filled with cold water, the hot water supplied by the heater back to the top of the storage tank is always at the desired temperature. Since the water is added to the top, a well-defined temperature gradient will be maintained, due to the stratification effect.

This ensures that even though the average temperature of the water in the reservoir may be much lower than the set-point value, a certain volume of water at the top will always be

ready for use at the highest temperature, even after the heating load was shed for a longer period. Furthermore, even if the reservoir is filled with colder water at the end of the load shedding period, a certain volume of water at the top will be ready for use shortly after the shedding period. It is therefore clear that the in-line configuration lends itself much better towards DSM compared to the conventional in-tank configuration.

During off-peak periods the resistance elements are controlled by the thermostat installed in the 'bottom' reservoir. The thermostat switches the heater on while the temperature at the bottom thermostat is lower than the lower thermostat set-point and visa versa. During peak periods the bottom thermostat is ignored while the thermostat installed at the top of the 'top' reservoir takes over the control. The heater is switched off during peak periods while the temperature at the top thermostat is higher than the top thermostat set-point, which is usually around 45 °C. If it should happen that the cold-water line reaches the top thermostat, the controller will switch on the heater resulting in the heater being switched on for a fraction of time during the peak demand period. Although this will result in a load during peak periods it will also result in sufficient hot water being supplied to the occupants. It must also be noted that this scenario will only occur in plants with an unusually high occupancy.

The previously mentioned simulation model is used to investigate the thermal performance of an in-line heater system. The plant specifications of the in-line heater system are identical to the specifications of the previously simulated conventional in-tank heater plant. The only difference between the two is the fact that the in-tank resistance elements are replaced with an in-line heater and that the reservoirs are connected in series rather than parallel. Table 3.2 provides a summary of the in-line heater system specifications.

Table 3.2: Summary of in-line heater system specifications.

Heating capacity	240 kW
Heating equipment	In-line resistance elements
Storage capacity	2 x 10 000 litre (Series connected)
Occupancy	1 150 residents
Hot-water consumption	75 litres per person per day
In-line heater temperature set-point	60 °C

The simulation is once again performed for a typical winter's day, in the Johannesburg region under the same operating conditions as for the conventional in-tank system. The weather data is obtained from the widely used CSIR climate database. Figure 3.7 shows the

simulated electrical demand profile during a typical winter's day with load shedding during the peak demand period (18:00 to 20:00). The total electricity consumed by the ILH adds up to 4 600 kWh compared to 4 600 kWh consumed by the conventional system. This indicates that the total energy consumed by the two systems compares very well showing that the ILH will not use much more or less electrical energy than the conventional system.

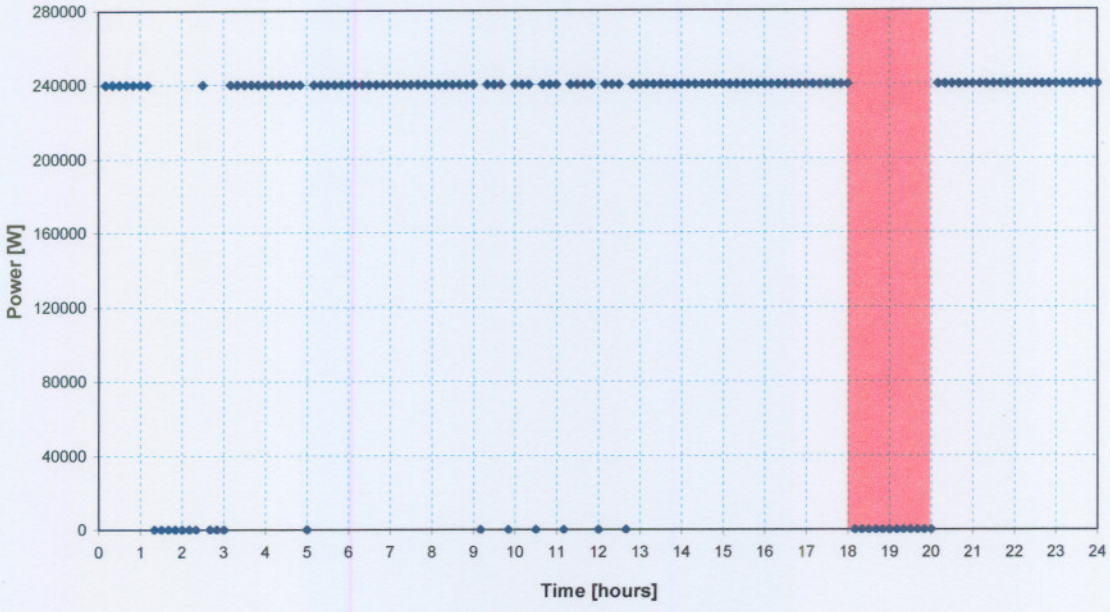

Figure 3.7: Simulated in-line heater electrical demand profile for a typical winter's day.

The simulated hot-water supply temperatures for the conventional in-tank system as well as the retrofitted in-line heater system are shown in Figure 3.8. It can be seen from the figure that the supply temperature of the in-line heater system almost stays constant and equal to the desired temperature throughout the entire day. In contrast with the conventional in-tank heater system, the temperature stays at the desired temperature during the load shedding period. After the load shedding period the in-line resistance elements are switched back on. This results in hot water being supplied to the top of the reservoir as well as to the occupants at the desired temperature. This is in contrast with the conventional in-tank system where the hot-water supply temperature drops below the desired temperature for an extended period after load shedding has occurred.

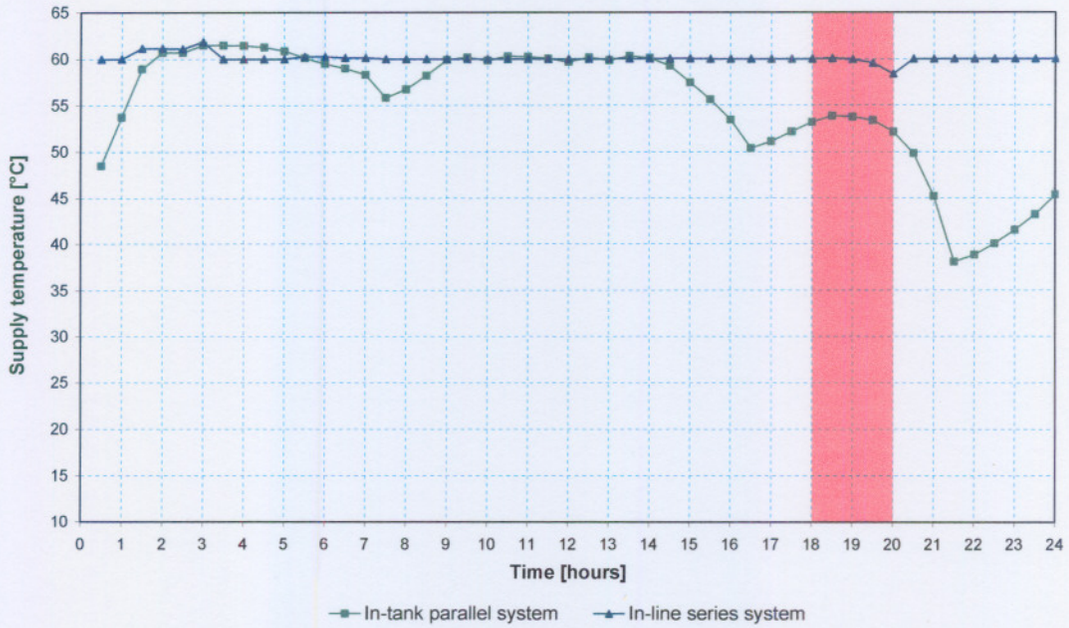

Figure 3.8: Simulated hot-water supply temperature for a typical winter's day.

The temperature distribution of the top reservoir from which the hot water is drawn, is shown in Figure 3.9. The temperature at the top of the reservoir is maintained at the desired temperature throughout the day. During the load shedding period, the temperature at the bottom of the top reservoir drops rapidly. This is due to the fact that colder water enters the reservoir from the bottom reservoir. As suspected, only the top layer of the top reservoir stays at the desired temperature during the load shedding period.

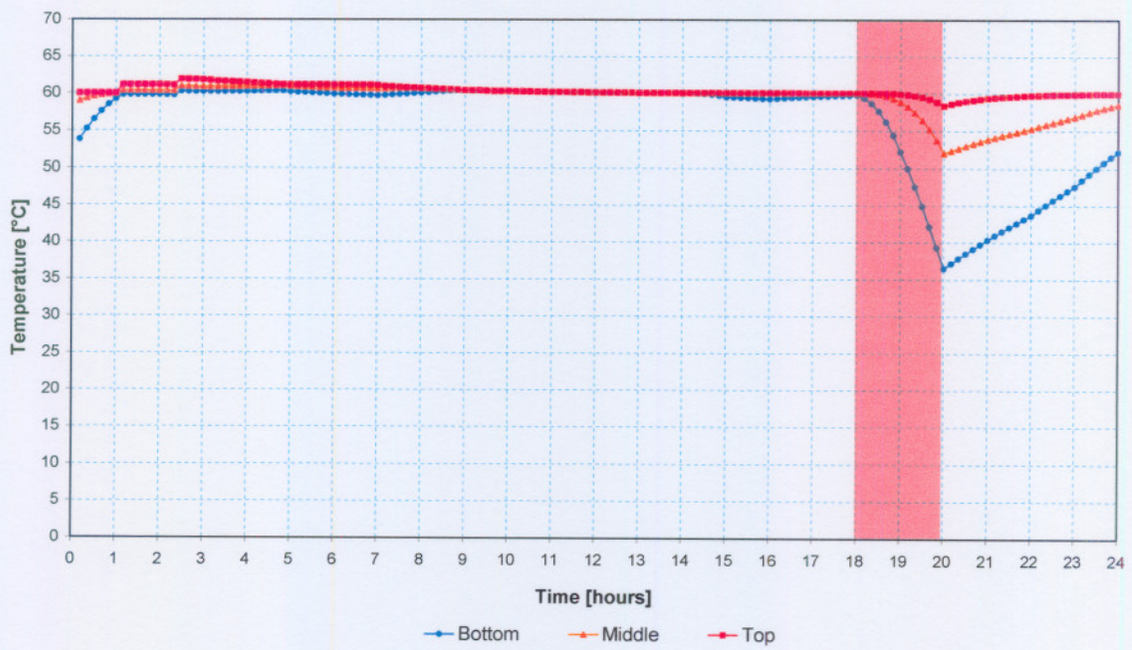

Figure 3.9: Simulated temperature distribution of top reservoir.

Figure 3.10 shows the vertical temperature distribution through the bottom reservoir where the cold water enters the system. A well-defined temperature gradient exists in the tank throughout the day. The temperature at the top of the reservoir drops substantially during the load shedding period (18:00 to 20:00). This is caused by hot water being drawn from the top of the reservoir to the second reservoir and cold water entering at the bottom of the reservoir.

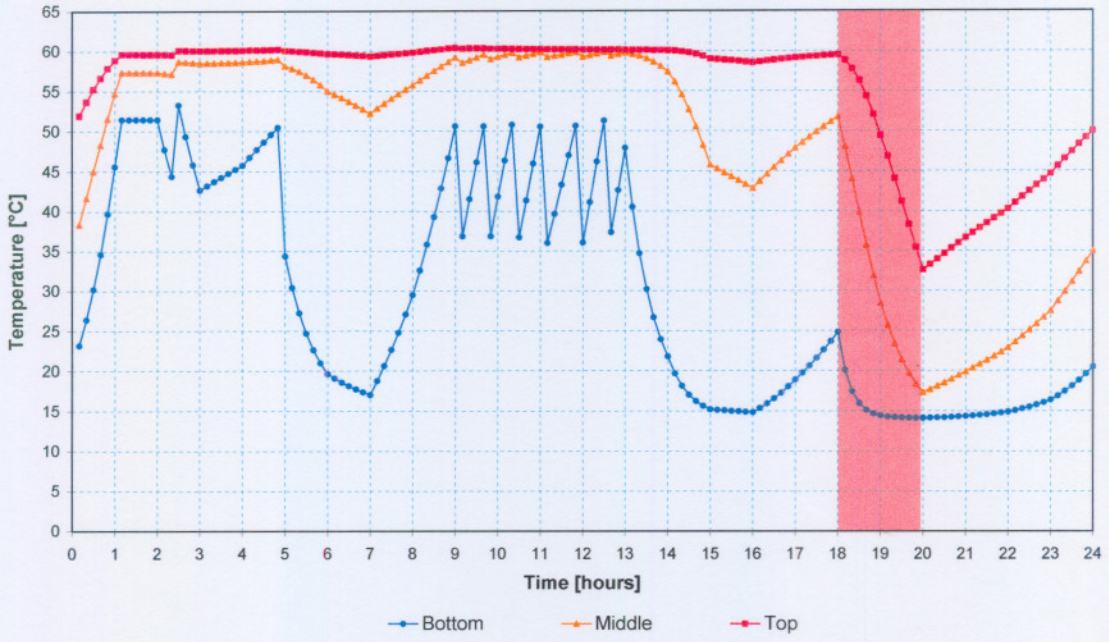

Figure 3.10: Simulated temperature distribution of bottom reservoir.

It is clear from the simulation results that the in-line heater system lends itself much more to DSM through load shedding than the conventional in-tank heater system. This makes the in-line heater system an ideal candidate for load shedding during peak demand periods.

3.4 Stratified in-tank (SIT) heater technology

In existing plants with high diversity factors (≥ 0.7), the ILH-technology remains the only technically feasible solution to achieve complete load shedding during peak demand periods, while still providing sufficient hot water to the building occupants at all times. However, many existing plants also have very low diversity factors. The diversity factor gives the probability of whether a system will be activated at a specific time during the day. This means that in their current configurations, these plants are essentially under-utilised. Therefore, even if all of the heating load can be shed during peak demand periods, the peak demand power savings will be limited. In such cases it is often not economically viable to

install the ILH-technology since it requires new equipment and relatively costly piping and electrical switchgear retrofits.

In order to make the most of the DSM-potential offered by these under-utilised plants the so-called stratified in-tank (SIT) heater technology was developed. Figure 3.11 shows a simplified schematic of the system layout for the SIT design methodology.

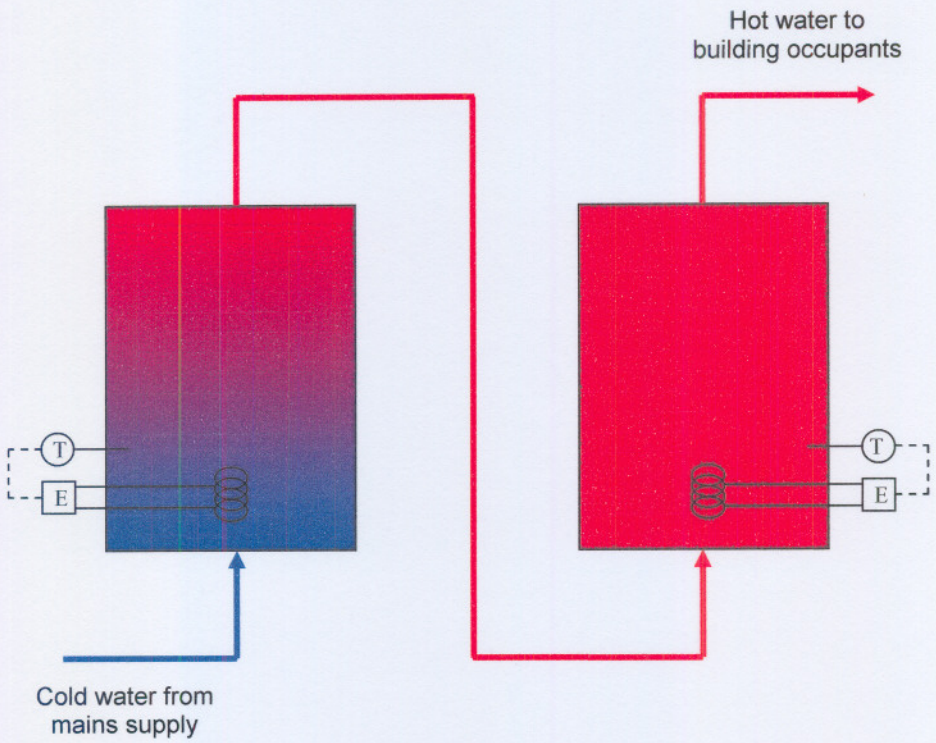

Figure 3.11: Stratified in-tank (SIT) design for multi-reservoir water heating plants.

As shown in this figure, the piping layout is again altered so that the reservoirs are connected in series rather than in parallel. From the flow's point of view, this has almost the same effect as if the reservoirs were situated one on top of the other. Since the cold feed water is drawn through the 'bottom' reservoir to the 'top' reservoir, the hot water will tend to accumulate in the top reservoir during load shedding periods while the cold water accumulates in the bottom reservoir. The controller will force the bottom heater to remain off, but if the cold-water line reaches the top reservoir during peak periods, the opportunity now exists to activate only the heater in the top reservoir to intervene and ensure that occupants are not supplied with cold water. Note that if only the top heater is switched on, there will be very little disruption of the natural temperature gradient. Furthermore, all of the water does not need to be heated at once, but only that entering the top reservoir.

An additional advantage is that only a part of the heating load is now activated during the peak demand period as opposed to all the heaters in the case of the conventional in-tank system. Once the off-peak period is entered, all the heaters may be reactivated while still maintaining most of the temperature gradient since the hot and cold water is essentially separated in the different reservoirs.

The thermal performance of a SIT-system is investigated through the previously mentioned simulation model. The plant specifications of the SIT-system are identical to the specifications of the previously simulated conventional in-tank heater plant. The only difference between the two is the fact that the reservoirs are connected in series rather than parallel. Table 3.3 provides a summary of the SIT-system specifications used as inputs to the simulation model.

Table 3.3: Summary of SIT-system specifications.

Heating capacity	240 kW
Heating equipment	In-tank resistance elements
Storage capacity	2 x 10 000 litre (Series connected)
Occupancy	1 150 residents
Hot-water consumption	75 litres per person per day
Temperature set-point	60 °C both tanks

The simulation is once again performed for a typical winter's day, in the Johannesburg region. The weather data is obtained from the widely used CSIR climate database. Figure 3.11 shows the simulated electrical demand profile during a typical winter's day with load shedding during the peak demand period (18:00 to 20:00). From this figure it can be seen that the entire load is not shed during the peak periods. The 'top' reservoir's resistance elements are activated during these times by the upper control thermostat. The total electricity consumed by the SIT-system for the simulated day accumulates to 4 580 kWh which is once again very close to the 4 600 kWh consumed by the conventional system. This indicates that the total energy consumed by the SIT-system and the conventional system compares very well showing that the SIT-system will not use much more or less electrical energy than the conventional system.

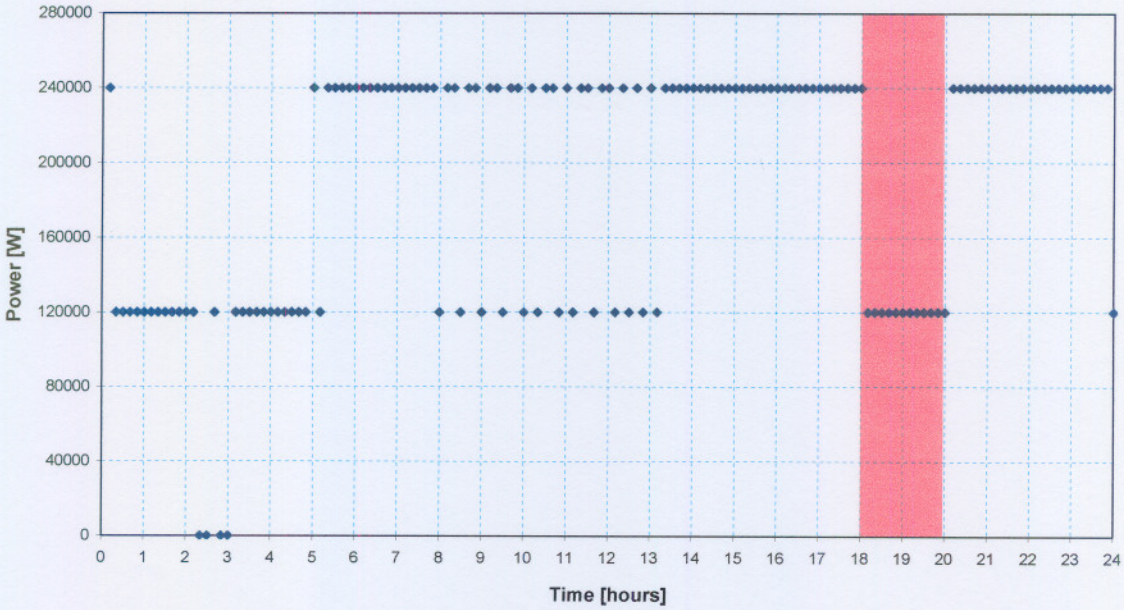

Figure 3.12: Simulated SIT-system electrical demand profile for a typical winter's day.

The simulated hot-water supply temperatures for both the conventional in-tank system and the SIT-system are shown in Figure 3.13. It can be seen from this figure that the supply temperature of the SIT-system stays near the desired hot-water temperature during peak hours. Although the power demand during peak hours is not shed entirely, the system provides sufficient hot water throughout the entire day together with a reduction in peak electricity demand. After the load shedding period all the in-tank resistance elements are switched back on. The result is a quick recovery in the top reservoir with the colder water trapped in the bottom reservoir and sufficient hot water drawn from the top reservoir.

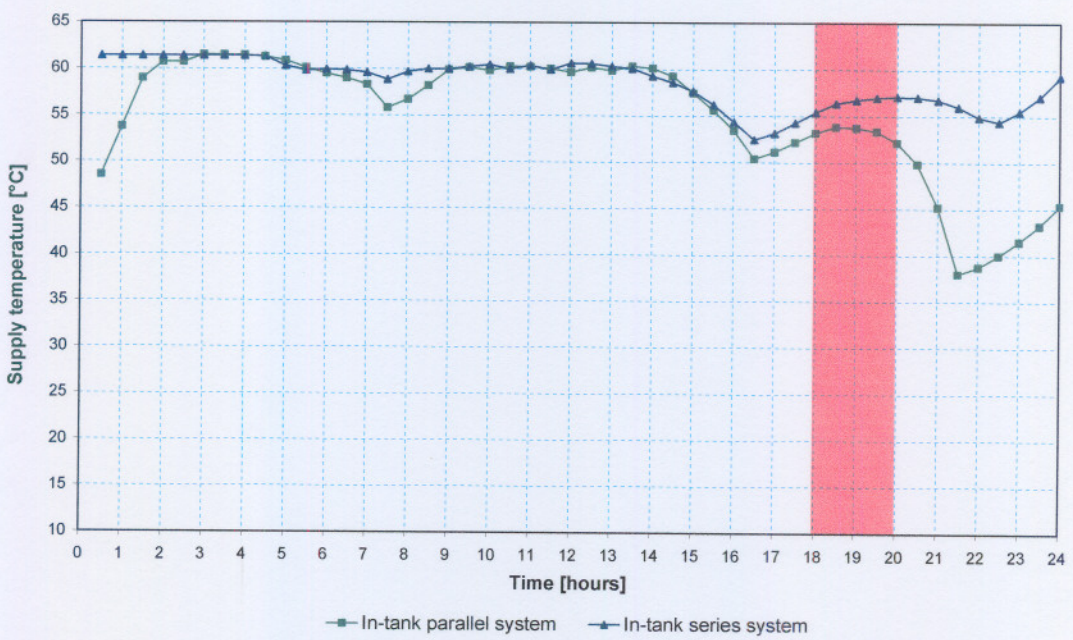

Figure 3.13: Simulated hot-water supply temperature for a typical winter's day.

The simulated vertical temperature distribution of the top reservoir from which the hot water is drawn, is shown in Figure 3.14. The temperature at the top of the reservoir is maintained close to the desired temperature throughout the day. During the load shedding period, the reservoir becomes fully mixed, due to the natural convection affect caused by the in-tank heaters which are switched on. The bottom temperature of the top reservoir drops, due to colder water entering from the bottom reservoir. This is the result of the resistance elements of the bottom reservoir being switched off during peak demand periods allowing colder water to accumulate in the bottom reservoir.

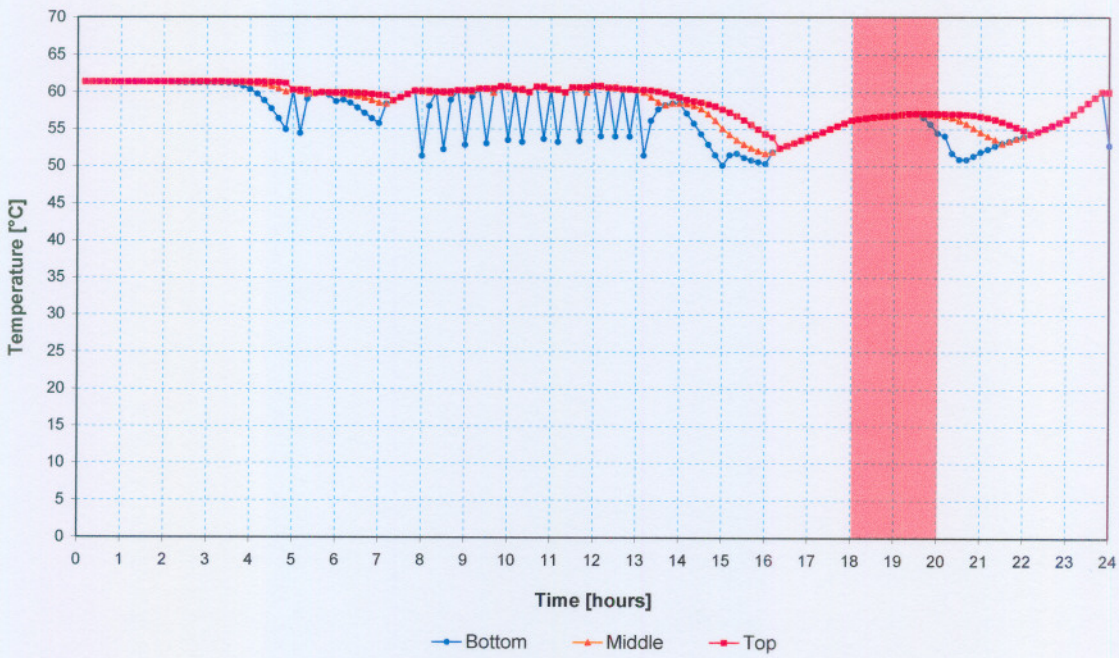

Figure 3.14: Simulated temperature distribution for the top reservoir.

Figure 3.15 shows the simulated vertical temperature distribution through the bottom reservoir, where the cold water enters the system. From this figure it is clear that the tank is fully mixed during most of the day. During the load shedding period a well-defined temperature gradient exists in the reservoir. The top temperature decreases rapidly as hot water is drawn from the top with cold water entering at the bottom during load shedding. After load shedding the resistance elements are activated and the reservoir almost instantly becomes fully mixed.

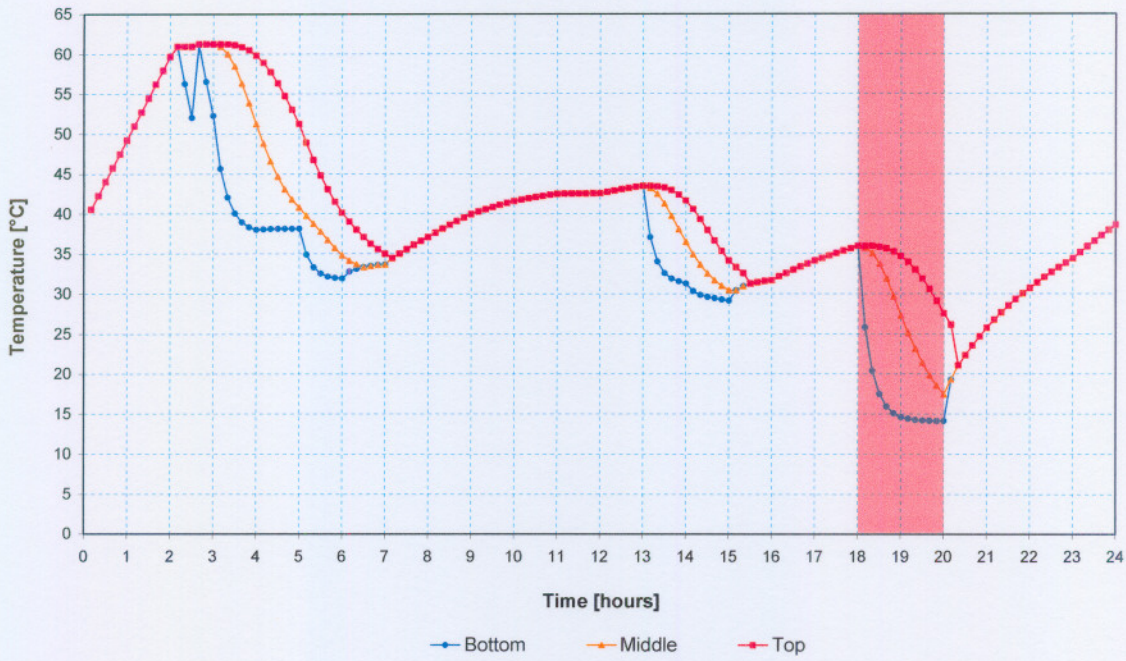

Figure 3.15: Simulated vertical temperature distribution for the bottom reservoir.

From the discussion it is clear that the SIT-technology provides a very real opportunity to realise the maximum DSM-potential, even in plants were comprehensive ILH-retrofits cannot be justified. However, it should also be clear that carefully designed and robust control is required to ensure smooth operation at all times.

3.5 Summary

This chapter investigated, via simulation, the thermal behaviour of two alternative water heating technologies developed to address the problems associated with the conventional heater design philosophy under load shedding conditions. It was found that the ILH-technology can achieve complete load shedding during peak demand periods, while still providing sufficient hot water to the building occupants at all times.

Furthermore, in plants were comprehensive ILH-retrofits are not economically viable it is clear that the SIT-technology provides a very real opportunity to realise the maximum DSM-potential. However, considering the SIT-configuration it is very important to have a carefully designed and robust control system to ensure smooth operation.

Chapter 4

EMPIRICAL INVESTIGATION

4.1 Introduction

In the previous chapter the operation of various new water heating configurations were evaluated via simulation under load shedding conditions. It was found that the newly developed, alternative water heating configurations lend themselves much better towards DSM, compared to conventional water heaters.

In order to evaluate the actual performance of the new water heating configurations under load shedding conditions, an empirical investigation is needed. This chapter presents the results obtained from an extensive empirical investigation conducted on a number of real-world water heating plants. The results obtained through the empirical investigation are also used to verify the water heating simulation model. This is done by comparing measured plant variables obtained from ten real-world water heating plants with the results obtained through the simulation model.

4.2 Real-world water heating plants

A number of real-world water heating plants are used to gather experimental data for the evaluation of the performance of the newly developed ILH-configuration under load shedding conditions. The empirical results obtained are also used to verify the simulation model developed by Rousseau *et al.* (2001) under real-world operating conditions. The plants used in the empirical investigation serve as centralised water heating systems for mine residences with each plant serving 200 to 1 000 occupants daily. All the plants are situated at a South African gold-mine in the Johannesburg region. The plants under investigation consist of two conventional in-tank (CIT) water heaters and eight ILH-systems.

Each of the plants is fitted with instruments in order to monitor the desired plant variables. In both the conventional in-tank and ILH-configurations the cold-water inlet temperature supplied from the mains as well as the temperature of the hot water supplied to the occupants is measured. These temperatures are monitored via accurate resistance thermometer devices (PT-100's) installed at the desired positions in the piping. The electrical energy consumption is measured using a 7300ION-meter installed on the electricity supply. The

water consumption is also measured using a veined wheel anemometer which provides digital pulses for every 25 litres of flow.

Figure 4.1 shows a schematic of a typical conventional in-tank configuration used in the empirical investigation. In some cases the plant may consist of more than one reservoir connected in parallel or in series with each other. In such cases the instrumentation layout stays exactly the same with the combined outlet temperature, inlet temperature and flow rate being measured. The only difference being the fact that the system might have more than one electrical heater installed, in which case the total electricity consumption of the installed heaters are measured.

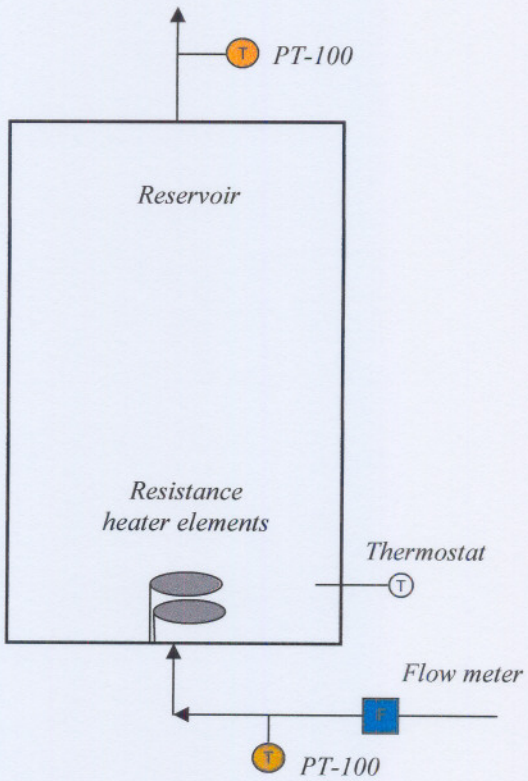

Figure 4.1: Schematic of the experimental set-up on a conventional in-tank water heater.

The instrumentation set-up on the ILH-plants is identical to that of the in-tank configuration. The only difference being the fact that the temperature distribution through the system is also monitored. This is done by installing three more PT-100's at different positions on the reservoirs. The first PT-100 is installed at the bottom of the 'bottom' reservoir; the second is installed close to the middle of the system, typically at the top of the 'bottom' reservoir assuming the system consists of two reservoirs; and the third PT-100 is installed at the top

of the 'top' reservoir near the hot-water outlet. Figure 4.2 shows a schematic of the instrumentation set-up of a typical ILH-system consisting of two reservoirs.

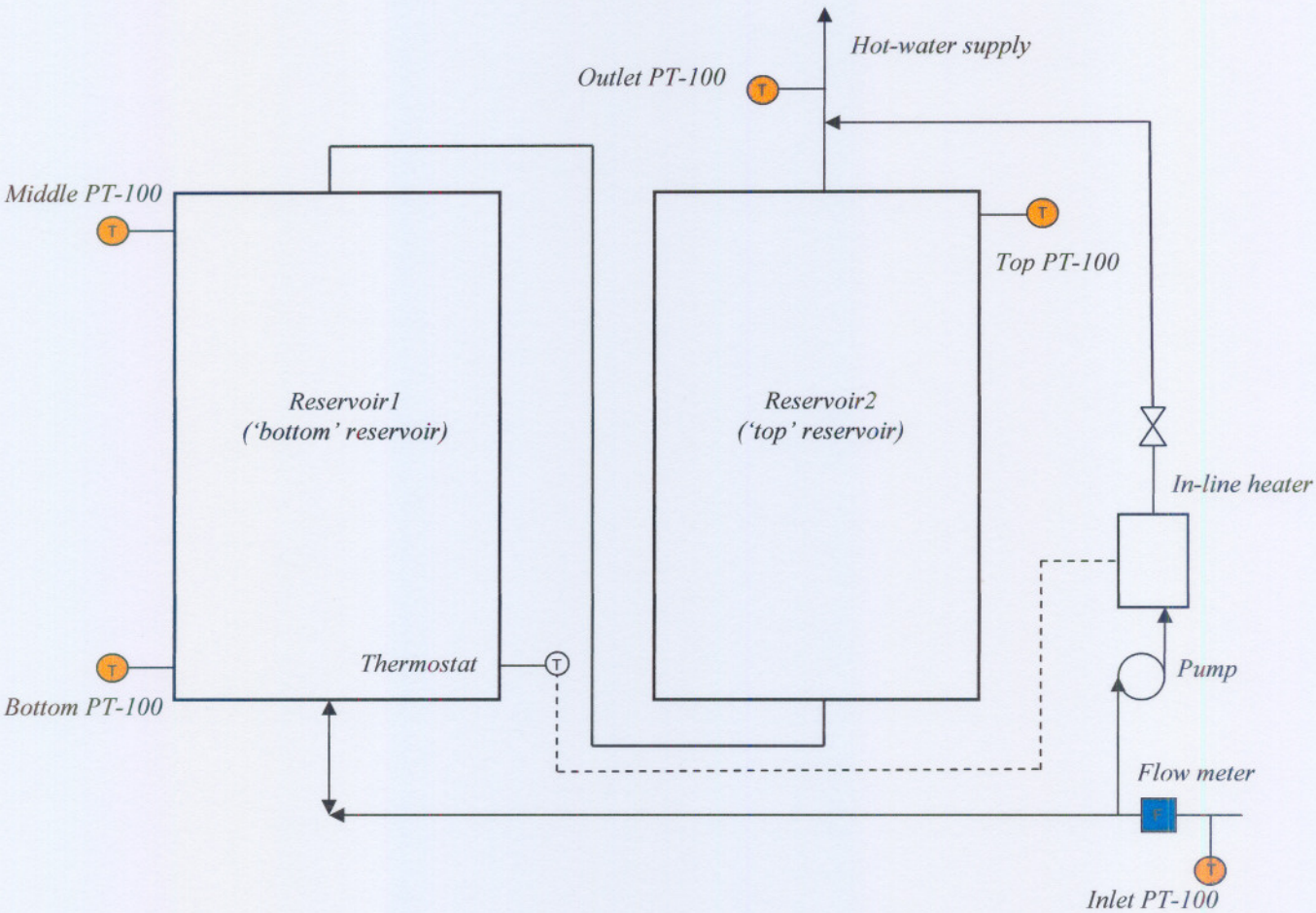

Figure 4.2: Schematic of typical experimental set-up of an ILH-configuration.

In the case where only one reservoir exists in an ILH-system the bottom, middle and top temperature sensors are installed at the bottom, middle and top respectively of the single reservoir.

4.3 Verification of simulation model

4.3.1 Calculation of standing losses

In order to obtain good correlations between the measured and simulated plant variables the standing heat losses suffered by the system to the environment should be determined. The main source of heat losses from the system is the reservoir surfaces. Although the reservoirs are well-insulated, the large heat transfer areas of the reservoirs cause heat to be lost to the surroundings, which are at a lower temperature than the reservoir surfaces. Another source

of heat loss is the pipe network supplying the occupants with hot water. Although most of the pipe network is usually insulated, the piping which feed the hot water to the occupants can be quite long in some cases resulting in notable heat losses from these pipes.

In order to calculate the exact heat loss of the entire system to the surroundings, a detailed heat transfer model could be used. However, this approach requires the real-time temperature of the surroundings to which the reservoirs as well as the pipe network are exposed. This creates a problem since the temperature inside the plant rooms, in which the reservoirs are situated, is not measured. An inaccurate temperature would affect the accuracy of the heat loss calculations directly since the heat loss is based on the temperature difference between the hot water in the reservoirs, or pipes, and the surroundings.

An alternative approach for calculating the heat losses from the system is to reduce the heat loss resistance network to a simple network with only one effective resistance value. This resistance value is based on an effective heat loss factor taking into account the losses suffered by the system as a whole. The value of the effective heat loss factor is determined by comparing experimental results for the heat losses of a series of days with the heat losses predicted by the simulation model. By comparing the heat losses suffered by a real-world plant with the simulated heat losses for the exact same plant, the effective heat loss factor can be determined by conducting a parametric study.

Figure 4.3 shows a schematic of the electrical analogue network representing the heat losses from the reservoir to the surroundings (Rousseau *et al.*, 2001). T_i represents the temperature of the water inside the reservoir at node *i*. Heat losses or gains through the reservoir wall are represented by the current flowing through R_{ii}, R_{li} *and* R_{oi}. These resistances represent the inside convective resistance, the wall, lagging and cladding material resistances and the outside convective resistances, respectively.

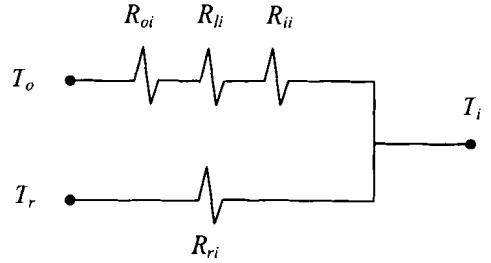

Figure 4.3: Schematic illustration of the electrical analogue network.

The reservoir wall is assumed to be a large flat plate and therefore the resistances are calculated as follows:

$$R_{ii} = \frac{1}{h_i A_{ii}} \tag{1}$$

$$R_{li} = \frac{x_w}{k_w A_{wi}} + \frac{x_l}{k_l A_{li}} + \frac{x_c}{k_c A_{ci}} \tag{2}$$

and

$$R_{oi} = \frac{1}{h_o A_{oi}}. \tag{3}$$

h_i and h_o are the internal and external convective heat transfer coefficients, respectively, with A_{ii} and A_{oi} the inside and outside surface areas. x_w, k_w and A_{wi} are the thickness, thermal conductivity and average heat transfer area of the reservoir wall, respectively. The subscripts l and c indicate the corresponding quantities for the lagging and cladding. T_o represents the outdoor temperature.

T_r in Figure 4.3 is the water temperature of the return flow from the load if a ring-main return pipe is present, and the resistance R_{ri} is added to allow for return flow if present at that node. R_{ri} is calculated as:

$$R_{ri} = \frac{1}{\dot{m}_{ri} c_p} \tag{4}$$

with $\dot{m}_{ri}$ the magnitude of the return flow at the node i. If no return flow is present at node i, then

$$R_{ri} = \infty. \tag{5}$$

In order to reduce the network shown in Figure 4.3 the following assumptions are made:

$$R_{ii} = \frac{1}{\infty} = 0 \tag{6}$$

$$R_{oi} = \frac{1}{\infty} = 0 \tag{7}$$

$$R_{li} = \frac{x_i}{k_i A_{oi}} \tag{8}$$

with x_i and k_i the effective thickness and thermal conductivity of the combined reservoir shell at node i. Replacing x_i and k_i with a combined value, we have that:

$$\frac{x_i}{k_i} = \frac{1}{k_{eff}} \tag{9}$$

with k_{eff} the effective heat loss factor for the system. Thus:

$$R_{li} = \frac{1}{k_{eff} A_{oi}} \tag{10}$$

and assuming no return flow,

$$R_{ri} = \infty . \tag{11}$$

All of the resistances can now be replaced by an effective resistance (R_{eff}) representing the total resistance at node i:

$$R_{eff} = \frac{1}{k_{eff} A_{oi}} \tag{12}$$

This reduces the network shown in Figure 4.3 to the network shown in Figure 4.4. T_i is the water temperature of node i with T_o an ambient temperature obtained from the widely used CSIR climate database. The database provides ambient temperatures for different regions of South Africa for each hour of every day of the year based on historical data of a specific region. The simulation model uses this database to obtain the typical ambient temperature to which the plant is subjected at a specific time of the day.

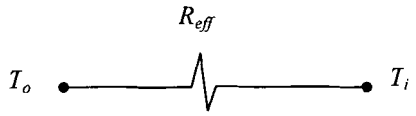

Figure 4.4: Reduced electrical analogue network.

The heat loss suffered by the system at node i can now be calculated as:

$$Q_{losses} = \frac{T_i - T_o}{R_{eff}} \tag{13}$$

From the definition of the heat loss (Q_{losses}) suffered by the system it is clear that although the value of the effective resistance (R_{eff}) is a constant, the heat loss remains a function of the ambient temperature as well as the water temperature at node i. Therefore, the simulation model calculates the heat loss at each node of the reservoir taking into account the ambient temperature obtained via the climate database as well as the water temperature inside the reservoir at each node for the specific time of the day. Although the value of the ambient temperature obtained via the climate database could differ from the actual temperature which the system is exposed to, R_{eff} can be adjusted to correct this difference by changing the value of k_{eff}.

In order to obtain the correct value for k_{eff}, a parametric study is conducted in which the standing heat losses suffered by a number of real-world plants are compared with the heat losses predicted by the simulation model for the exact same plants. In each case k_{eff} is adjusted until a good correlation between the measured and simulated heat losses is obtained.

4.3.2 Empirical results

The standing heat losses of a number of real-world water heating plants are used to determine the typical value of k_{eff} for centralised water heating systems. First of all the standing heat losses suffered by a conventional in-tank water heating plant are investigated. The plant is monitored for a period of 26 consecutive days in order to obtain a quasi-steady state representation of the plant operation. The standing heat losses suffered by the system are given by the difference between the total energy input to the system and the total energy output from the system over the 26-day period. The energy input to the system can be readily obtained by using the measured electricity consumption of the plant over the 26-day period. E_{in} is calculated as:

$$E_{in} = \sum 3.6 E_{elec} \tag{14}$$

with E_{in} the total energy input expressed in MJ over the 26-day period and E_{elec} the electricity consumption expressed in kWh for each half-hour during the 26-day period.

The energy withdrawn from the system can be calculated using the measured inlet temperature, outlet temperature and the water flow rate through the system. The energy withdrawn from the system over the 26-day period is calculated by using the following equation:

$$E_{out} = \sum \frac{m_w c_p (T_{out} - T_{in})}{1000} \tag{15}$$

with m_w the mass of the water leaving the system during each half-hour interval. T_{out} and T_{in} are the average outlet temperature and average inlet temperature measured over half-hour intervals, respectively.

Table 4.1 provides a summary of the real-world plant specifications of the conventional in-tank water heating system under investigation.

Table 4.1: Summary of conventional in-tank system specifications.

Heating capacity	82 kW
Heating equipment	In-tank resistance elements
Storage capacity	1 x 5 000 litre (Vertically mounted)

The thermal behaviour of the plant is simulated using the simulation model discussed in Chapter 2, with the heat loss model adapted to reflect the heat loss model as discussed in paragraph 4.3.1. The value of k_{eff} is adjusted between 2 and 8 W/m^{2}K. Figure 4.5 shows the results obtained with k_{eff} set to 6 W/m^{2}K. It can be seen from this figure that the measured and simulated energy input as well as the energy output compares well with each other.

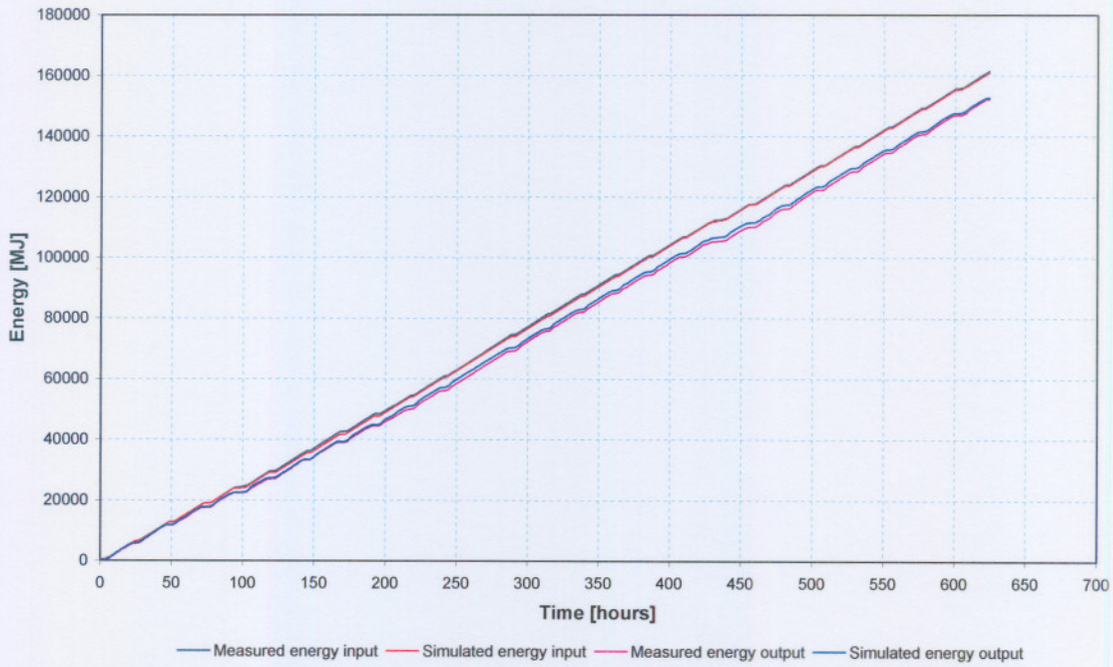

Figure 4.5: Measured and simulated energy input and output.

The measured amount of energy provided to the system via the electricity supply adds up to 161 453 MJ with the measured energy withdrawn from the system accumulating to 152 279 MJ. The energy input being 9 174 MJ more than the energy withdrawn from the system. This indicates that 5.7% of the electrical energy consumed by the system is lost to the environment via standing heat losses.

The amount of standing heat losses is also calculated using the simulation model with a number of different values for k_{eff}. Table 4.2 provides a summary of the results obtained for four different values of k_{eff}.

Table 4.2: Summary of simulation results for a number of effective loss coefficients.

k [W/m^{2}K]	E_{in} [MJ]	E_{out} [MJ]	Losses [%]
2	159 161	156 546	1.6
4	160 097	154 717	3.4
6	160 884	152 760	5.1
8	162 016	151 231	6.7

It is clear from Table 4.2 that when k_{eff} is equal to 6 W/m^{2}K the measured losses of 5.7% compare well with the simulated losses of 5.1%.

The same procedure is followed to calculate the standing heat losses suffered by an ILH-system over a 21-day period. Table 4.3 provides a summary of the ILH-system specifications used for the investigation.

Table 4.3: Summary of ILH-system specifications.

Heating capacity	106 kW
Heating equipment	In-line resistance elements
Storage capacity	1 x 5 000 litre (Vertically mounted)

Figure 4.6 shows the results obtained with k_{eff} equal to 6 W/m^{2}K for the ILH system. It can be seen from this figure that the measured and simulated energy input as well as the energy output compares well with each other.

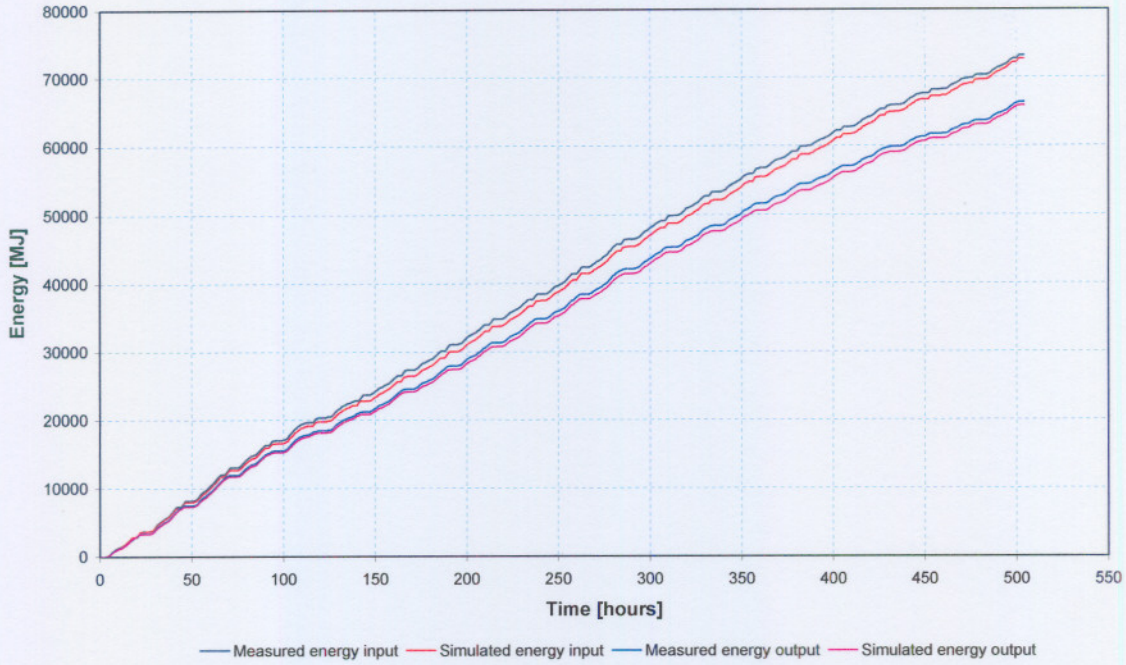

Figure 4.6: Measured and simulated energy input and output.

The amount of energy provided to the system via the electricity supply adds up to 73 235 MJ with the energy withdrawn from the system via the supplied hot water adding up to 66 348 MJ. The energy input being 6 887 MJ more than the energy withdrawn from the system. This indicates that 9.4% of the electrical energy consumed by the system is lost due to standing heat losses to the environment. The amount of standing heat losses is once again calculated using the simulation model with different values for k_{eff}. Table 4.4 provides a summary of the results obtained for four different values of k_{eff}.

Table 4.4: Summary of simulation results for a number of effective loss coefficients.

k [W/m^{2}K]	E_{in} [MJ]	E_{out} [MJ]	Losses [%]
2	70 214	66 449	5.4
4	71 486	66 118	7.5
6	72 695	65 856	9.4
8	73 776	65 590	11.1

It is once again clear from Table 4.4 that when k_{eff} is equal to 6 W/m^{2}K the measured losses of 9.4% compare very well with the simulated losses of 9.4% as in the case of the conventional in-tank system.

In order to verify the results obtained for the above-mentioned water heating systems, the standing heat losses for a number of additional plants are investigated under different operating conditions. The results obtained from these investigations also suggest that an effective loss factor of 6 W/m^2K provides satisfactory results. The results obtained for the additional plants are available in Appendix A.

Considering the results obtained for the different water heating systems, it can be assumed that an effective loss factor of 6 W/m^2K provides a typical value for centralised water heating systems. Therefore, k_{eff} will be set as 6 W/m^2K for all of the following simulations presented in the rest of this chapter.

4.4 Empirical investigation of water heating plants

To be able to evaluate the performance of the newly developed ILH water heating configuration data is gathered on a number of real-world water heating plants. The performances of two conventional in-tank water heating systems are investigated after which the performances of eight ILH-plants are investigated. The data gathered on the above-mentioned plants is also used to verify the simulation model. This is done by simulating a typical day of operation for each plant and comparing the measured variables with the same variables as predicted by the simulation model.

When comparing the measured and simulated results for the verification of the simulation model, the performance numbers of Kleinbach *et al.* (1993) are employed and compared with that reported in the reference.

The first performance number (QD) defined by Kleinbach *et al.* (1993) is a measure of the simulation model's ability to correctly predict the temperature of the water at the top of the reservoir. QD is defined as:

$$QD = \frac{Q_{del,sim} - Q_{del,exp}}{Q_{del,exp}} \tag{15}$$

with

$$Q_{del} = \int_{day} \dot{m}_{del} c_p (t_s - t_c) dt. \tag{16}$$

$\dot{m}_{del}$ is the mass flow rate of the hot water delivered to the users, c_p is the specific heat capacity of water, t_s is the temperature of the water actually supplied to the users and t_c is the temperature of the cold feed water taken from the supply mains. The subscripts 'sim' and 'exp' refer to the simulated and experimentally determined results, respectively.

The second performance number (QI) defined by Kleinbach *et al.* (1993) is a measure of the simulation model's ability to correctly predict the temperature of the water returned to the inlet side of the in-line heater i.e. the temperature at the bottom of the reservoir. QI is defined as:

$$QI = \frac{Q_{in,sim} - Q_{in,exp}}{Q_{in,exp}} \tag{17}$$

with

$$Q_{in} = \int_{day} \dot{m}_{heat} c_p (t_w - t_i) dt. \tag{18}$$

$\dot{m}_{heat}$ is the mass flow rate of the hot water through the in-line heater while t_w and t_i are the temperatures of the water leaving at the hot outlet and cold inlet of the in-line heater, respectively. QI cannot be evaluated for the in-tank configuration since the heater is not situated outside the reservoir and does not have its own well-defined flow rate, inlet and outlet temperatures. In this case QI can also not be evaluated for the ILH-configuration since the inlet and outlet temperatures of the ILH are not measured at all. However, considering the definition of QI it can be seen that Q_{in} actually represents the heat which is put into the system, hence the electrical power. Thus, QI is actually a measure which compares the actual energy input of the system with the simulated energy input. This can be obtained through the measured electricity consumption together with the simulated electricity consumption. QI can therefore be replaced by an equivalent performance number (QE) which is a measure of the simulation model's ability to correctly predict the energy consumption of the resistance elements situated inside or in parallel with the reservoir. QE can be evaluated for both the in-tank and ILH-configurations. QE is defined as:

$$QE = \frac{E_{in,sim} - E_{in,exp}}{E_{in,exp}} \tag{19}$$

with

$$E_{in(sim,\exp)} = \int_{day} \mathrm{P}dt. \qquad (20)$$

P is the power drawn from the electricity supply expressed in kW. QD and QE can now be used as criteria to quantify the accuracy of the simulation model in simulating a number of real-world water heating plants.

The following sections present extensive results obtained from an empirical investigation conducted under different operating conditions on each of the plants mentioned earlier.

4.4.1 Plant no.1

The first plant is a conventional in-tank water heating system with a single, vertically mounted reservoir. The plant has a heating capacity of 82 kW with a storage capacity of 5 000 litres serving approximately 350 occupants daily. The plant operation is monitored over a number of days by measuring the cold-water supply temperature, the hot-water temperature supplied to the occupants as well as the flow rate and electricity consumption as discussed in section 4.2. A typical day representing the typical operation of the plant is selected. This day is also simulated by using the water heating simulation software under the exact same operating conditions in order to evaluate the accuracy of the simulation model.

Since the initial conditions of the real system, e.g. the average temperature inside the reservoir, are unknown the simulation is run for a series of consecutive days to obtain a quasi-steady state solution before simulating the selected day. This is done by running the simulation model for a number of pre-days. These pre-days consist of the actual operating conditions of a number of days before the selected day. In doing this before the selected day is simulated, the initial conditions at the start of the day under investigation should be very close to the actual conditions in the system. The specific day which is selected is 1 July, 2004. This day represents a typical winter's day during which the plant is highly utilised. Table 4.5 provides a summary of the plant specifications and operation during the selected day.

Table 4.5: Summary of plant specifications.

Heating capacity	82 kW
Heating equipment	In-tank resistance elements
Storage capacity	1 x 5 000 litre (Vertically mounted)
Typical occupancy	± 350
Hot-water consumption	49 225 litres
Temperature set-point	80 °C

Figure 4.7 shows the measured as well as the simulated hot-water supply temperature during the selected day. It can be seen from this figure that the measured hot-water supply temperature does not coincide with the simulated hot-water supply temperature during the first few hours of the day. This is due to the fact that there is very little mass flow through the system between the hours of 00:00 and 03:30. This causes the water, situated in the outlet pipe in the vicinity of the outlet temperature sensor, to cool down due to heat loss to the surroundings. After this period more water is consumed by the occupants resulting in hot water from the reservoir flowing past the temperature sensor. From 04:30 up to the end of the day, the measured hot-water supply temperature compares very well with the simulated hot-water supply temperature.

The average hot-water supply temperature for the selected day is found to be around 46 °C with the set-point of the thermostat at 80 °C. This indicates that the plant is over utilised since the outlet temperature rarely reaches the set-point value.

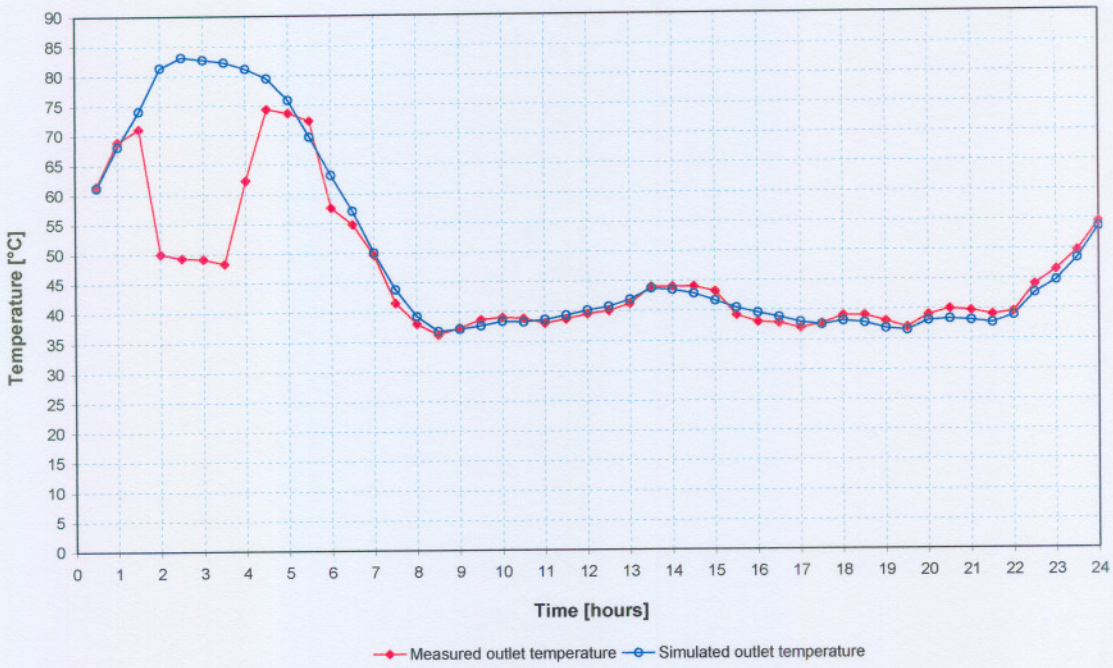

Figure 4.7: Measured and simulated hot-water supply temperatures for selected day.

Figure 4.8 shows the half-hourly hot-water consumption profile of the selected day. It can be seen that there are no distinct peaks in the consumption during the day, indicating an overall high consumption during most of the day.

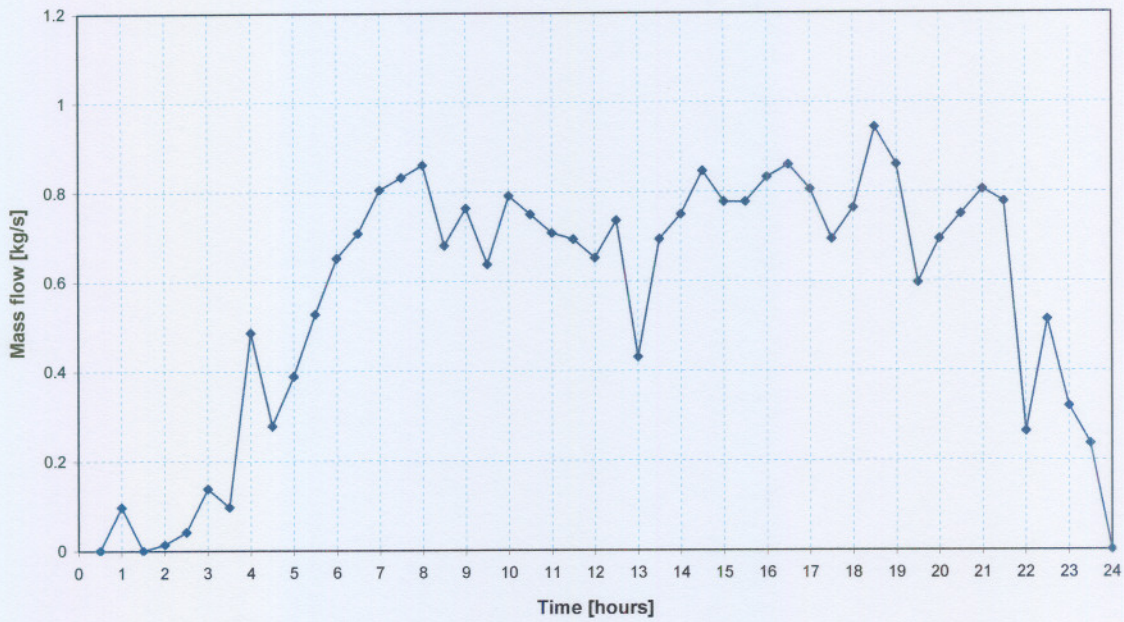

Figure 4.8: Measured hot-water consumption profile.

The measured and simulated electricity demand is shown by Figure 4.9. It can be seen that the plant operates at full capacity during most of the day indicating that the temperature of the water inside the reservoir rarely reaches the thermostat set-point. Note that the measured electricity demand compares very well with the simulated electricity demand during the entire day. The plant consumes a total of 1 779 kWh measured during the day with the simulated electricity consumption adding up to 1 831 kWh.

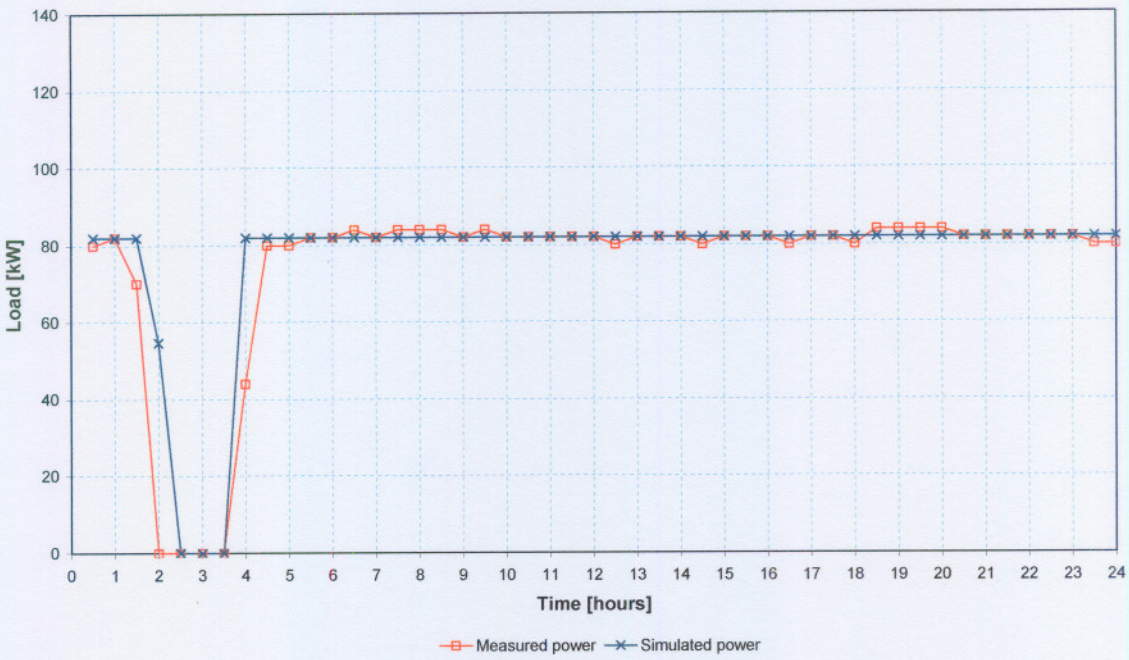

Figure 4.9: Measured and simulated electricity demand profile for selected day.

The performance number QD is found to be 0.055 indicating a 5.5% difference between the measured and simulated outlet temperature over the entire day. QE is found to be 0.029 indicating a 2.9% difference between the measured and simulated electricity consumption.

4.4.2 Plant no.2

The second of the conventional in-tank water heating plants has a heating capacity of 142 kW consisting of two in-tank heaters of 71 kW each. The storage capacity is 8 200 litres in the form of two equally sized, vertically mounted reservoirs connected in series. The plant serves approximately 450 occupants daily. A typical day representing the typical operation of the plant is once again selected. The selected day is used to evaluate the performance of the plant as well as the accuracy of the simulation model. Table 4.6 provides a summary of the plant specifications and operation during the selected day.

Table 4.6: Summary of plant specifications.

Heating capacity	142 kW
Heating equipment	In-tank resistance elements
Storage capacity	2 x 4 100 litre (Vertically mounted)
Temperature set-point	76°C for both reservoirs
Typical occupancy	± 450
Hot-water consumption	31 500 litres
Date of selected day	5 May 2004

Figure 4.10 shows the water consumption profile for the selected day together with the measured and simulated hot-water outlet temperatures. It can be seen from this figure that there exists a distinct peak in the consumption between 14:00 and 15:00. This can also be seen in the behaviour of the outlet temperature which drops slightly during this period. The measured and simulated output temperatures compare well with each other. The measured outlet temperature drops substantially at the end of the day, due to the fact that there is almost no flow during this time, allowing the water in the vicinity of the outlet temperature sensor to cool down.

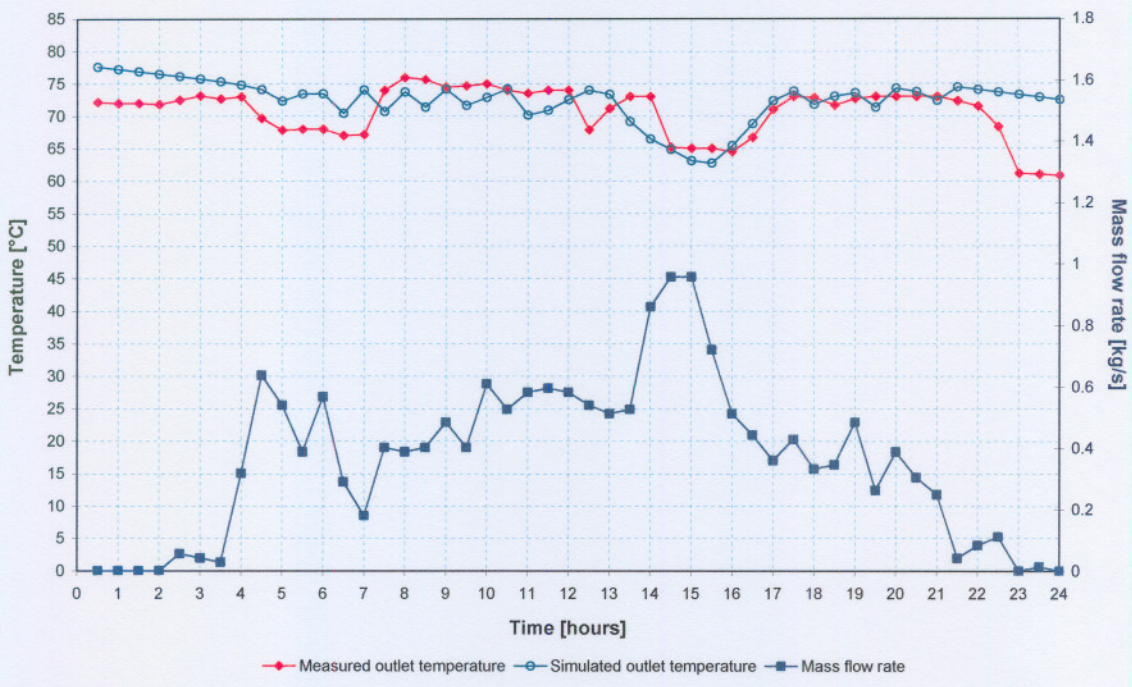

Figure 4.10: Water consumption profile together with measured and simulated hot-water supply temperatures for the selected day.

The measured and simulated electricity demand is shown by Figure 4.11. It can be seen that the plant is highly utilised with the electrical heaters only switching off during the hours of 22:00 to 04:00. The plant consumes a total of 1 859 kWh measured during the day with the simulated electricity consumption accumulating to 2 000 kWh. The measured electricity demand compares well with the simulated electricity demand during the entire day.

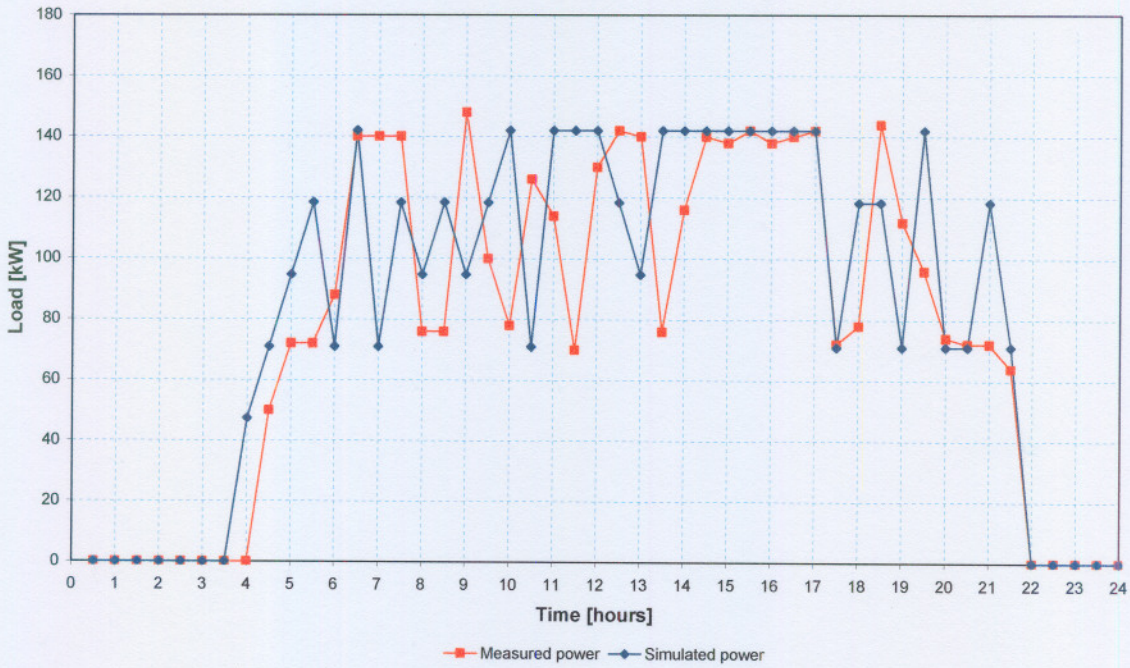

Figure 4.11: Measured and simulated electricity demand profile for the selected day.

The performance number QD is found to be 0.029 indicating a 2.9% difference between the measured and simulated outlet temperature over the entire day. QE is found to be 0.076 indicating a 7.6% difference between the measured and simulated electricity consumption.

4.4.3 Plant no.3

The third plant under investigation consists of an ILH with a heating capacity of 230 kW and storage capacity of 20 000 litres in the form of two 10 000 litre reservoirs connected in series. The only difference in the operation between this plant and the above-mentioned conventional in-tank plants is the fact that the entire load is now shed during the peak demand period (18:00 to 20:00). Table 4.7 provides a summary of the plant specifications and operation during the selected day of operation.

Table 4.7: Summary of plant specifications.

Heating capacity	230 kW
Heating equipment	In-line heater
Storage capacity	2 x 10 000 litre (Vertically mounted)
ILH-temperature set-point	51 °C
Typical occupancy	± 1 000
Hot-water consumption	78 050 litres
Date of selected day	4 November 2004

The measured hot-water consumption profile together with the measured and simulated hot-water supply temperatures is shown in Figure 4.12. It can be seen from the consumption profile that no distinct peaks exist in the hot-water consumption during the day suggesting a highly utilised plant.

The measured outlet temperature remains above 48 °C for the entire day of operation with the ILH set-point at 51 °C. Even with the full load shed during the load shedding period (18:00 to 20:00) the outlet temperature never drops below 48 °C. The water consumption during the load shedding period accumulates to 8 300 litres representing 42% of the total storage capacity. This indicates that a large percentage of the 'bottom' reservoir is filled with cold water at the end of the load shedding period with the 'top' reservoir expected to be filled with hot water due to stratification.

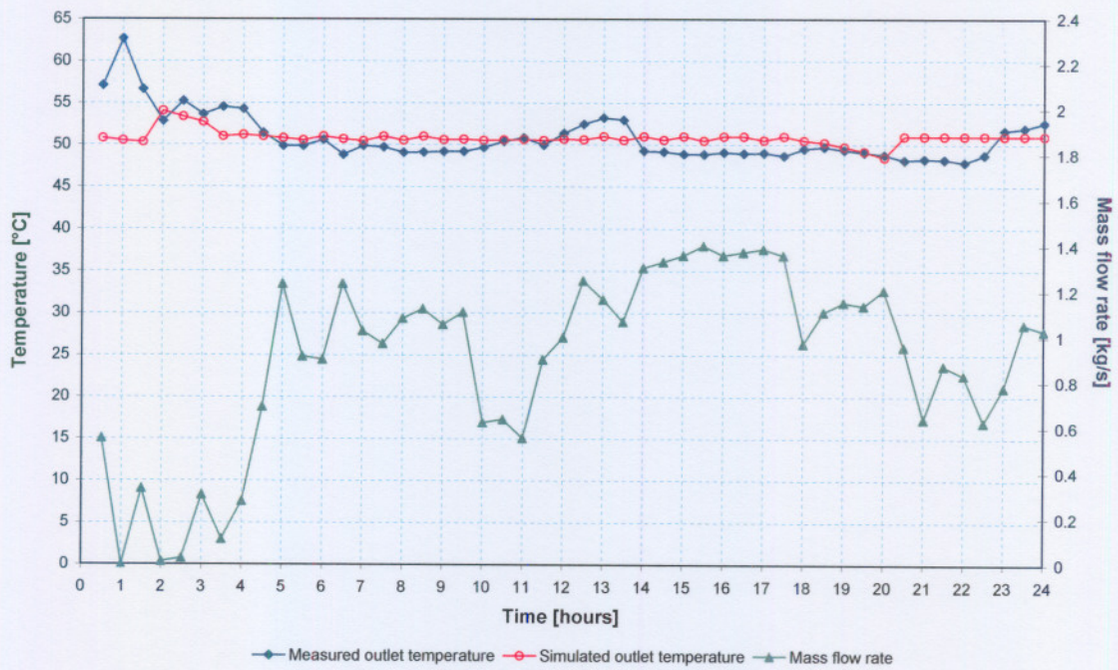

Figure 4.12: Water consumption profile together with measured and simulated hot-water supply temperatures for the selected day.

The simulated outlet temperature compares well with the measured outlet temperature over the entire day. The minimum outlet temperature measured during the load shedding period is found to be 48.8 °C compared to 48.5 °C predicted by the simulation model.

The measured and simulated temperatures near the top of the 'top' reservoir are shown in Figure 4.13. The temperature at the top of the reservoir remains above 47 °C throughout the entire day. This can be expected since the ILH supplies water to the top of this reservoir at a temperature close to the ILH set-point.

The simulated top temperature compares very well with the measured top temperature except for a slight deviation after the load shedding period. This is due to the fact that the timer employed on the actual plant to control the ILH during the peak demand period is slightly delayed in switching the ILH back on after the peak demand period. Therefore, the simulated outlet temperature recovers more rapidly after the load shedding period than the actual measured temperature.

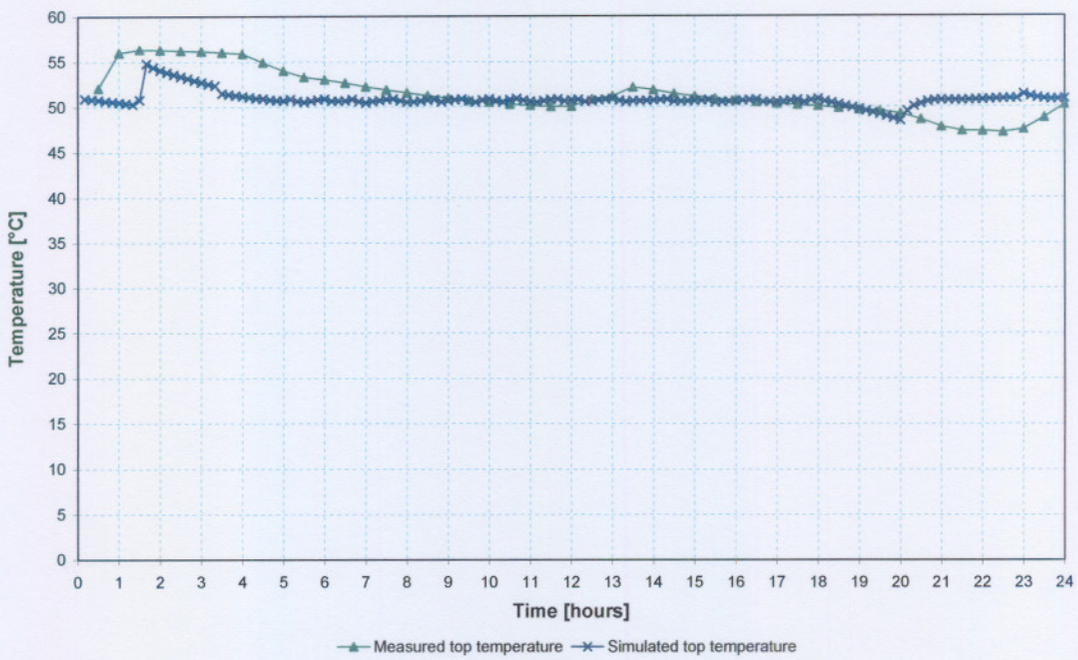

Figure 4.13: Measured and simulated temperature at the top of the 'top' reservoir.

The middle temperature of the reservoir system is also measured with the aid of the 'middle' PT-100 situated at the top of the 'bottom' reservoir. Figure 4.14 shows the measured middle temperature together with the simulated middle temperature. Note that both the measured and simulated middle temperatures drop substantially during the peak demand period (18:00

to 20:00). This is due to the fact that when the ILH is switched off, cold water enters the system at the bottom of the 'bottom' reservoir. Considering that 8 300 litres of water is consumed during the peak demand period, the largest percentage of the 'bottom' reservoir is filled with cold water. This results in a drop in the middle temperature during the peak demand period.

The temperature reached by the middle temperature at the end of the load shedding period is measured as 22.1 °C compared to the top temperature reaching a temperature of 49.3 °C at exactly the same time. This indicates the high degree of stratification achieved by the reservoir system.

The simulated temperature drop experienced during the peak demand period occurs slightly earlier than the measured temperature drop. This indicates that the simulation model predicts the outlet temperature quite conservatively. A possible reason for the conservativeness of the simulation model could be the relatively large time-step of ten minutes between calculations used by the simulation model. A smaller time-step could result in better results.

Another reason for the slight deviation could be due to the fact that the stratification achieved in the actual system is slightly better than predicted by the simulation model. The stratification effect of the simulation model can be improved by increasing the number of increments in which the reservoir is divided during simulation. This would result in more layers of water with different temperatures in the reservoir, hence less mixing and resulting in improved stratification. Improved stratification would insure the availability of more hot water at the top of the reservoir for a longer period during load shedding. At present the reservoir is divided into 21 increments in comparison with 11 increments used by Rousseau *et al.* (2001) during the experimental verification of the simulation model.

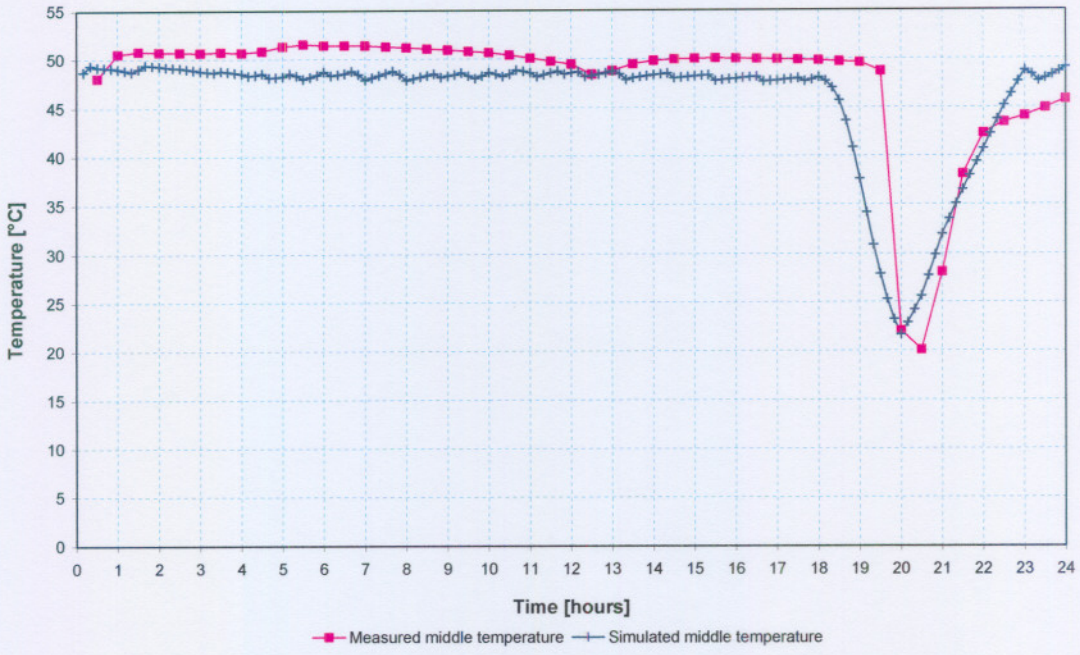

Figure 4.14: Measured and simulated temperature at the top of the 'bottom' reservoir.

The temperature at the 'bottom' of the system is measured by the PT-100 installed near the bottom of the 'bottom' reservoir. Figure 4.15 shows the measured temperature versus the simulated temperature near the bottom of this reservoir. The bottom temperature stays relatively constant throughout the day with a substantial drop in temperature occurring during the load shedding period. As soon as the ILH is switched back on the bottom temperature starts to recover, reaching a temperature of 42.3 °C three hours after the load has been reactivated.

The simulated bottom temperature compares well with the measured temperature. The oscillation effect seen in the simulated bottom temperature is due to the fact that the thermostat controlling the ILH during off-peak periods is situated near the bottom temperature sensor. Whenever the temperature at the bottom of the reservoir is lower than the thermostat set-point, the ILH is switched on fully. This results in hot water being pushed downwards from the top of the reservoir increasing the temperature at the bottom temperature sensor. As soon as the ILH is switched off by the thermostat, cold water is allowed to flow upwards through the reservoir, lowering the temperature at the bottom temperature sensor, hence the oscillating effect. This oscillating effect is not seen in the measured data since the measured temperature is not an instantaneous measurement but an average value logged over a 30-minute interval. In the case of the simulation the temperature is predicted every ten minutes.

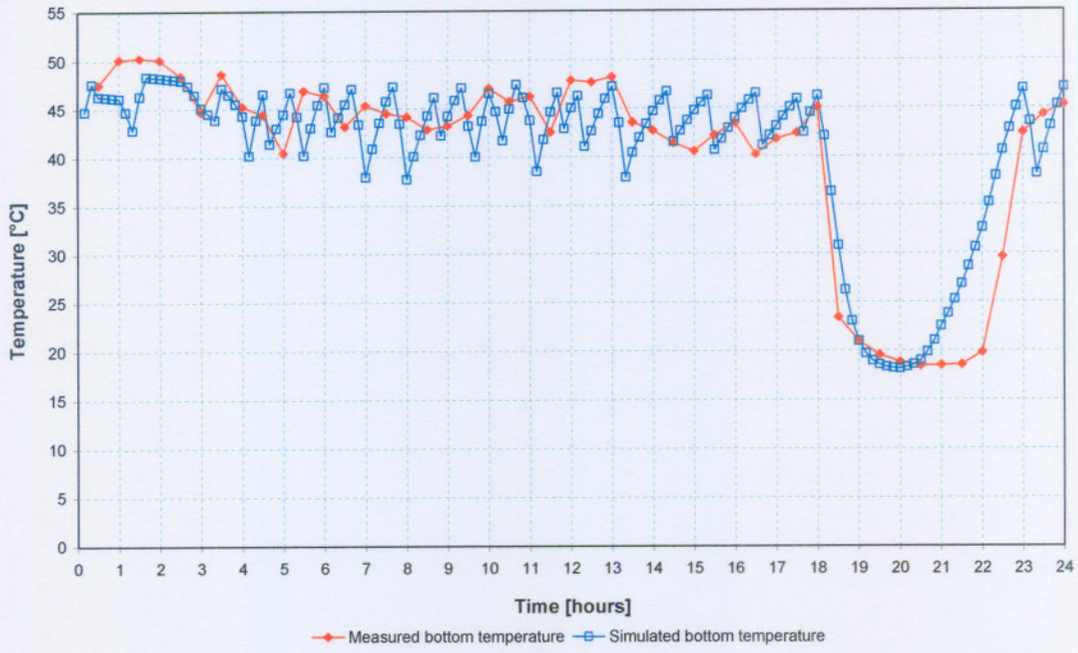

Figure 4.15: Measured and simulated temperatures near the bottom of the 'bottom' reservoir.

Figure 4.16 compares the measured and simulated electricity demand profile for the selected day. It can be seen from this figure that the measured electricity demand compares well with the simulated electricity demand. The full load is shed during the peak demand period (18:00 to 20:00) for both the measured as well as the simulated electricity demand. The measured electricity consumption added up to 3 264 kWh during the day compared to 3 297 kWh predicted by the simulation model.

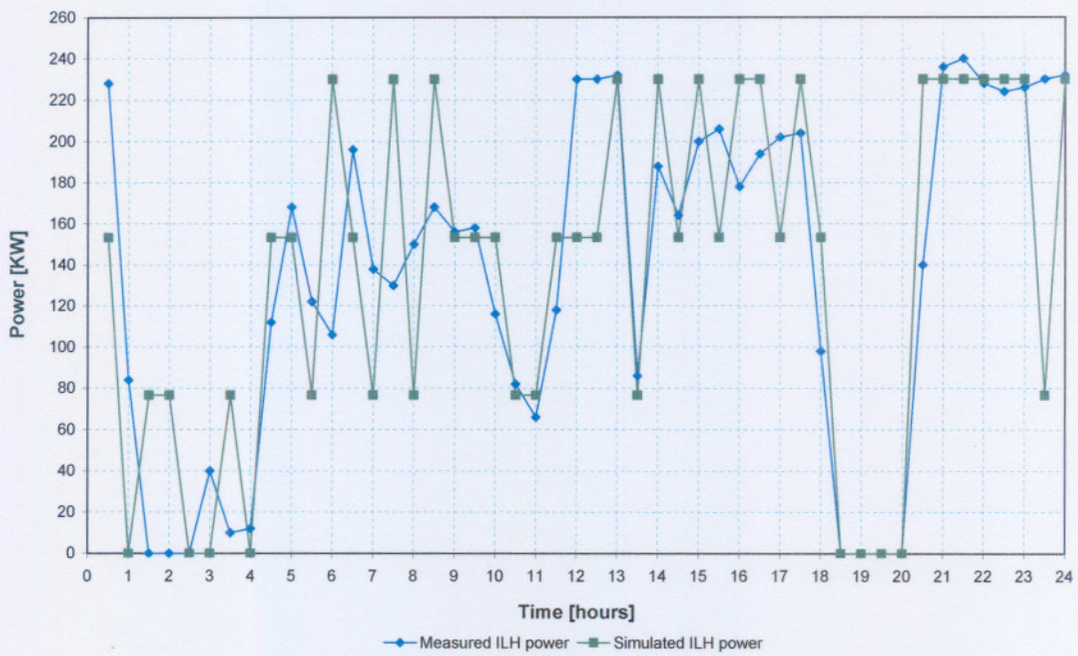

Figure 4.16: Measured and simulated electricity demand profile for the selected day.

The difference between the measured and simulated outlet temperatures over the entire day is quantified using the performance number QD. QD is found to be -0.009 indicating a 0.9% difference between the measured and simulated outlet temperatures. QE is employed to quantify the difference between the measured and simulated electricity consumption. QE is found to be 0.01 indicating a 1.0% difference between the measured and simulated electricity consumption.

4.4.4 Plant no.4

The fourth plant which is also the second of the ILH-plants consists of an ILH with a heating capacity of 154 kW and storage capacity of 8 200 litres in the form of two 4 100 litre reservoirs connected in series. Table 4.8 provides a summary of the plant specifications and operation during the selected day of operation.

Table 4.8: Summary of plant specifications.

Heating capacity	154 kW
Heating equipment	In-line heater
Storage capacity	2 x 4 100 litre (Vertically mounted)
ILH-temperature set-point	51 °C
Typical occupancy	± 500
Hot-water consumption	45 100 litres
Date of selected day	22 October 2004

The measured water consumption profile together with the measured and simulated hot-water supply temperatures is shown in Figure 4.17. Two distinct peaks are noticed in the hot-water consumption profile. The first peak occurs between the hours of 05:00 and 06:00 in the morning with the second peak occurring between 15:00 and 16:00 in the afternoon.

It can be seen from the figure that the measured outlet temperature remains very close to the ILH-temperature set-point of 51 °C. The measured outlet temperature supplied to the occupants merely drops during the peak demand period (18:00 to 20:00) although the entire load is shed during this period. The water consumption during the load shedding period accumulates to 4 675 litres representing 57% of the total storage capacity. This indicates that the whole of the 'bottom' reservoir as well as part of the 'top' reservoir is filled with cold water at the end of the load shedding period.

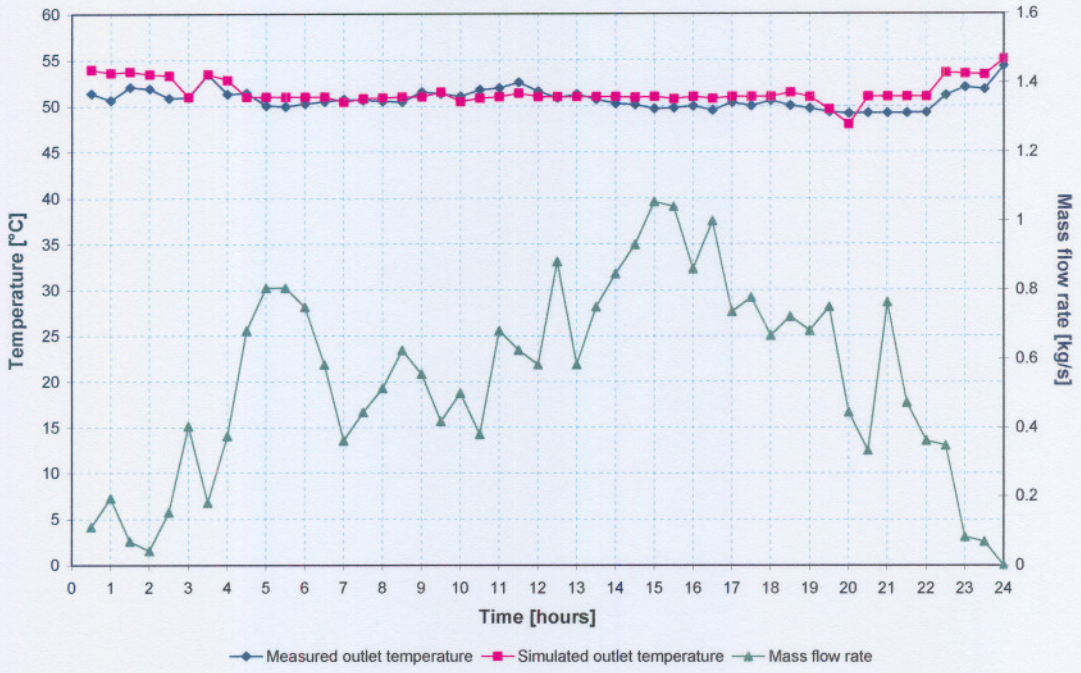

Figure 4.17: Water consumption profile together with measured and simulated hot-water supply temperatures for the selected day.

It is clear from Figure 4.18 that the simulated outlet temperature compares well with the measured outlet temperature. A minimum outlet temperature of 49.2 °C is measured during the load shedding period. This value compares well with the predicted temperature of 48.0 °C at the same time.

The measured and simulated temperatures near the top of the 'top' reservoir are shown in Figure 4.18. The temperature near the top of this reservoir remains in the region of 51 °C throughout the entire day. This can be expected since the water is supplied to the top of this reservoir at 51 °C whenever the ILH is switched on.

The simulated top temperature compares well with the measured top temperature for the selected day.

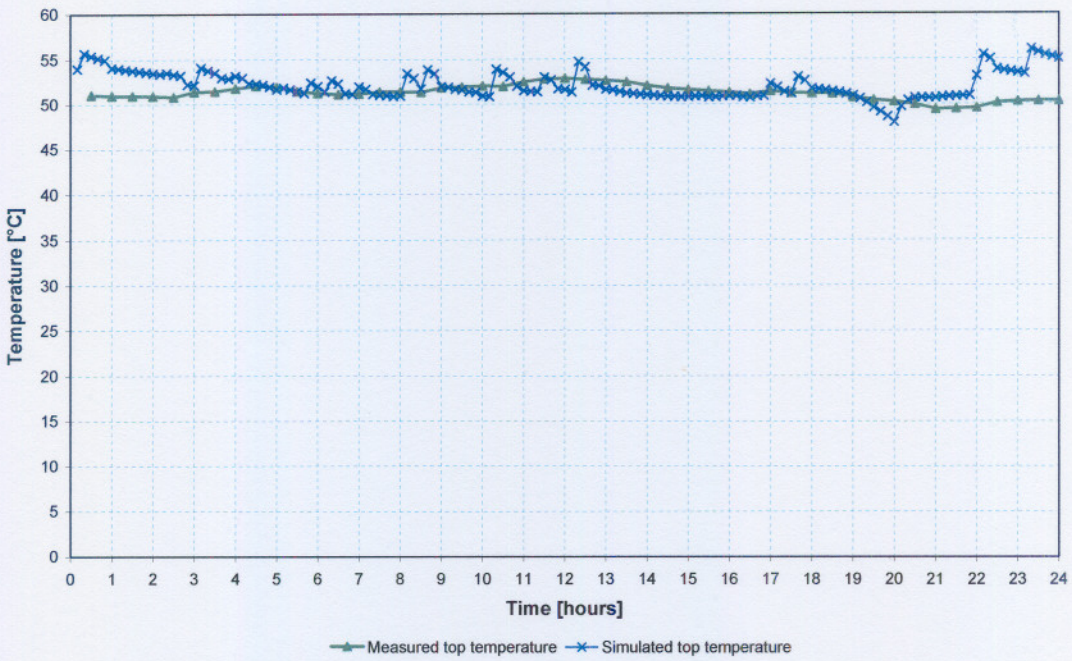

Figure 4.18: Measured and simulated temperature at the top of the 'top' reservoir.

The middle temperature of the reservoir system is measured with the aid of the 'middle' PT-100 situated at the top of the 'bottom' reservoir. Figure 4.19 shows the measured middle temperature together with the simulated middle temperature. It can be seen from this figure that the middle temperature drops substantially during the peak demand period (18:00 to 20:00). A total of 4 675 litres of cold water enters the 'bottom' reservoir during the load shedding period. This causes the middle temperature to drop substantially considering that the whole of the 'bottom' reservoir is filled with cold water at the end of this period.

The middle temperature reaches a measured value of 20.1 °C at the end of the load shedding period compared to the top temperature reaching a value of 50.3 °C at the same time. This emphasises the high degree of stratification achieved by the ILH water heating system during the load shedding period. The measured and simulated middle temperatures once again compare well with each other.

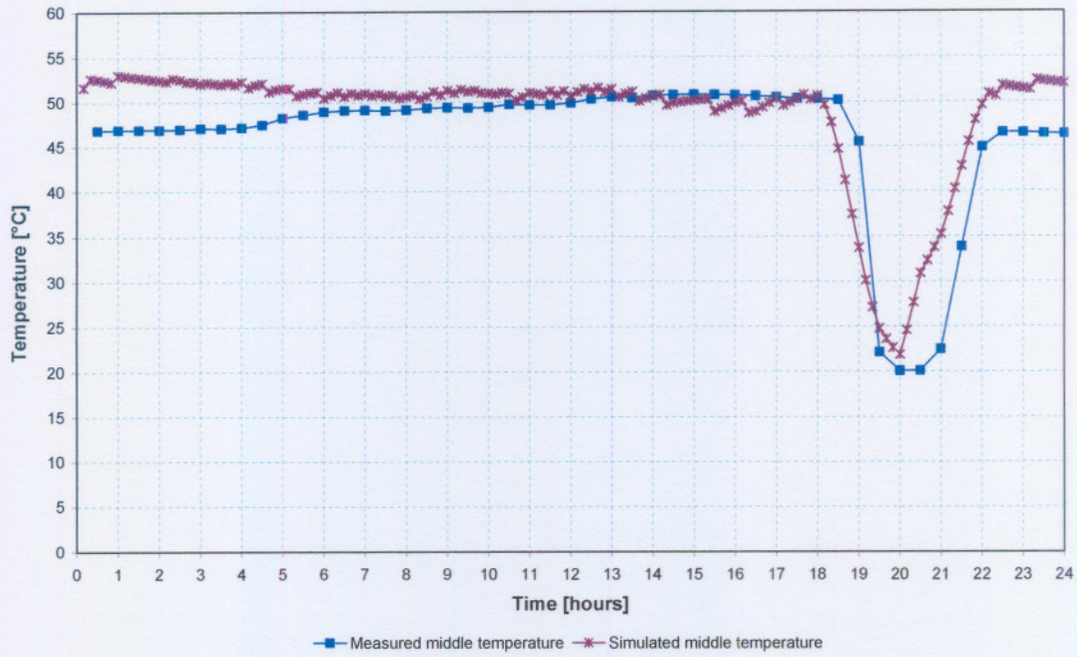

Figure 4.19: Measured and simulated temperature at the top of the 'bottom' reservoir.

The temperature at the 'bottom' of the system is measured near the bottom of the 'bottom' reservoir. Figure 4.20 shows the measured temperature versus the simulated temperature near the bottom of this reservoir. The bottom temperature stays relatively constant up to the load shedding period during which the temperature decreases rapidly. As soon as the ILH is switched back on the bottom temperature starts to recover. The measured and simulated bottom temperatures once again compare well with each other.

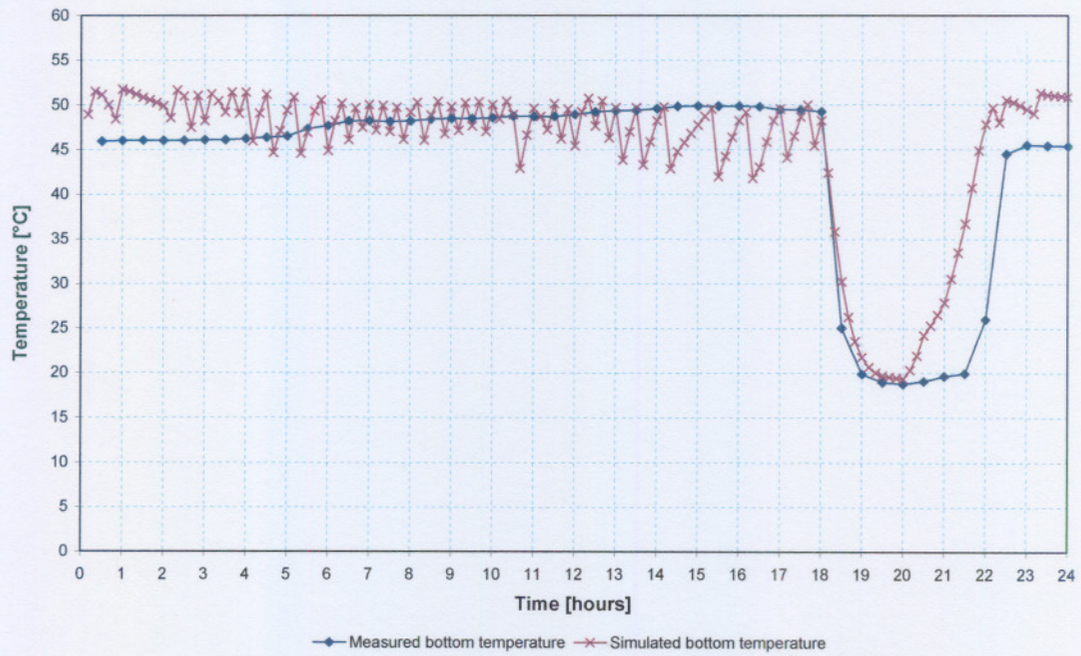

Figure 4.20: Measured and simulated temperature near the bottom of the 'bottom' reservoir.

Figure 4.21 compares the measured and simulated electricity demand profile for the selected day. It can be seen from the figure that the measured electricity demand compares very well with the simulated electricity demand. The full load is once again shed during the peak demand period for both the measured as well as the simulated electricity demand. The measured electricity consumption added up to 1 811 kWh for the selected day compared to 1 951 kWh predicted by the simulation model.

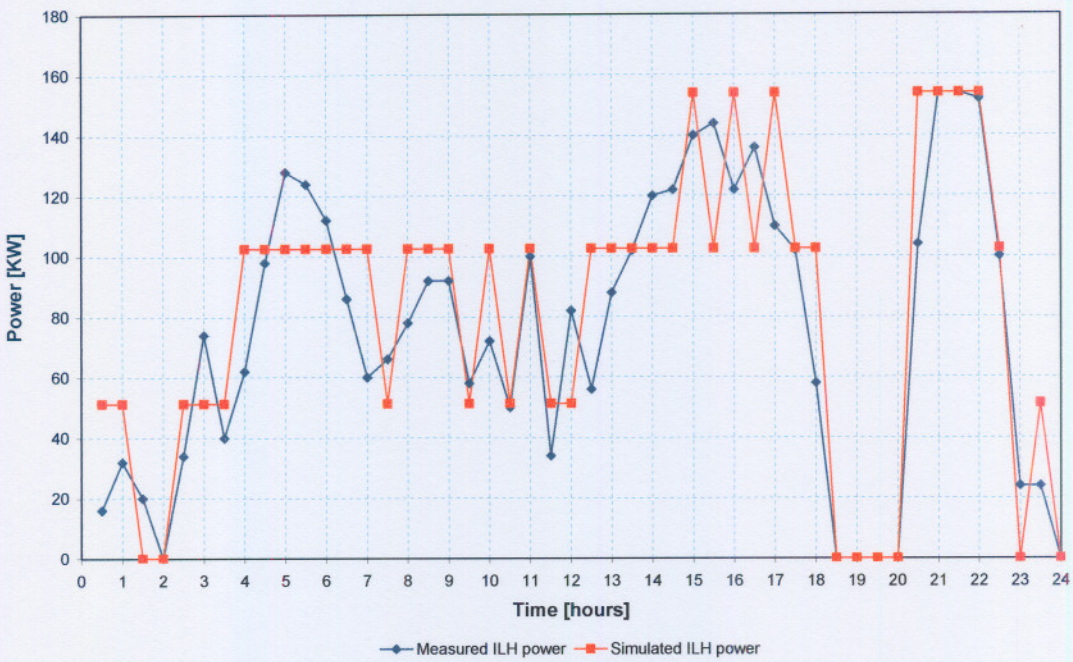

Figure 4.21: Measured and simulated electricity demand profile for the selected day.

The performance number QD is found to be 0.038 indicating a 3.8% difference between the measured and simulated outlet temperatures over the entire day. QE is found to be 0.077 indicating a 7.7% difference between the measured and simulated electricity consumption.

4.4.5 Plant no.5

The fifth plant under investigation consists of an ILH with a heating capacity of 116 kW and storage capacity of 10 000 litres in the form of two 5 000 litre reservoirs connected in series. Table 4.9 provides a summary of the plant specifications and operation during the selected day of operation.

Table 4.9: Summary of plant specifications.

Heating capacity	116 kW
Heating equipment	In-line heater
Storage capacity	2 x 5 000 litre (Vertically mounted)
ILH-temperature set-point	48°C
Typical occupancy	± 500
Hot-water consumption	37 275 litres
Date of selected day	12 November 2004

The measured hot-water consumption profile together with the measured and simulated hot-water supply temperatures are shown in Figure 4.22. Two distinct peaks exist in the water consumption profile. The first peak occurs between the hours of 06:00 and 07:00 in the morning with the second peak occurring between 15:00 and 16:00 in the afternoon. The fact that the peak water consumption is quite higher than the average consumption throughout the day suggests that the plant is not over utilised.

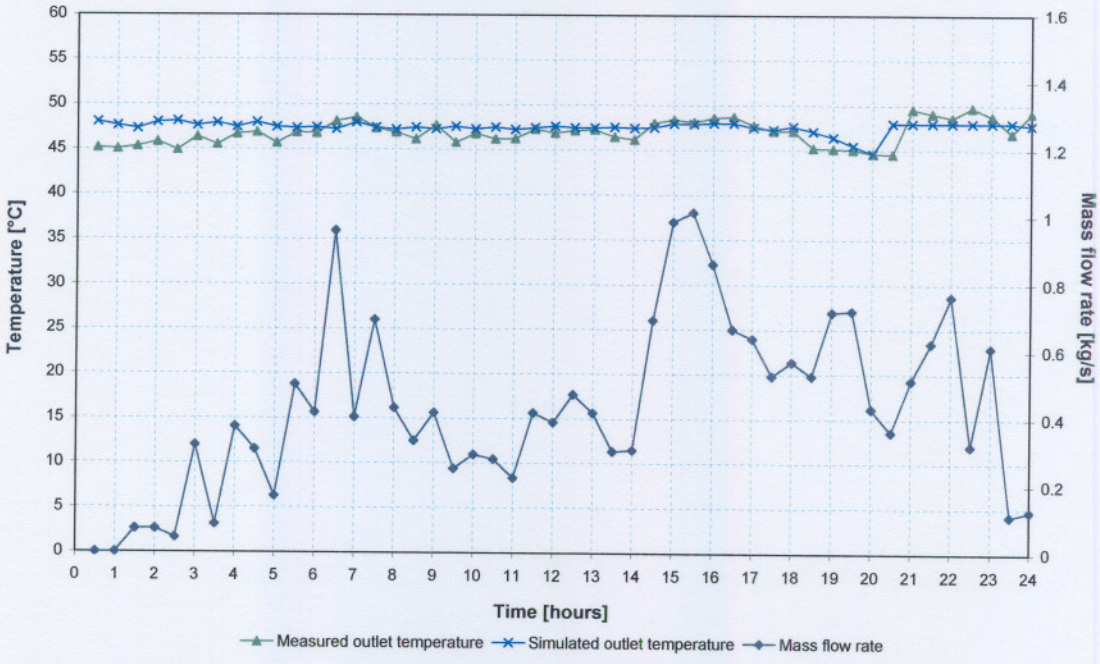

Figure 4.22: Water consumption profile together with measured and simulated hot-water supply temperatures for the selected day.

It can be seen from the figure that the measured outlet temperature remains between 45 °C and 50 °C throughout the selected day with the entire load being shed during the peak demand period (18:00 to 20:00). The hot-water consumption during the load shedding period accumulates to 4 325 litres representing 43% of the total storage capacity. This

indicates that 86% of the 'bottom' reservoir is filled with cold water at the end of the load shedding period. It is therefore expected that the 'top' reservoir should be filled with sufficient hot water due to the stratification effect achieved by the system.

Figure 4.22 also indicates that the simulated outlet temperature compares well with the measured outlet temperature. The minimum outlet temperature of 44.6 °C measured during the load shedding period compares well with the predicted temperature of 44.6 °C.

The measured and simulated temperatures near the top of the 'top' reservoir are shown in Figure 4.23. The temperature near the top of this reservoir remains around 47 °C throughout the day except during the load shedding period during which it drops to a minimum of 43.2 °C. This can be expected since the water is supplied to the top of this reservoir at 48 °C whenever the ILH is switched on. Figure 4.24 also suggests a good comparison between the measured and simulated top temperature.

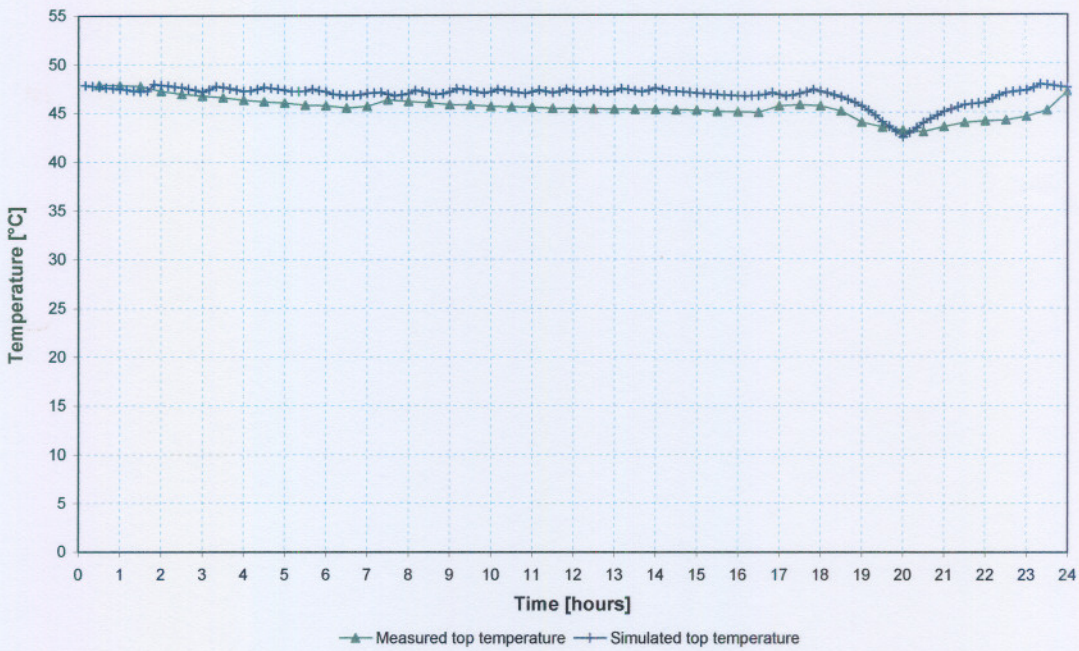

Figure 4.23: Measured and simulated temperature at the top of the 'top' reservoir.

The middle temperature of the reservoir system is measured with the aid of the 'middle' PT-100 situated at the top of the 'bottom' reservoir. Figure 4.24 shows the measured middle temperature together with the simulated middle temperature. It can be seen from the figure that the middle temperature drops substantially during the peak demand period (18:00 to 20:00). A total of 4 325 litres of cold water enters the 'bottom' reservoir during the load

shedding period. This causes the middle temperature to drop substantially considering the fact that 86% of the 'bottom' reservoir is filled with cold water.

The middle temperature reaches a measured value of 21.9 °C at the end of the load shedding period compared to the top temperature reaching a value of 43.2 °C at the same time. This emphasises the high degree of stratification achieved by the ILH-system. The measured and simulated middle temperatures once again compare well with each other.

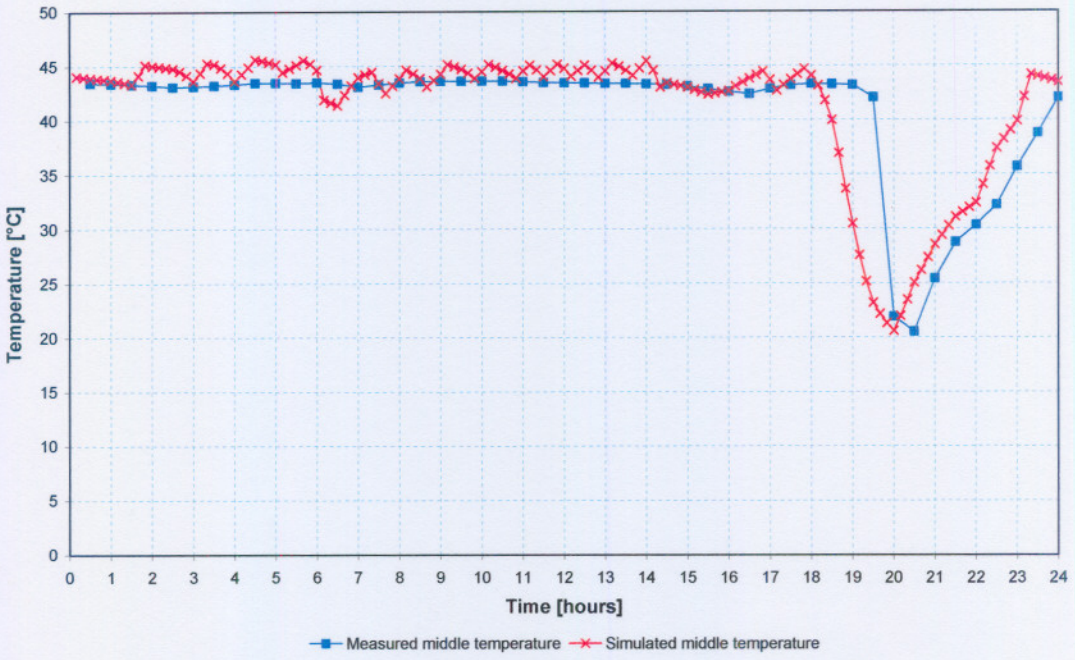

Figure 4.24: Measured and simulated temperature at the top of the 'bottom' reservoir.

The temperature at the 'bottom' of the system is measured near the bottom of the 'bottom' reservoir. Figure 4.25 shows the measured temperature versus the simulated temperature near the bottom of this reservoir. The bottom temperature stays relatively constant up to 14:30 when the peak consumption is achieved. The fact that the temperature at the bottom of the 'bottom' reservoir decreases during this time indicates that the ILH cannot supply the full amount of water consumed. The peak in consumption causes water to be drawn from the ILH as well as the storage reservoir causing cold water to enter the 'bottom' reservoir. The bottom temperature recovers rapidly before the load shedding period after which it decreases substantially. As soon as the ILH is switched back on the bottom temperature starts to recover. The measured and simulated bottom temperatures once again compare well with each other.

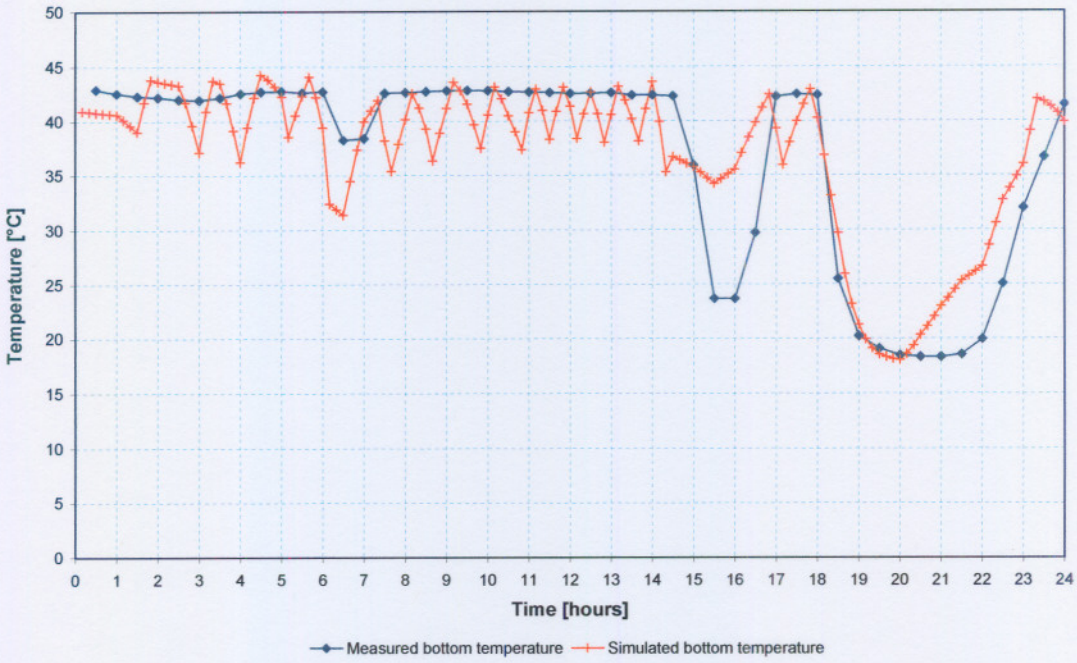

Figure 4.25: Measured and simulated temperature near the bottom of the 'bottom' reservoir.

Figure 4.26 compares the measured and simulated electricity demand profile for the selected day. It can be seen from the figure that the measured electricity demand compares very well with the simulated electricity demand. The full load is once again shed during the peak demand period for both the measured as well as the simulated electricity demand. The measured electricity consumption added up to 1 402 kWh during the entire day compared to 1 431 kWh predicted by the simulation model.

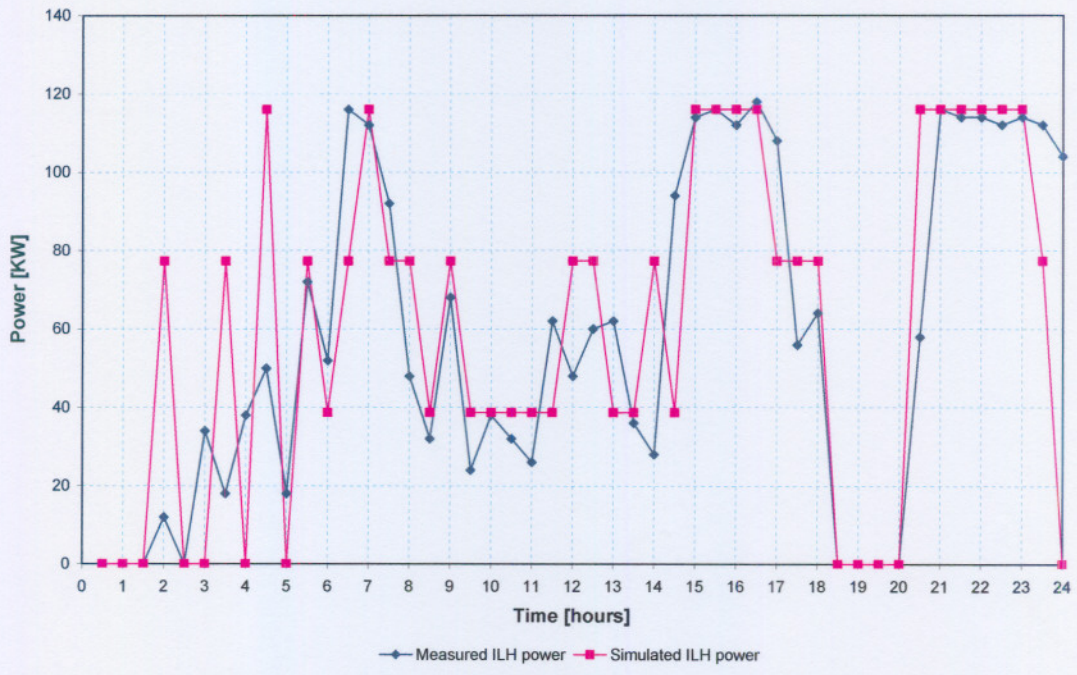

Figure 4.26: Measured and simulated electricity demand profile for the selected day.

The performance number QD is found to be -0.106 indicating a 10.6% difference between the measured and simulated outlet temperatures over the entire day. QE is found to be 0.020 indicating a 2.0% difference between the measured and simulated electricity consumption.

The empirical results obtained for five additional ILH-plants operating under different conditions are evaluated and compared to simulated results in Appendix B.

4.5 Summary

This chapter presented an extensive empirical investigation used to evaluate the performance of the newly developed ILH-configuration. It is clear from the results obtained by the investigation that the ILH indeed lends itself much better towards DSM-applications than conventional water heating configurations. In most of the applications the ILH-plants could shed the entire load during peak demand periods while still supplying sufficient hot water to the occupants at all times.

The empirical results were also employed to verify the water heating simulation model. It was found that the standing losses suffered by a typical centralised water heating system could be expressed using an effective loss factor. A loss factor of 6 W/m^2K was found to represent a typical value for all of the plants under investigation.

Figure 4.27 shows the results of the performance number QD for the CIT-configuration obtained in the empirical investigation as well as the results reported by Strauss (1999). The results shown for the empirical investigation are based on the average value of QD for the two CIT-plants investigated. From the figure it is clear that the results obtained from the empirical investigation compare favourably with the results obtained in the study conducted by Strauss (1999). Strauss (1999) reported an average QD of 0.118 with the average value of QD for the empirical study found to be 0.042.

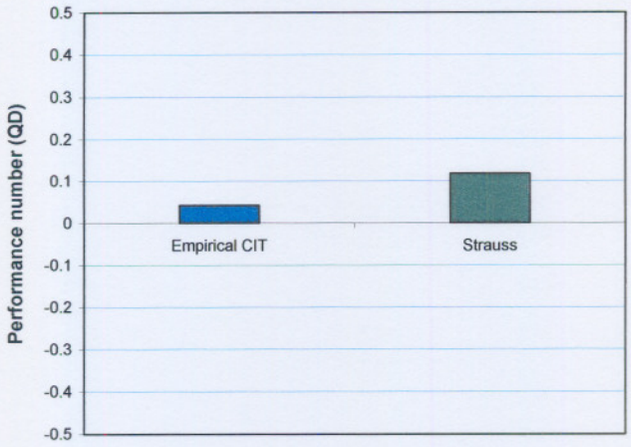

Figure 4.27: Performance numbers obtained for the CIT-configurations from the empirical investigation as well as those reported in the literature.

Figure 4.28 shows the results obtained for the ILH-plants in terms of the performance number QD. The figure compares the results obtained via the empirical study with the results reported by Strauss (1999) as well as Kleinbach *et al.* (1993). The results obtained via the empirical study are once again based on the average value of QD for the eight ILH-plants investigated. In the study by Strauss (1999), an average performance number of 0.02 is reported with Kleinbach *et al.* (1993) reporting 0.035 for low flow regimes and 0.11 for high flow regimes. The current empirical investigation resulted in an average performance number of 0.06 which compares favourably with the above-mentioned results.

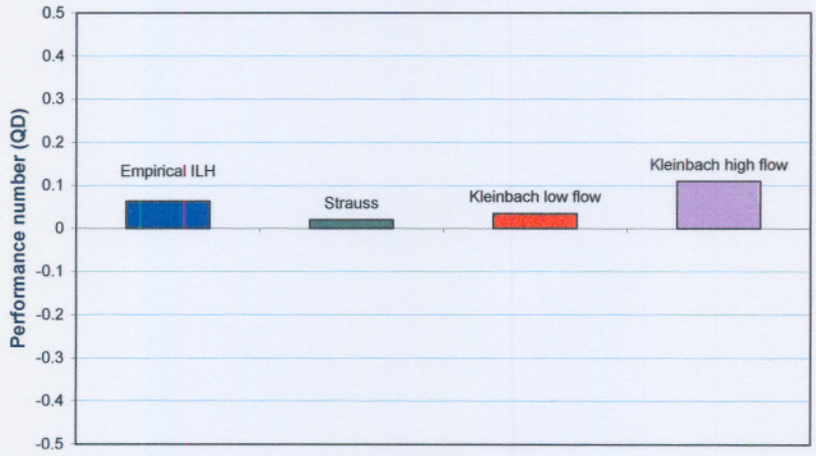

Figure 4.28: Performance numbers obtained for the ILH-configurations from the empirical investigation as well as those reported in the literature.

Considering the results of the performance numbers it can be concluded that the current simulation model can be used with confidence to accurately predict the performance of both CIT and ILH water heating configurations.

Chapter 5

IMPACT ASSESSEMENT

5.1 Introduction

In the previous chapter the results obtained from an extensive empirical investigation were presented in order to evaluate the performance of the newly developed ILH water heating configuration. The empirical results were also used to verify the simulation model used to predict the thermal behaviour of the various water heating plants. It was found that the ILH-configuration performs as expected in a real-world application under load shedding conditions. The results also showed that the simulation model can be used with confidence to predict the thermal performance of both the CIT- and ILH-configurations.

This chapter presents an impact assessment performed on a number of real-world conventional water heating systems, which have been retrofitted with ILH-systems. The impact assessment is performed in order to determine the impact of the newly developed ILH-configuration on the electricity supply grid as well as on the facility.

5.2 Demand baseline

In order to determine the impact of the newly developed ILH-configuration a baseline is required which represents the load profile of the conventional in-tank water heaters which operated on the facility before the systems were retrofitted with ILH-systems.

Since the total installed capacity of the conventional in-tank systems differs from the total installed capacity of the retrofitted ILH-systems, a normalised baseline is required. The normalised baseline is based on the daily energy consumption rather than the installed capacity of the plants. The baseline is constructed by using measured data obtained over a period of three months of operation on ten real-world conventional water heating plants. Furthermore, the baseline is only constructed for a typical weekday, due to the fact that load shedding is not important to Eskom during weekends.

The fact that the conventional in-tank water heating systems are situated at different locations and the periods over which the plants are monitored differ slightly, the average facility load profile could not be determined directly. In order to determine the average

facility load, an average weekday load profile is constructed for each of the individual plants. These individual weekday load profiles are then added together in order to construct the typical weekday load profile of the entire facility.

To be able to compare the baseline load profile with the load profile of the retrofitted ILH-systems the average facility load profile has to be normalised due to the fact that the installed capacities of the two systems are not the same. The normalisation is done by determining the total energy consumed during the average weekday baseline load profile. The average weekday baseline load profile is then devided by the total energy consumed during the averaged weekday. This gives a normalised load profile representing the average load profile for the monitored conventional in-tank water heaters for a total energy consumption of 1 kWh.

Figure 5.1 shows the normalised load profile constructed for an average weekday together with the cumalitive energy consumption of the normalised load profile. It can be seen from the figure that the cumulative energy consumption adds up to 1 at the end of the day, indicating a total energy consumption of 1 kWh.

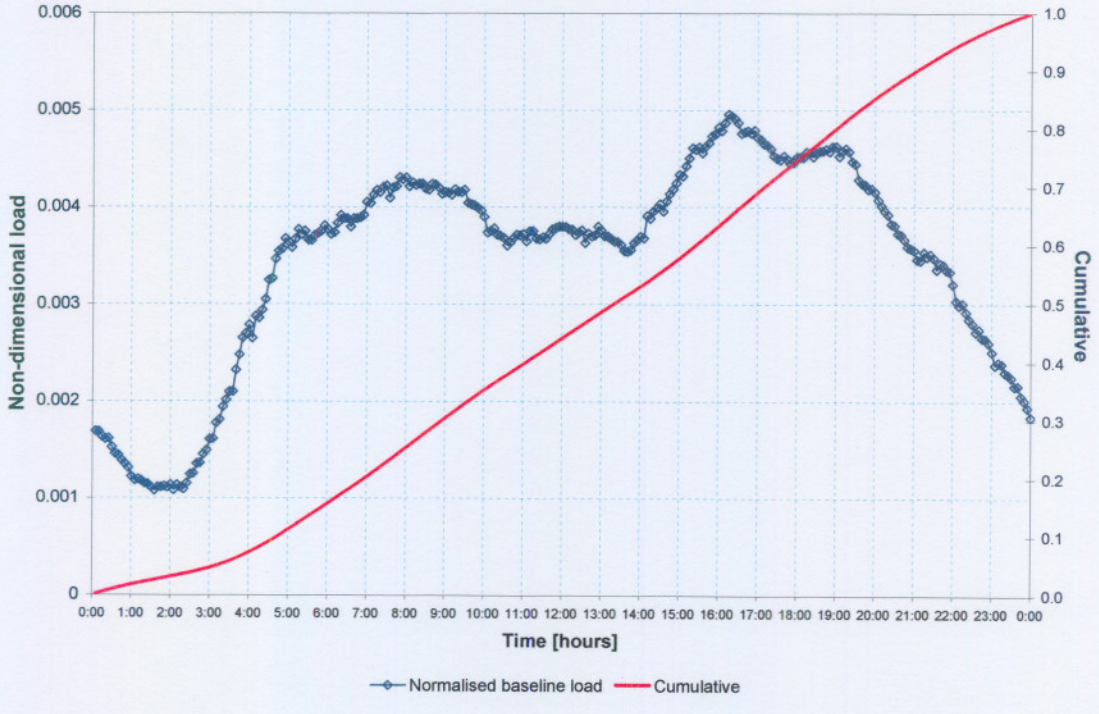

Figure 5.1: Normalised weekday baseline load and cumulative energy consumption.

5.3 Impact on electricity supply grid

In order to compare the baseline load profile with that of the rertrofitted facility under load shedding conditions a typical weekday load for each of the retrofitted plants is constructed. This is done by using the data obtained from the empirical investigation conducted in Chapter 4. These individual load profiles are then added together to represent the weekday load profile of the retrofitted facility.

The total energy consumption of the retrofitted facility load profile is then determined and the normalised baseline load profile is adjusted accordingly. In doing this, the baseline load and the retrofitted load represents the same amount of energy without having the same installed capacity.

Figure 5.2 shows the adjusted baseline load for the monitored conventional in-tank water heating plants together with the average load profile obtained through measuring the load of the eight retrofitted ILH-plants described in Chapter 4. The ILH-plants have a combined capacity of approximately 1 060 kW. It was found that the ILH-plants consume a total of 13 289 kWh over the selected weekday. The normalised baseline is adjusted in such a way that it consumes the same amount of energy.

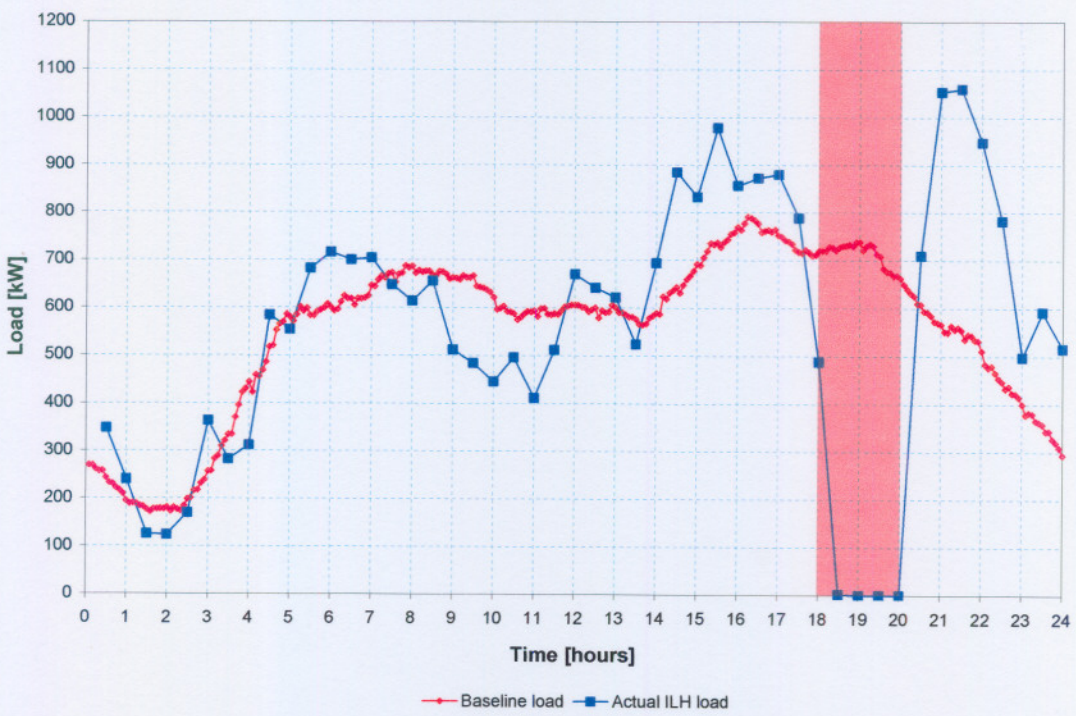

Figure 5.2: Actual ILH-load versus baseline load for a typical day.

It can be seen from the figure that the entire load is shed by the retrofitted systems during the peak demand period (18:00 to 20:00). Considering the adjusted baseline load, similar conventional in-tank water heating plants would of created an average load of 713.1 kW during the peak demand period (18:00 to 20:00). This indicates that an average of 713.1 kW is shifted from the peak demand period to off-peak periods by retrofitting all of the systems with ILH-configurations.

5.4 Impact on facility

With the impact of the retrofitted ILH-plants on the electricity supply grid addressed, the impact on the facility is considered. In order to assess the impact on the facility due to the retrofitted ILH-systems the cost incurred by the facility before and after the retrofit is evaluated.

Only the active energy cost incurred by the facility is addressed. Since the water heating system does not exclusively contribute to the maximum demand (MD) of the facility it is difficult to quantify the actual effect of the retrofitted system on the MD-cost.

The facility under investigation is on Eskom's Megaflex tariff structure. The Megaflex tariff structure consists of an active energy charge component calculated on a TOU pricing structure together with a MD-charge calculated on a monthly basis.

The active energy charge pricing structure consists of different prices charged per kWh according to the TOU-periods. The TOU-periods are different for weekdays, Saturdays and Sundays. Figure 5.3 shows the different TOU-periods for Eskom's Megaflex tariff structure. The TOU-periods are divided into three different groups consisting of peak, standard and off-peak periods.

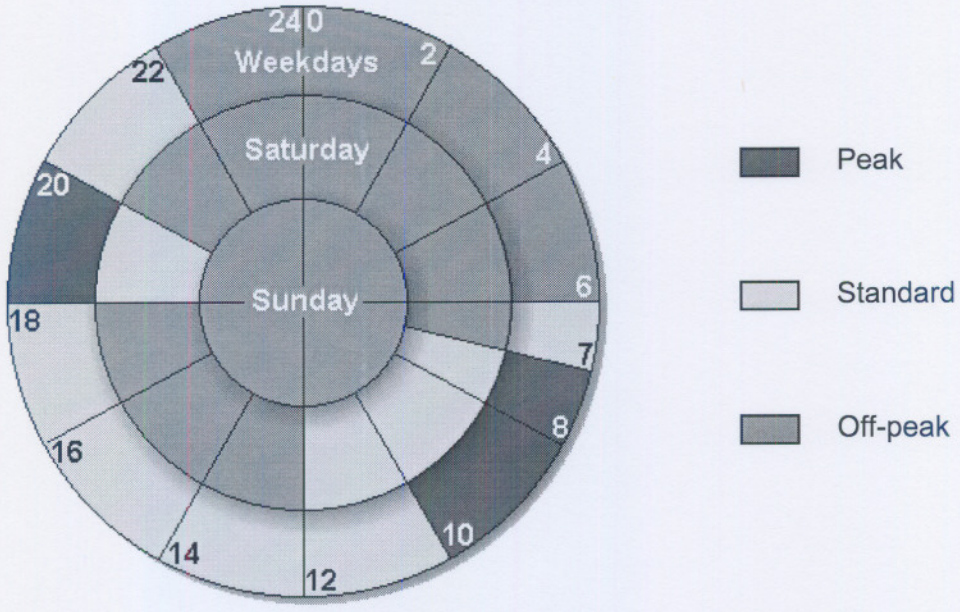

Figure 5.3: Eskom's Megaflex time-periods (Eskom, 2005).

Table 5.1 shows the pricing structure used for each of the different TOU-periods. The active energy charge is different for the so-called low-demand season and the high-demand season. The low-demand season stretches from September up to the end of May with the high-demand season stretching from June to the end of August. It can be seen from the table that the active energy charge during the peak demand period is considerably higher during the high-demand season.

Table 5.1: Megaflex – active energy charge pricing structure (Eskom, 2005).

Low-demand season (September – May)	Time-period	High-demand season (June – August)
16.07 c/kWh	Peak	56.65 c/kWh
9.98 c/kWh	Standard	14.98 c/kWh
7.07 c/kWh	Off-peak	8.15 c/kWh

Employing the above-mentioned tariff structure the typical weekday operating cost of the load profiles shown in Figure 5.2 can be determined for the high-demand season as well as the low-demand season. The adjusted baseline together with the actual ILH load profile shown in Figure 5.2 is used to compare the operating cost incurred by the facility before and after the systems have been retrofitted. Note that this cost is only determined for a typical weekday since the active energy charge over weekends is substantially lower than during weekdays.

Figure 5.4 shows the cumulative weekday operating cost incurred by the facility according to the adjusted baseline load as well as the actual ILH-load during the high-demand season. It can be seen from this figure that the baseline and retrofitted operating cost stays relatively the same during the first part of the day up to the point where most of the load is shed by the retrofitted plants between the hours of 18:00 and 20:00. During this time the baseline operating cost rises steeply, due to the high cost of electricity during this period.

The total weekday cost based on the baseline load adds up to R 3 218 with the total retrofitted operating cost being R 2 456. This indicates a saving of 24% on the active energy cost during the high-demand season.

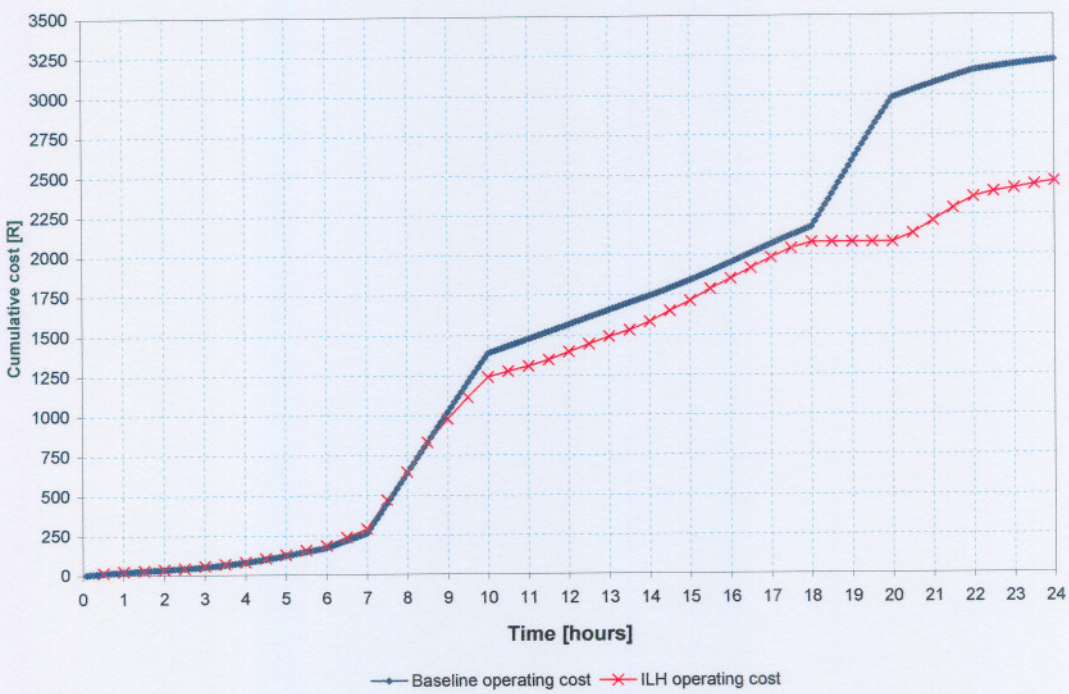

Figure 5.4: Baseline operating cost and actual ILH operating cost for a typical day during the high-demand season.

The same is done for the low-demand season using the pricing structure as shown in Table 5.1. Figure 5.5 shows the cumulative cost incurred by the facility for a typical weekday during the low-demand season before and after the systems have been retrofitted. It can be seen from the figure that the cumulative operating cost before the load shedding period (18:00-20:00) is almost the same for both the conventional water heating systems and the retrofitted ILH-systems. During the load shedding period the retrofitted systems shed the

entire load causing the operating cost to stay constant over this period. On the other hand, the baseline operating cost rises steeply during the peak demand period (18:00 to 20:00) but not as steep as under the high-demand pricing structure. This is due to the fact that the peak demand periods during the low-demand season are not as expensive as during the high-demand season.

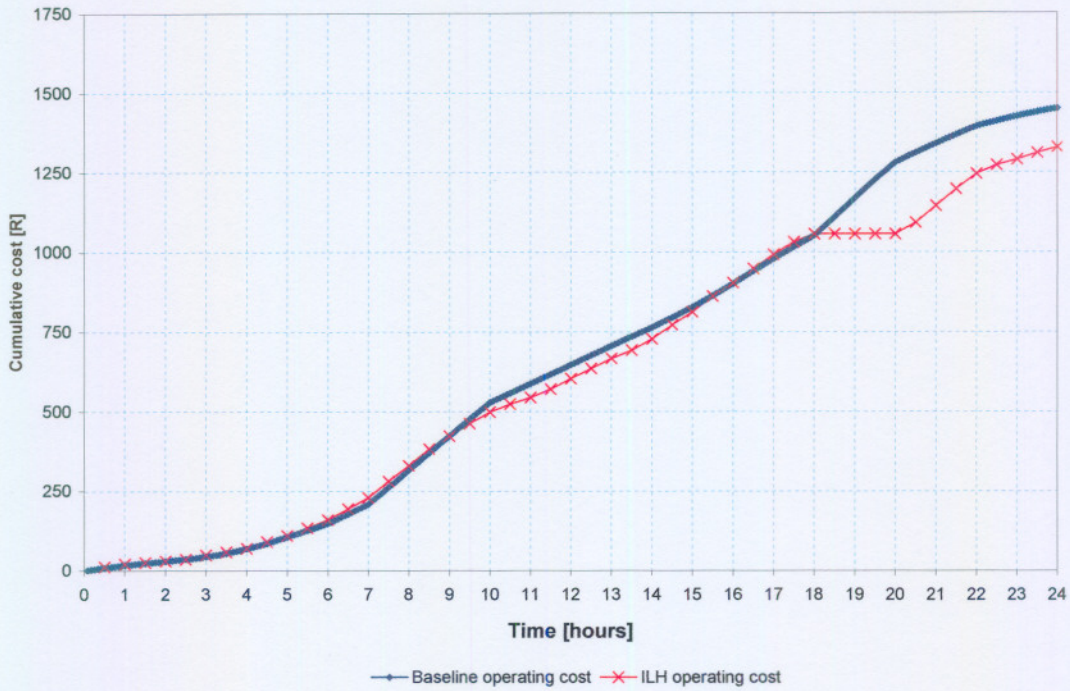

Figure 5.5: Baseline operating cost and actual ILH operating cost for a typical day during the low-demand season.

During the low-demand season the total weekday cost based on the baseline load adds up to R 1 451 with the total retrofitted operating cost being R 1 328. This indicates a saving of 8.5% on the active energy cost during the low-demand season.

5.5 Summary

This chapter assessed the impact of the ILH water heating configuration on both the electricity supply grid and the facility. It was found that the ILH-technology is able to shift a substantial amount of the load from the peak demand periods to off-peak periods.

Furthermore, in assessing the impact of the ILH-technology on the facility it was found that the operating cost is decreased by 24% during the high-demand season and 8.5% during the

low-demand season. This makes the ILH a very attractive option for any DSM-initiative, with substantial advantages for the electricity utility as well as the facility.

Chapter 6

CONCLUSION

6.1 Introduction

In this chapter a summary is provided, presenting the most important results obtained in each of the previous chapters. From these results conclusions are made as well as recommendations for further research.

6.2 Chapter summary

Chapter 1 provided the basic background to the current problem caused by conventional water heating installations concerning the peak load on the national electricity supply grid. This problem is mainly due to the conventional water heating design philosophy used in the majority of water heating installations found in South Africa. The objectives of the study were to evaluate the performance of newly developed water heating configurations via simulation together with an empirical investigation. Another objective was to determine the impact of the newly developed water heating configurations on the peak electricity demand.

An extensive literature survey was presented in Chapter 2. The survey showed that sanitary water heating forms a critical part of the peak demand imposed on the national electricity supply grid. By far the largest portion of the total sanitary hot-water consumption in South Africa is heated by means of resistance heaters. It was also found that resistance heaters, almost exclusively conventional in-tank heaters, account for 68% of the total number of residents served. A lot of research has been done on DSM on sanitary water heaters. The majority of DSM control strategies for in-tank water heaters use a reactive, direct load control strategy switching water heaters on or off during peak demand periods without taking customer satisfaction into account. The simulation model used to simulate the thermal behaviour of different types of water heating systems was also discussed. From this chapter a need for alternative water heating configurations which lend themselves better towards DSM was identified.

In Chapter 3, the thermal performances of two alternative water heating technologies were investigated via simulation. These technologies were developed to address the problems associated with the conventional in-tank heater design philosophy under load shedding

conditions. It was found that the ILH-technology could achieve complete load shedding during peak demand periods, while still providing sufficient hot water to the occupants at all times. In plants where comprehensive ILH-retrofits could not be justified it was found that the SIT-technology provided a very real opportunity to realise the maximum DSM-potential.

Chapter 4 presented an extensive empirical investigation in which the performance of the newly developed ILH-configuration was evaluated. The chapter also provided a generic model for simulating the standing heat losses suffered by typical water heating systems. It was found that the standing heat loss model provided sufficient results. The empirical results obtained from a number of conventional in-tank water heating systems and ILH-systems showed that the ILH-configuration indeed performed as expected. The empirical results were also used to verify the simulation model used to predict the thermal performance of the water heating plants. It was found that the simulation model provided acceptable results compared to results reported in the literature.

An impact assessment was performed in Chapter 5 to determine the impact of the ILH water heating configuration on both the electricity supply grid and the facility. It was found that the ILH-technology was able to shift a huge amount of the load from the peak demand period to off-peak periods making this configuration a very attractive option for DSM-initiatives. Furthermore, the energy cost of the facility was decreased by 24% during Eskom's high-demand season and a decrease of 8.5% was found during Eskom's low-demand season. This also made the ILH-configuration a very attractive option for the facility to reduce the operating cost of existing water heating systems.

6.3 Conclusion

This study evaluated alternative water heating configurations which proved to lend themselves much better towards DSM, in the form of load shedding, than conventional water heating configurations. Two newly developed, alternative water heating configurations were evaluated in the form of the ILH- and SIT- configurations.

It was found that the ILH-configuration performs excellent under load shedding conditions. The ILH-configuration was able to shed the entire load during peak demand periods while still supplying sufficient hot water to the occupants at all times under a range of different operating conditions. The SIT-configuration proved to be a good alternative in cases where the installation of an ILH was not entirely justified. Although the SIT-configuration did not

form part of the empirical investigation, the simulation results showed that the SIT-configuration was able to shed at least half of its load during peak demand periods. This was done while supplying sufficient hot water to the occupants at all times.

An extensive empirical investigation showed that the ILH-configuration performs as expected under load shedding conditions in a real-world application. The empirical investigation also showed that the model used to simulate the thermal performance of the different types of water heaters provided acceptable agreement with the empirical results.

Furthermore, the impact of the newly developed ILH-configuration on the electricity supply grid as well as on the facility was assessed. It was found that retrofitting conventional in-tank water heating systems with the ILH-technology could provide the utility with substantial load shedding potential. It was also found that the facility could reduce its water heating electricity cost by 24% during the high-demand season and 8.5% during the low-demand season.

Considering these results, the ILH-technology together with the SIT-technology provides a very attractive option for DSM-initiatives in which customer satisfaction is a priority.

6.4 Recommendations for further research

It is recommended that the following aspects be considered for further research:

- An empirical investigation could be conducted in order to evaluate the performance of the SIT-configuration in a real-world application.
- The stratification model used in the simulation model could be further verified in order to determine the factors which influence the stratification achieved by different water heating systems.
- An impact study could be performed to determine the potential national impact of the newly developed water heating systems on the DSM-targets set by Eskom.

REFERENCES

Akridge, J.M. and Keebaugh, D. 1990. An investigation of off-peak domestic water heating. *ASHRAE Journal*, 32:21-25.

Becker, B. R. and Stogdill, K. E. 1990. A domestic hot-water use database. *ASHRAE Journal*, 32:21-25.

Bhattacharyya, K. and Crow, M.L. 1996. A Fuzzy Logic Based Approach to Direct Load Control. *IEEE Transactions on Power Systems* , 11(2):708-714.

Bzura, J.J. 1989. Radio control of water heaters in Rhode Island. *IEEE Transactions on Power Systems*, 4(1):26-29.

Calmeyer, J.E. and Delport, G.J. 1999. Hot water control within communal living environments such as residences and hostels. *Proceedings of the international conference on domestic use of energy,* 1999, South Africa.

El-Amin, I.M., Al-Ali, A.R. and Suhail, M.A. 1999. Direct load control using a programmable logic controller. *Electric power systems research*, 52:211-216.

Els, R. 2002. Energy evaluations and load shift feasibility in South African mines. Thesis, Philosophiae Doctor, Potchefstroom University.

Eskom. 2004. Demand Side Management. [Web:] http://www.eskom.co.za [Date accessed: 26 July 2004].

Eskom. 2005. Tariffs and Charges. [Web:] http://www.eskom.co.za [Date accessed: 9 May 2005].

Forlee, C. 1999. A flexible hot water load control system. *Proceedings of the international conference on domestic use of energy,* 1999, South Africa.

Forlee, C. 1997. Water heating in South Africa facts & figures from 1997 "notch testing" program. *Proceedings of the international conference on domestic use of energy,* 1997, South Africa.

Horn, G.F. and De Kock, J.A. 2004. A comparison of two bulk hot water heating systems for an university hostel. *Proceedings of the international conference on industrial and commercial use of energy on 10-11 May 2004*, Somerset West, South Africa.

Kar, A.K. and Al-Dossary, K.M. 1995. Thermal performance of water heaters in series. *Applied Energy*, 52:47-53.

Kar, A.K. and Kar, U. 1996. Optimum design and selection of residential storage-type electric water heaters for energy conservation. *Energy conservation and management*, 37:1445-1452.

Kleinbach, E.M., Beckman, W.A. and Klein, S.A. 1993. Performance study of one-dimensional models for stratified thermal storage tanks. *Solar Energy*, 50:155-166.

Lacroix, M. 1999. Electric water heater designs for load shifting and control of bacterial contamination. *Energy conservation and management*, 40:1313-1340.

LaMeres, B.J., Nehrir, M.H. and Gerez, V. 1999. Controlling the average residential electric water heater power demand using fuzzy logic. *Electric power systems research*, 52:267-271.

Lane, I.E. and Beute, N. 1996. A model of the domestic hot water load. *IEEE Transactions on Power Systems*, 11(4):1850-1855.

Laurent, J.C., Desaulniers, G. and Malhamè, R.P. 1995. A column generation method for optimal load management via control of electric water heaters. *IEEE Transactions on Power Systems*, 10(3):1389-1399.

Lee, S.H. and Wilkens, C.L. 1983. A practical approach to appliance load control analysis: A water heater case study. *IEEE Transactions on Power Apparatus and Systems*, PAS-102(4):1007-1013.

Lemmer, E.F. and Delport, G.J. 1999. The Influence of a Variable Water Heater on The Domestic Load Profile. *IEEE Transactions on Energy Conversion*, 14(4):1558-1563.

Lemmer, E.F., Delport, G.J., Kern, C.F. 1998. A comparative RTP case study with a variable volume water heater. *Proceedings of the international conference on domestic use of energy,* 1998, South Africa.

Minguez, J.M. 1987. Water-heaters in series. *Energy Research*, 11:145-151.

Nehrir, M.H. and LaMeres, B.J. 2000. A multiple-block logic-based electric water heater demand-side management strategy for levelling distribution feeder demand profile. *Electric power systems research*, 56:225-230.

Rautenbach, B. and Lane, I.E. 1996. The multi-objective controller: A novel approach to domestic hotwater load control. *IEEE Transactions on Power Systems*, 11(4):1832-1837.

Roman, R. and Wilson, R. 1995. Commercial demand-side management using a programmable logic controller. *IEEE Transactions on Power Systems*, 10(1):376-379.

Rousseau, P.G. and Greyvenstein, G.P. 2000. Enhancing the impact of heat pump water heaters in the South African commercial sector. *Energy*, 11:51-70.

Rousseau, P.G., Strauss J.P. and Greyvenstein, G.P. 2001. Demand side management for water heating installations in South African commercial buildings. *International journal of energy research*, 25:291-317.

Strauss, J.P. 1999. Demand-side management for water-heating installations in commercial buildings, Masters dissertation, Potchefstroom University.

Van Harmelen, G. and Van Tonder, J.C. 1998. Hot water load control in the South African context: where to next? *Proceedings of the international conference on domestic use of energy,* 1998, South Africa.

Van Tonder, J.C. and Lane, I.E. 1996. A Load Model to Support Demand Management Decisions on Domestic Storage Water Heater Control Strategy. *IEEE Transactions on Power Systems*, 11(4):1844-1849.

Wilken, A.S. and Delport, G.J. 2000. Hot water load control – A new perspective. *Proceedings of the international conference on domestic use of energy,* 2000, South Africa.

Appendix A

ADDITIONAL STANDING LOSS EMPIRICAL RESULTS

This section provides the empirical results obtained for three additional water heating plants employed to verify the standing losses suffered by the different systems. In each case the standing heat losses suffered by the system over a number of days are simulated using different values for the effective loss factor k_{eff}. The simulated losses are compared with the measured losses for different values of k_{eff} in order to obtain a typical value of k_{eff} for centralised water heating systems as discussed in paragraph 4.3.

Additional Plant no.1

The first of the additional plants used to verify the simulation of the standing losses suffered by a typical centralised water heating system, consists of an ILH connected to two 10 000 litre vertically mounted storage reservoirs connected in series. In this case the plant operation is monitored over a period of 14 consecutive days. Table A.1 provides a summary of the ILH-system specifications used for the investigation.

Table A.1: Summary of ILH-system specifications.

Heating capacity	230 kW
Heating equipment	In-line resistance elements
Storage capacity	2 x 10 000 litre (Vertically mounted)

Figure A.1 shows the results obtained with k_{eff} equal to 6 W/m^{2}K for the ILH-system. It can be seen from the figure that the measured and simulated energy input as well as the energy output compares well with each other.

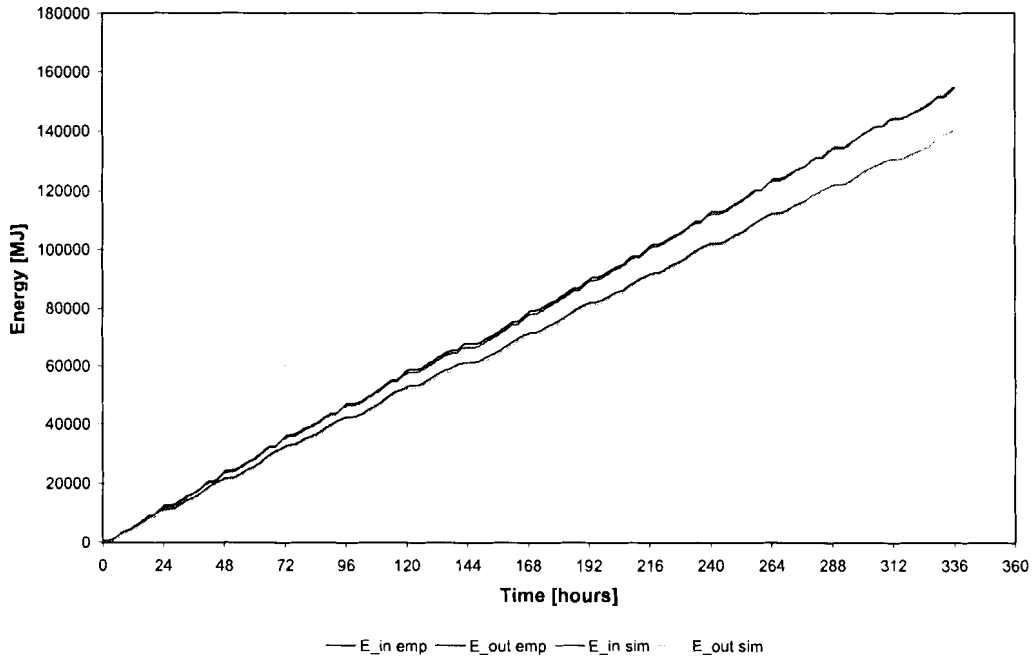

Figure A.1: Measured and simulated energy input and output.

The amount of energy provided to the system via the electricity supply adds up to 154 576 MJ with the energy withdrawn from the system via the supplied hot water adding up to 140 401 MJ. The energy input being 14 175 MJ more than the energy withdrawn from the system. This indicates that 9.2% of the electrical energy consumed by the system is lost due to standing heat losses to the environment. The amount of standing heat losses are also calculated using the simulation model with different values for k_{eff}. Table A.2 provides a summary of the results obtained for different values of k_{eff}.

Table A.2: Summary of simulation results for a number of effective loss coefficients.

k [W/m^{2}K]	E_{in} [MJ]	E_{out} [MJ]	Losses [%]
2	148 764	141 193	5.1
6	154 836	140 518	9.2
8	158 010	140 344	11.2

It is clear from Table A.2 that when k_{eff} is equal to 6 W/m^{2}K the measured losses of 9.2% compare very well with the simulated losses of 9.2%.

Additional Plant no.2

Exactly the same is done for the second additional plant with the plant monitored over a period of 24 consecutive days. Table A.3 provides a summary of the plant specifications.

Table A.3: Summary of plant specifications.

Heating capacity	102 kW
Heating equipment	In-line resistance elements
Storage capacity	2 x 5 000 litre (Vertically mounted)

Figure A.2 shows the results obtained with k_{eff} equal to 6 W/m^{2}K for the energy input to the system and energy output from the system. It can be seen from the figure that the measured and simulated energy input as well as the energy output compares well with each other.

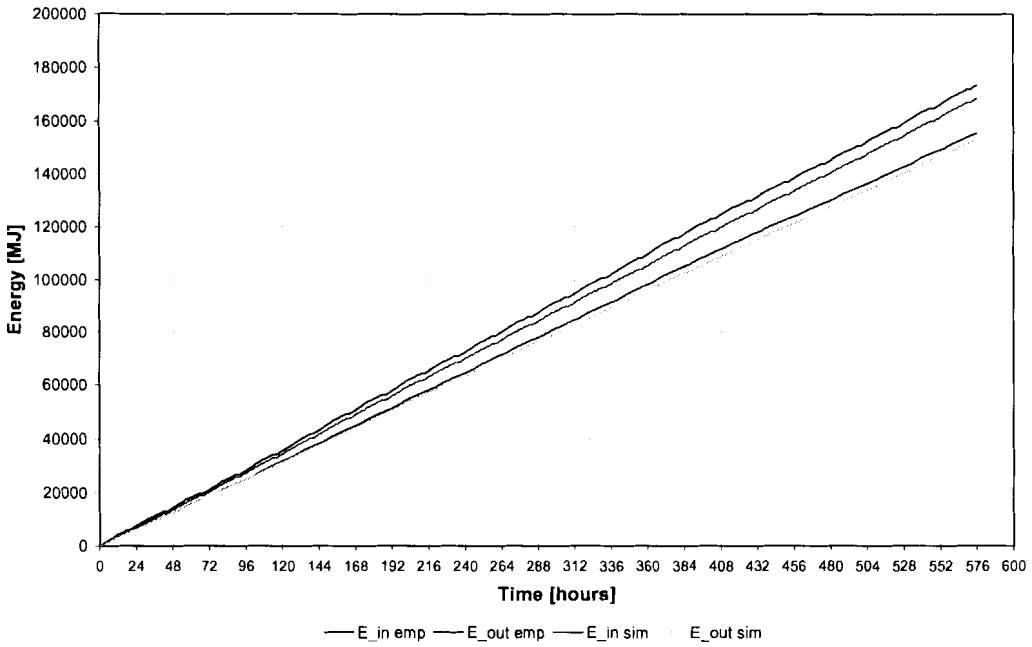

Figure A.2: Measured and simulated energy input and output.

In comparing the measured energy input with the measured energy extracted from the system the standing heat losses are found to be 10.3%. Table A.4 provides a summary of the results obtained using the simulation model to predict the standing heat losses for different values of k_{eff}.

Table A.4: Summary of simulation results for a number of effective loss coefficients.

k [W/m^{2}K]	Losses [%]
2	4.3
4	6.8
6	9.0
8	11.2

It is clear from Table A.4 that when k_{eff} is equal to 6 W/m^{2}K the measured losses of 10.3% once again compare very well with the simulated losses of 9.0%.

Additional Plant no.3

The third additional plant is also monitored over a period of 24 consecutive days. Table A.5 provides a summary of the plant specifications.

Table A.5: Summary of plant specifications.

Heating capacity	106 kW
Heating equipment	In-line resistance elements
Storage capacity	2 x 5 000 litre (Vertically mounted)

Figure A.3 shows the results obtained with k_{eff} equal to 6 W/m^{2}K for the energy input and output. It can be seen from the figure that the measured and simulated energy input as well as the energy output compares well with each other.

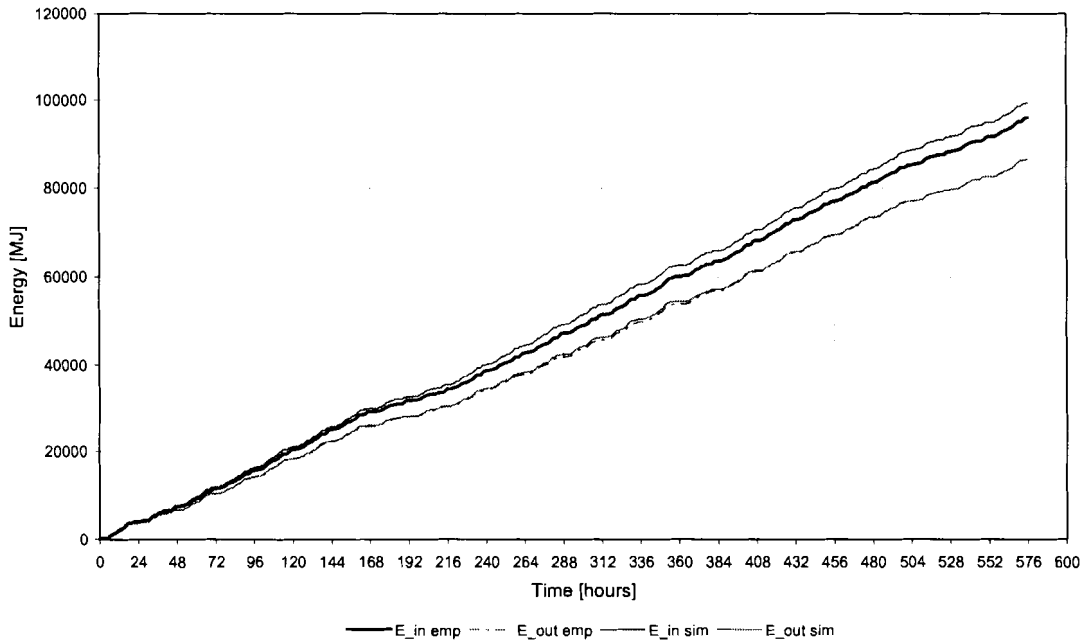

Figure A.3: Measured and simulated energy input and output.

In comparing the measured energy input with the measured energy extracted from the system the standing heat losses are found to be 9.8%. Table A.6 provides a summary of the results obtained using the simulation model to predict the standing heat losses for different values of k_{eff}.

Table A.6: Summary of simulation results for a number of effective loss coefficients.

k [W/m^{2}K]	Losses [%]
2	6.7
4	9.9
6	13.0
8	15.7

In this case the standing heat losses are simulated more accurately by using a value of 4 W/m^{2}K in the simulation, instead of 6 W/m^{2}K used in all of the previous cases. Although the standing heat losses are simulated more accurately with this value for k_{eff}, the losses simulated with k_{eff} equal to 6 W/m^{2}K are within an expectable range of the measured losses.

The fact that the losses are simulated more accurately with a different value for k_{eff} could be caused by a difference in this particular plant operation. A possible difference could be the fact that more/less ring-main returns are present at this particular plant. However, this is not certain since no ring-main return measurements are available for the plants.

Appendix B

ADDITIONAL ILH EMPIRICAL RESULTS

This section provides the empirical results obtained for five additional ILH-plants supplementing the results obtained for the five plants presented in paragraph 4.4. All of the ILH-plants presented here operate under load shedding conditions with the entire load being shed during the peak demand period (18:00 to 20:00). The results obtained for each of the above-mentioned plants are discussed briefly together with the calculated performance numbers as set out in paragraph 4.4.

Plant no.6

The sixth plant is the exact same plant as the first plant except for the fact that the in-tank resistance heaters have been retrofitted with an ILH with a heating capacity of 106 kW. The storage capacity of the plant remained unchanged, consisting of a single 5 000 litre reservoir. The only difference in the operation of the plant is the fact that the entire load is now shed during the peak demand period (18:00 to 20:00). Table B.1 provides a summary of the plant specifications and operation during the selected day.

Table B.1: Summary of plant specifications.

Heating capacity	106 kW
Heating equipment	In-line heater
Storage capacity	1 x 5 000 litre (Vertically mounted)
ILH-temperature set-point	49 °C
Typical occupancy	± 350
Hot-water consumption	32 025 litres
Date of selected day	27 October 2004

The measured water consumption profile together with the measured and simulated outlet water temperatures supplied to the occupants is shown in Figure B.1. The outlet temperature remains nearly constant between 45 °C and 50 °C for most of the day. A distinct drop in the outlet temperature occurs at the end of the load shedding period between 19:30 and 20:00. This drop in temperature is due to the fact that the entire load is shed between 18:00 and 20:00, allowing cold water to enter at the bottom of the reservoir. Another reason for the drop in temperature is the unusually high consumption of 4 400 litres during the load

shedding period. This results in almost 90% of the reservoir being filled with cold water making a drop in the outlet temperature, inevitable. Unlike the expected behaviour of the conventional in-tank configuration the outlet temperature recovers very quickly after the load shedding period to the desired outlet temperature.

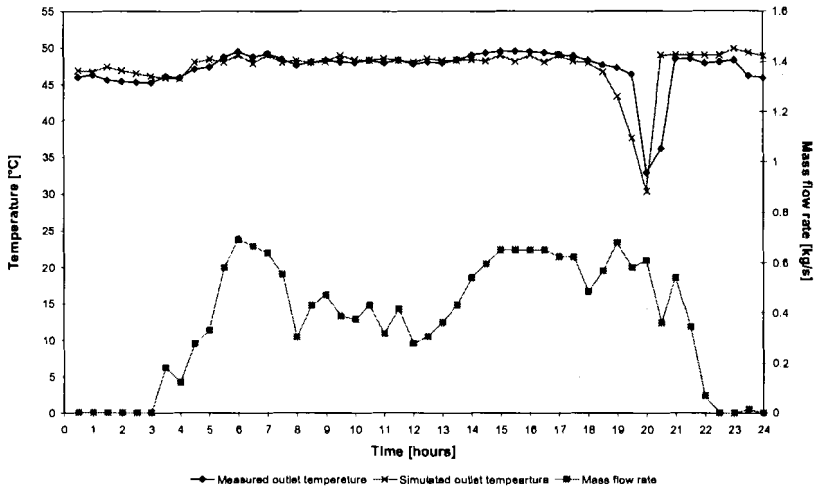

Figure B.1: Water consumption profile together with measured and simulated hot-water supply temperatures for the selected day.

It can be seen from Figure B.1 that the simulated outlet temperature compares well with the measured outlet temperature for the entire day. The simulated temperature drop experienced during the peak demand periods occurs at a slightly earlier time than the measured temperature drop. This indicates that the simulation model predicts the outlet temperature conservatively. The reason for the conservativeness of the simulation model could be because of relatively large time-step of ten minutes between calculations used by the simulation model. A smaller time-step could result in better results.

Another reason for the slight deviation could be due to the fact that the stratification achieved in the actual system is slightly better than predicted by the simulation model. The stratification effect of the simulation model can be improved by increasing the number of increments in which the reservoir is divided during simulation. This would result in more layers with a different temperature in the reservoir and less mixing, resulting in improved stratification. Improved stratification would insure that more hot water is available at the top of the reservoir for a longer period during load shedding. At present the reservoir is divided into 21 increments in comparison with 11 increments used by Rousseau *et al.* (2001) during the experimental verification of the simulation model.

The measured and simulated temperatures near the top of the reservoir are shown in Figure B.2. The temperature at the top of the reservoir stays almost constant and equal to the outlet temperature of the system during most of the day. This can be expected since the ILH supplies water to the top of the reservoir at the same temperature as the outlet temperature. As in the case of the outlet temperature, the top temperature drops distinctively during the load shedding period (18:00 to 20:00) after which it recovers quickly as soon as the ILH is switched back on.

The simulated top temperature compares well with the measured top temperature. The same effect is seen here as in the case of the outlet temperature where the simulated temperature decreases a while earlier than the measured temperature.

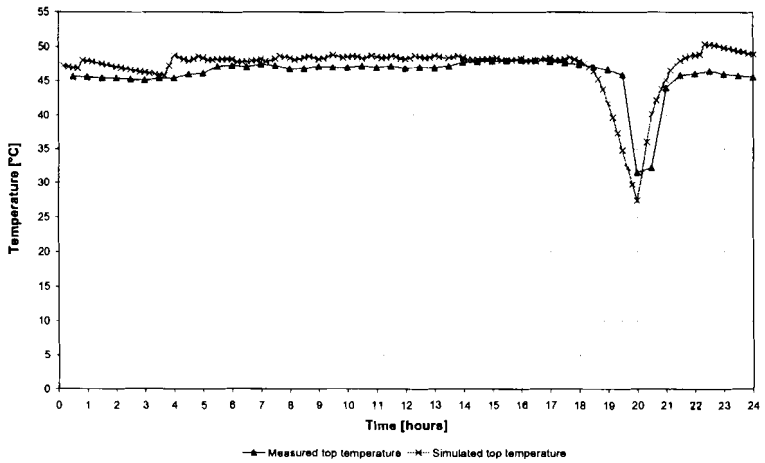

Figure B.2: Measured and simulated reservoir top temperature.

The middle temperature of the reservoir is also measured with the aid of the 'middle' PT-100. It can be seen from Figure B.3 that the middle temperature drops substantially during the peak demand period (18:00 to 20:00). The middle temperature reaches a minimum of about 16 °C compared to the top temperature reaching about 32 °C, indicating the stratification existing in the reservoir. The measured and simulated middle temperature compares well with each other.

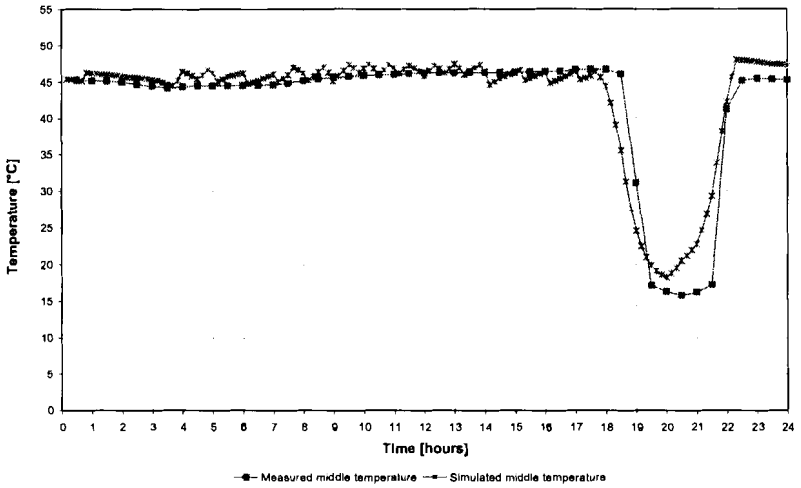

Figure B.3: Measured and simulated reservoir middle temperature.

The temperature at the bottom of the reservoir is measured by the 'bottom' PT-100. Figure B.4 shows the measured temperature versus the simulated temperature at the bottom of the reservoir. The measured bottom temperature compares well with the measured middle and top temperature. It can be seen from the figure that the bottom temperature stays relatively constant throughout the day with a substantial drop in temperature occurring from 18:00 when the load is shed up to 22:00 at which time the bottom temperature starts to recover.

The simulated bottom temperature compares well with the measured temperature. The oscillation effects seen in the simulated bottom temperature is due to the fact that the thermostat controlling the ILH during off-peak periods is situated near the bottom temperature sensor. Whenever the temperature at the bottom of the reservoir is lower than the thermostat set-point, the ILH is switched on fully. This results in hot water being pushed downwards from the top of the reservoir increasing the temperature at the bottom temperature sensor. As soon as the ILH is switched off by the thermostat, cold water is allowed to flow upwards through the reservoir, lowering the temperature at the bottom temperature sensor, hence the oscillating effect. The oscillation effect is not seen in the measured data since the measured temperature is not an instantaneous measurement, but an average value over a 30-minute interval. In the case of the simulation the temperature is predicted every ten minutes.

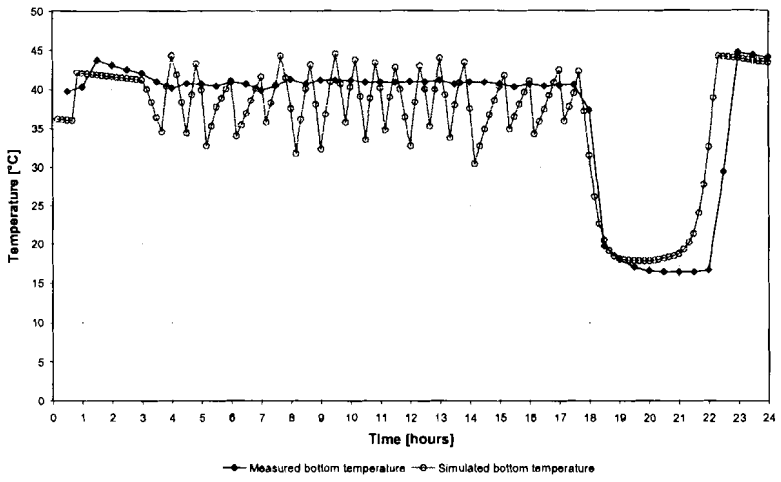

Figure B.4: Measured and simulated reservoir bottom temperature.

Figure B.5 compares the measured and simulated electricity demand profile for the selected day. It can be seen from the figure that the measured electricity demand compares well with the simulated electricity demand. The full load is shed during the peak demand periods for both the measured as well as the simulated electricity demand. The actual plant consumes 1 254 kWh during the entire day compared to 1 219 kWh predicted by the simulation model.

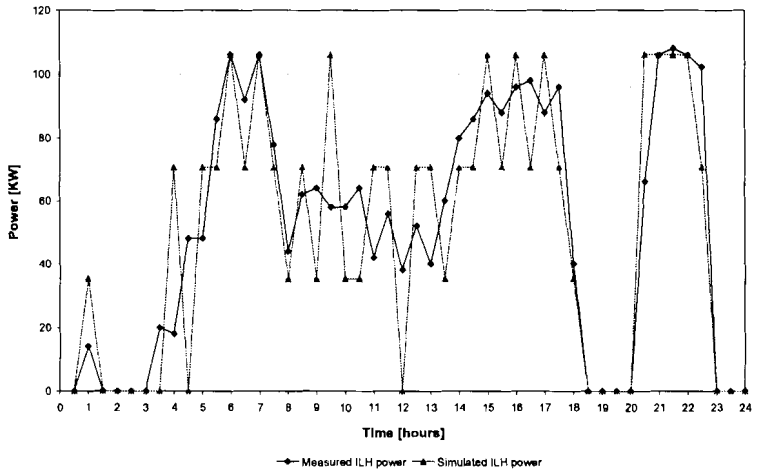

Figure B.5: Measured and simulated electricity demand profile for the selected day.

The performance number QD is found to be -0.035 indicating a 3.5% difference between the measured and simulated outlet temperature over the entire day. QE is found to be -0.028 indicating a 2.8% difference between the measured and simulated electricity consumption.

Plant no.7

The seventh plant consists of an ILH with a heating capacity of 146 kW and storage capacity of 8 200 litres in the form of two 4 100 litre reservoirs connected in series. Table B.2 provides a summary of the plant specifications and operation during the selected day.

Table B.2: Summary of plant specifications.

Heating capacity	146 kW
Heating equipment	In-line heater
Storage capacity	2 x 4 100 litre (Vertically mounted)
ILH-temperature set-point	46 °C
Typical occupancy	± 450
Hot-water consumption	32 025 litres
Date of selected day	2 September 2004

Figure B.6 shows the measured water consumption profile together with the measured and simulated hot-water supply temperatures. The consumption profile is quite flat except for a distinct peak occurring between 14:00 and 17:00. The fact that the peak in consumption is substantially higher than the average consumption during the selected day, indicates that the plant is not over utilised at all.

The measured outlet temperature of the plant almost remains constant between 43 °C and 48 °C throughout the entire day with the ILH-temperature set-point set to 46 °C. Even during the load shedding period (18:00 to 20:00) the outlet temperature remains above 42 °C with the full load being shed during this period. The water consumption during the load shedding period accumulates to 3 275 litres which is 40% of the storage capacity.

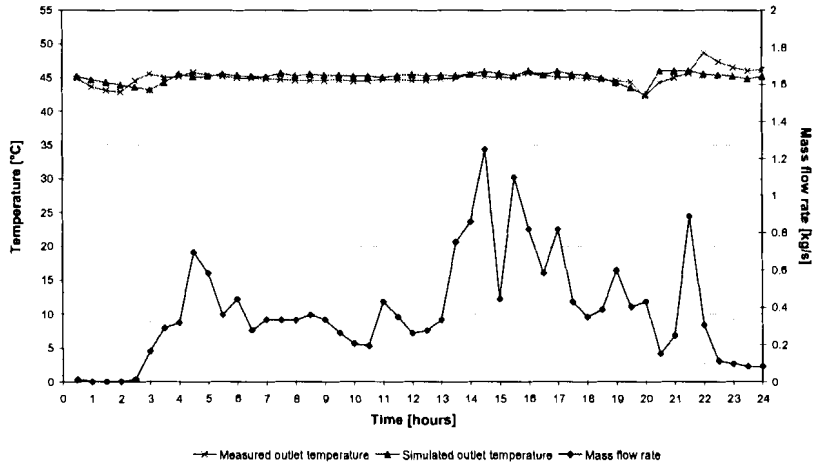

Figure B.6: Water consumption profile together with measured and simulated hot-water supply temperatures for the selected day.

The simulated outlet temperature compares very well with the measured outlet temperature. The minimum outlet temperature measured is found to be 42.2 °C with the minimum hot-water supply temperature predicted by the simulation model being 42.5 °C.

The measured and simulated temperatures near the outlet of the 'top' reservoir are shown in Figure B.7. The temperature at the top of the reservoir remains almost constant and equal to the outlet temperature of the ILH throughout the entire day. This can be expected since the ILH supplies water to the top of this reservoir at the temperature of the ILH set-point. The top temperature only decreases slightly at the end of the load shedding period (18:00 to 20:00) after which it quickly recovers as soon as the ILH is switched back on. The simulated top temperature compares very well with the measured top temperature.

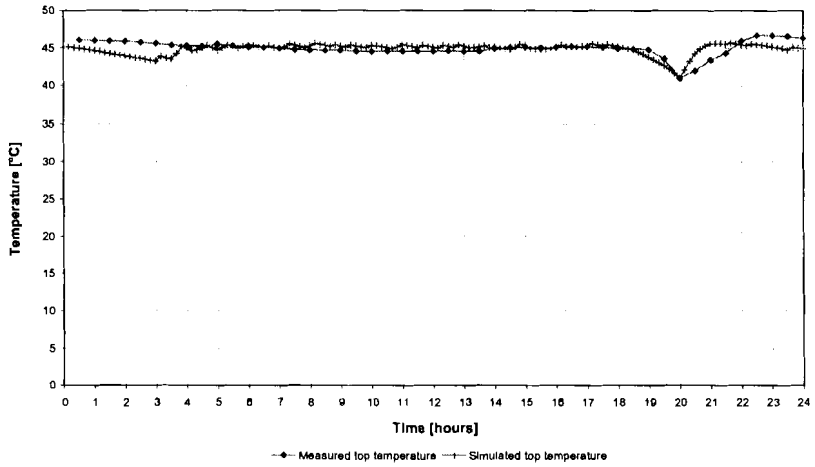

Figure B.7: Measured and simulated temperature at the top of the 'top' reservoir.

The middle temperature of the reservoir system is measured with the aid of the 'middle' PT-100 situated at the top of the 'bottom' reservoir. It can be seen from Figure A.8 that the middle temperature drops substantially during the peak demand period (18:00 to 20:00). The middle temperature reaches a minimum of 17 °C compared to the top temperature reaching a minimum of 41 °C, indicating the stratification existing in the reservoir system. The measured and simulated middle temperature once again compares well with each other.

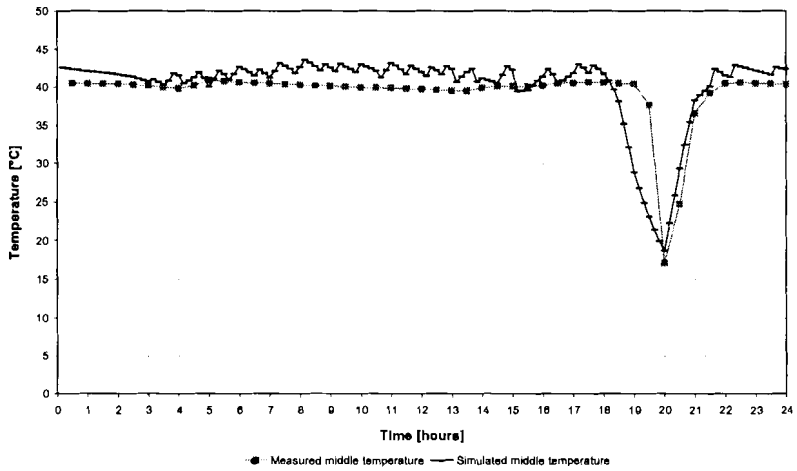

Figure B.8: Measured and simulated temperature at the top of the 'bottom' reservoir.

The temperature at the 'bottom' of the system is measured by the PT-100 installed near the bottom of the 'bottom' reservoir. Figure B.9 shows the measured temperature versus the simulated temperature near the bottom of this reservoir. The measured bottom temperature is slightly lower than the middle and top temperatures as expected due to the stratification effect. It can be seen from the figure that the bottom temperature stays relatively constant throughout the day with a substantial drop in temperature occurring from 18:00 when the load is shed up to 20:00. As soon as the ILH is switched back on the bottom temperature starts to recover rapidly. It can also be seen that the measured temperature drops to about 24 °C at 15:00, due to the peak in consumption measured between 14:00 and 15:30.

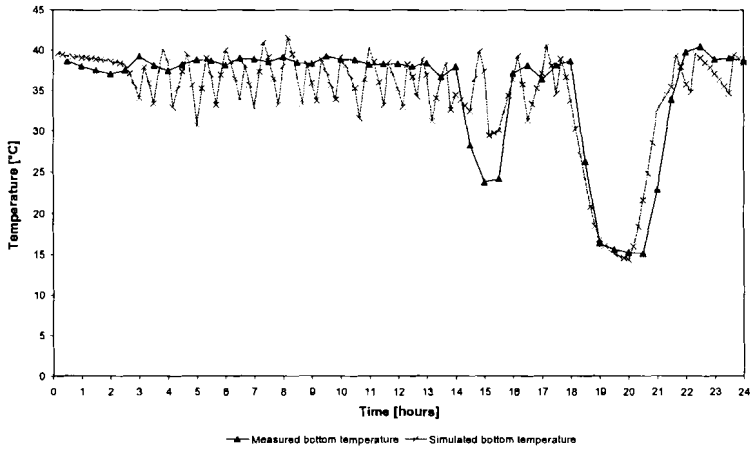

Figure B.9: Measured and simulated temperature near the bottom of the 'bottom' reservoir.

Figure B.10 compares the measured and simulated electricity demand profile for the selected day. It can be seen from the figure that the measured electricity demand compares well with the simulated electricity demand. The full load is shed during the peak demand period for

both the measured as well as the simulated electricity demand. The actual plant consumes 1 206 kWh during the entire day compared to 1 363 kWh predicted by the simulation model.

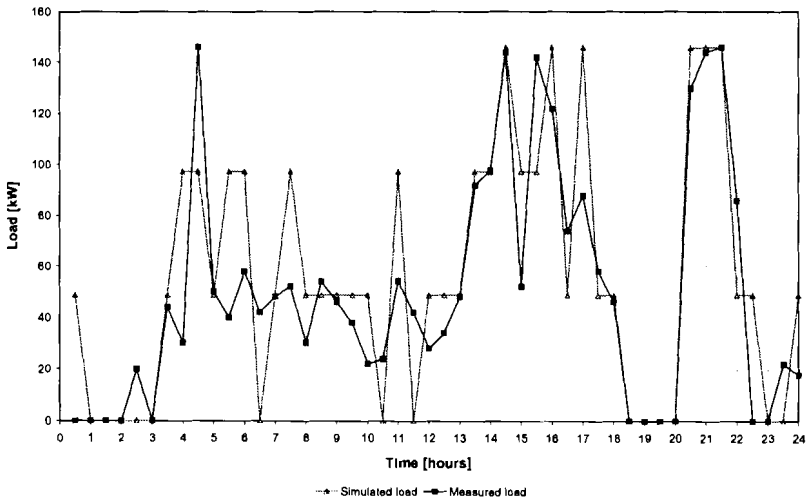

Figure B.10: Measured and simulated electricity demand profile for the selected day.

The performance number QD is calculated to be -0.114 indicating an 11.4% difference between the measured and simulated outlet temperature over the entire day. QE is found to be 0.130 indicating a 13.0% difference between the measured and simulated electricity consumption.

Plant no.8

The eighth plant under investigation consists of an ILH with a heating capacity of 102 kW and storage capacity of 10 000 litres in the form of two 5 000 litre reservoirs connected in series. Table B.3 provides a summary of the plant specifications and operation during the selected day of operation.

Table B.3: Summary of plant specifications.

Heating capacity	102 kW
Heating equipment	In-line heater
Storage capacity	2 x 5 000 litre (Vertically mounted)
ILH-temperature set-point	54 °C
Typical occupancy	200 - 350
Hot-water consumption	41 050 litres
Date of selected day	24 October 2004

The measured water consumption profile together with the measured and simulated hot-water supply temperatures is shown in Figure B.11. It can be seen from the figure that there

exists no distinct peaks in the hot-water consumption during the selected day. The water consumption remains almost constant even during the early hours of the morning and late at night, suggesting a highly utilised plant.

The measured outlet temperature remains relatively constant between 52 °C and 60°C during most of the day. The measured outlet temperature decreases slightly to a minimum of 49.7 °C just after the load shedding period. The water consumed during the load shedding period accumulates to 3 200 litres representing 32% of the total storage capacity. This indicates that just over 60% of the 'bottom' reservoir is filled with cold water at the end of the load shedding period with the entire 'top' reservoir expected to be filled with hot water, due to stratification.

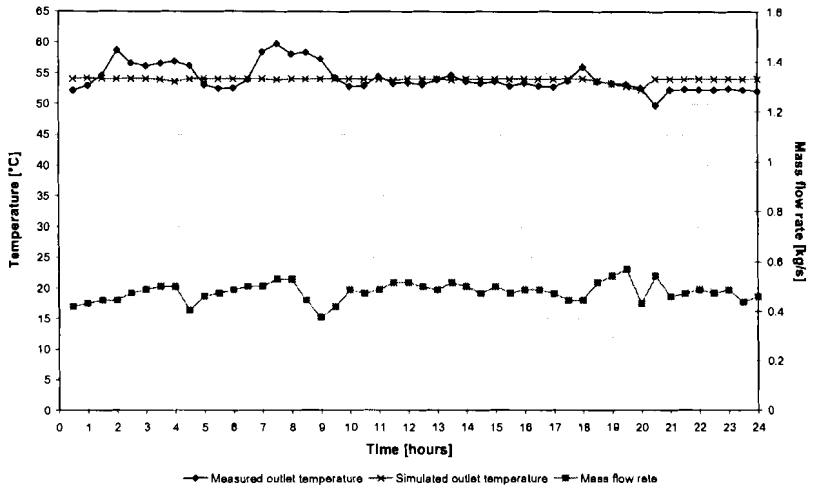

Figure B.11: Water consumption profile together with measured and simulated hot-water supply temperatures for the selected day.

The simulated outlet temperature compares well with the measured outlet temperature. The minimum outlet temperature measured during the load shedding period is found to be 52.6 °C compared to 52.6 °C predicted by the simulation model.

The measured and simulated temperatures near the top of the 'top' reservoir are shown in Figure B.12. The temperature at the top of the reservoir remains above 50 °C throughout the entire day. This can be expected since the ILH supplies water to the top of this reservoir at 54 °C. The simulated top temperature compares very well with the measured top temperature.

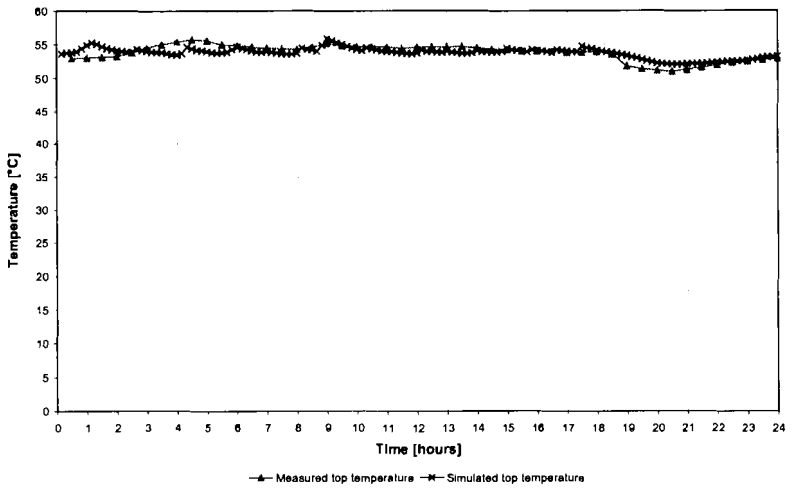

Figure B.12: Measured and simulated temperature at the top of the 'top' reservoir.

The middle temperature of the reservoir system is measured with the aid of the 'middle' PT-100 situated at the top of the 'bottom' reservoir. Figure B.13 shows the measured middle temperature together with the simulated middle temperature. It can be seen from the figure that the middle temperature starts to decrease as just after the load is shed with cold water entering the system.

The temperature reached by the middle temperature at the end of the load shedding period is measured as 20.8 °C compared to the top temperature reaching a temperature of 51.1 °C at exactly the same time. This indicates the high degree of stratification present in the system. The measured and simulated middle temperatures once again compare well with each other.

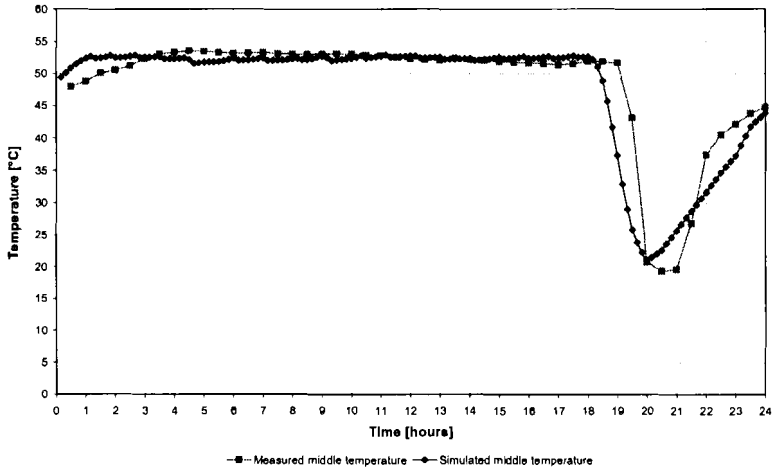

Figure B.13: Measured and simulated temperature at the top of the 'bottom' reservoir.

The temperature at the 'bottom' of the system is measured by the PT-100 installed near the bottom of the 'bottom' reservoir. Figure B.14 shows the measured temperature versus the simulated temperature near the bottom of this reservoir. The bottom temperature varies quite a lot during the day with a substantial decrease in the bottom temperature experienced during the load shedding period.

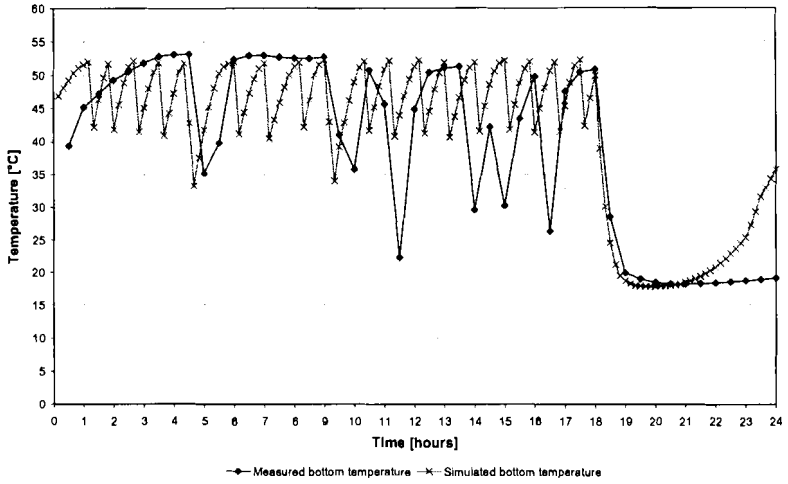

Figure B.14: Measured and simulated temperature near the bottom of the 'bottom' reservoir.

Figure B.15 compares the measured and simulated electricity demand profile for the selected day. It can be seen from the figure that the measured electricity demand compares well with the simulated electricity demand. The measured electricity consumption accumulates to 1 892 kWh during the entire day compared to 1 904 kWh predicted by the simulation model.

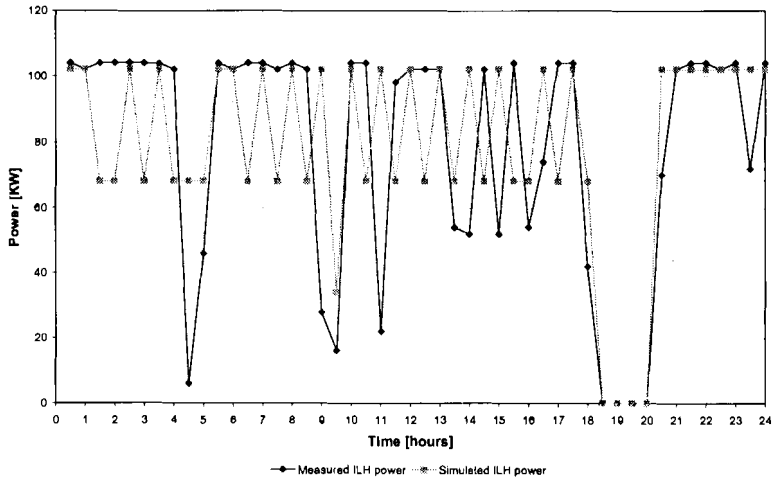

Figure B.15: Measured and simulated electricity demand profile for the selected day.

The difference between the measured and simulated outlet temperatures over the entire day is quantified, using the performance number QD. QD is found to be 0.008 indicating a 0.8% difference between the measured and simulated outlet temperatures. QE is employed to quantify the difference found between the measured and simulated electricity consumption. QE is found to be 0.006 indicating a 0.6% difference between the measured and simulated electricity consumption.

Plant no.9

The ninth plant consists of an ILH with a heating capacity of 80 kW and storage capacity of 8 000 litres in the form of two 4 000 litre reservoirs connected in series. Table B.4 provides a summary of the plant specifications and operation during the selected day of operation.

Table B.4: Summary of plant specifications.

Heating capacity	80 kW
Heating equipment	In-line heater
Storage capacity	2 x 4 000 litre (Vertically mounted)
ILH-temperature set-point	52 °C
Typical occupancy	± 450
Hot-water consumption	21 875 litres
Date of selected day	10 August 2004

The measured water consumption profile together with the measured and simulated hot-water supply temperatures is shown in Figure B.16.

The measured outlet temperature remains above 48 °C for most of the day except for a short while after the load shedding period when the temperature drops to 44 °C. The water consumption during the load shedding period accumulates to 2 323 litres representing only 23% of the total storage capacity. This indicates that the plant is not over utilised at all.

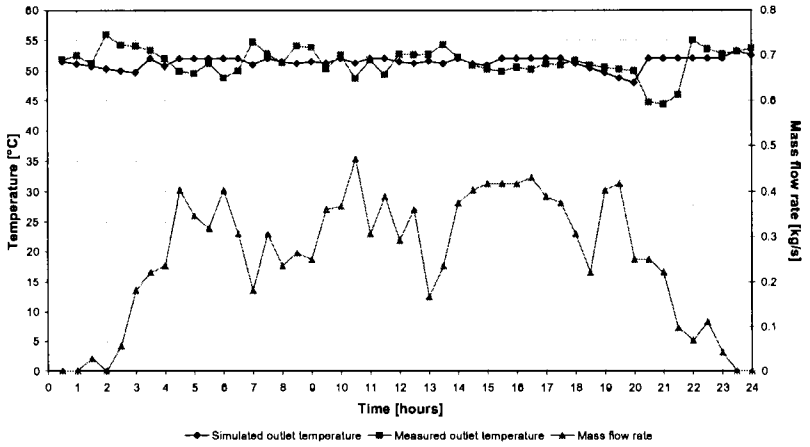

Figure B.16: Water consumption profile together with measured and simulated hot-water supply temperatures for the selected day.

Figure B.16 also indicates that the simulated outlet temperature compares well with the measured outlet temperature. A minimum outlet temperature of 44.3 °C is measured during the entire day with a minimum predicted temperature of 47.9 °C.

The measured and simulated temperatures near the top of the 'top' reservoir are shown in Figure B.17. The temperature near the top of this reservoir remains around 50 °C throughout the day, even during the load shedding period the temperature does not drop significantly.

The simulated top temperature compares well with the measured top temperature throughout the entire day.

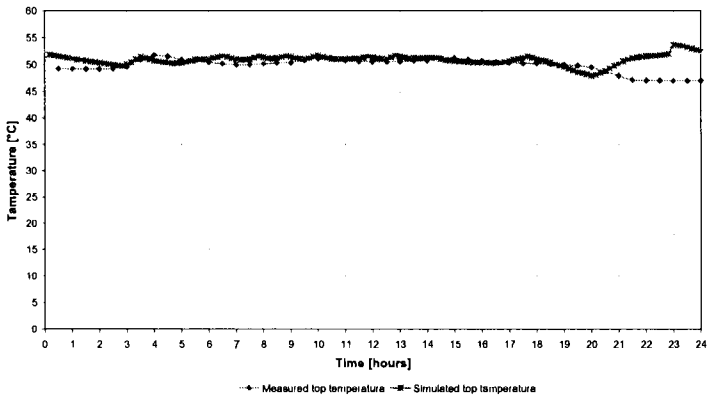

Figure B.17: Measured and simulated temperature at the top of the 'top' reservoir.

The middle temperature of the reservoir system is measured with the aid of the 'middle' PT-100 situated near the top of the 'bottom' reservoir. Figure B.18 shows the measured middle

temperature together with the simulated middle temperature. It can be seen from the figure that middle temperature does not drop substantially during the peak demand period (18:00 to 20:00). A total of 2 323 litres of cold water enters the 'bottom' reservoir during the load shedding period. This represents about 46% of the 'bottom' reservoir capacity. It is therefore expected that the middle temperature will not decrease as much since less than half of the reservoir is filled with cold water. This can be seen from the figure as the middle temperature only drops to 34 °C for a short period of time. The measured and simulated middle temperatures once again compare well with each other.

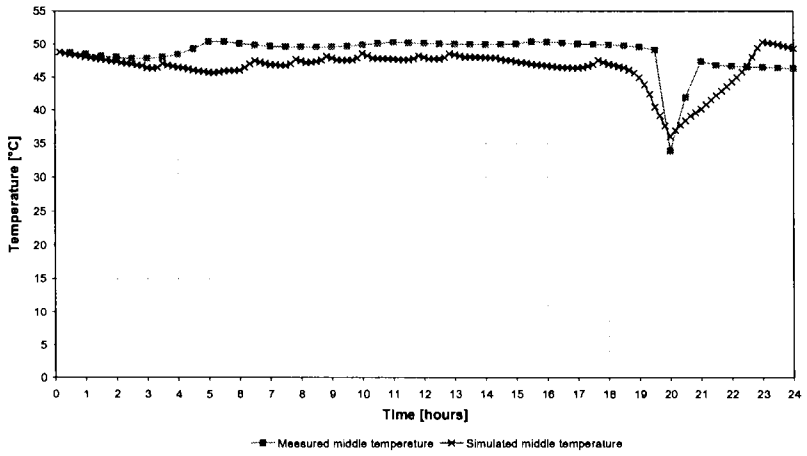

Figure B.18: Measured and simulated temperature at the top of the 'bottom' reservoir.

The temperature at the 'bottom' of the system is measured near the bottom of the 'bottom' reservoir. Figure B.19 shows the measured temperature versus the simulated temperature near the bottom of this reservoir. The bottom temperature stays relatively constant up to the load shedding period. The bottom temperature decreases rapidly during the load shedding period, after which it recovers rapidly as soon as the ILH is switched back on. The minimum temperature reached near the bottom of the 'bottom' reservoir is measured to be 12 °C at the end of the load shedding period. The corresponding temperature near the top of the same reservoir is measured to be 34 °C. This indicates the high degree of stratification achieved by the system during the load shedding period.

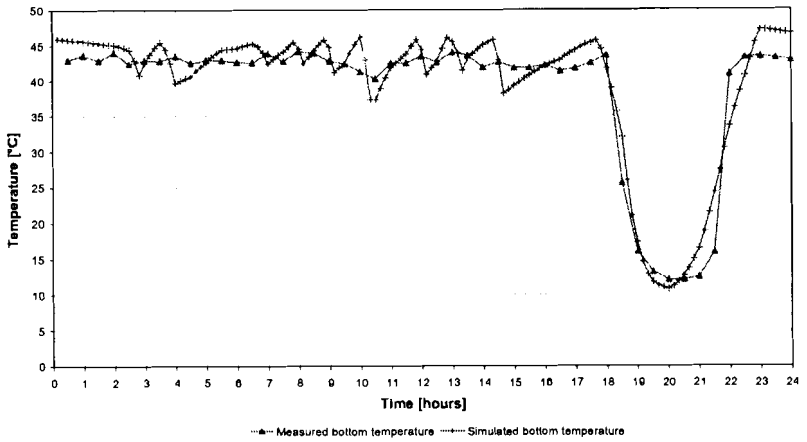

Figure B.19: Measured and simulated temperature near the bottom of the 'bottom' reservoir.

Figure B.20 compares the measured and simulated electricity demand profile for the selected day. It can be seen from the figure that the measured electricity demand compares very well with the simulated electricity demand. The full load is once again shed during the peak demand period for both the measured as well as the simulated electricity demand. The measured electricity consumption accumulated to 1 115 kWh during the entire day compared to 1 173 kWh predicted by the simulation model.

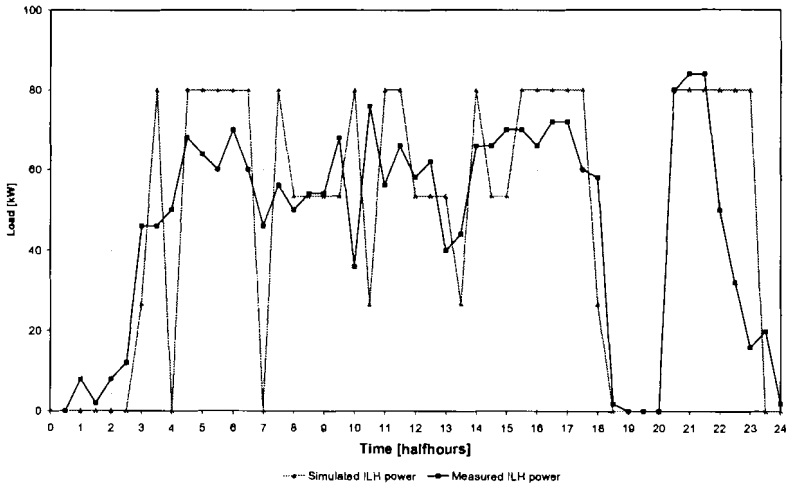

Figure B.20: Measured and simulated electricity demand profile for the selected day.

The performance number QD is found to be -0.144 indicating a 14.4% difference between the measured and simulated outlet temperatures over the entire day. QE is found to be 0.052 indicating a 5.2% difference between the measured and simulated electricity consumption.

Plant no.10

The tenth plant consists of an ILH with a heating capacity of 110 kW and storage capacity of 10 000 litres in the form of two 5 000 litre reservoirs connected in series. Table B.5 provides a summary of the plant specifications and operation during the selected day of operation.

Table B.5: Summary of plant specifications.

Heating capacity	110 kW
Heating equipment	In-line heater
Storage capacity	2 x 5 000 litre (Vertically mounted)
ILH-temperature set-point	47 °C
Typical occupancy	200 - 350
Hot-water consumption	35 825 litres
Date of selected day	2 November 2004

The measured water consumption profile together with the measured and simulated hot-water supply temperatures is shown in Figure B.21. A distinct peak occurs in the water consumption profile between 14:30 and 17:00.

It can be seen from the figure that the measured outlet temperature remains between 45 °C and 50 °C during most of the day, even though the entire load is shed. The water consumption during the load shedding period accumulates to 3 475 litres representing 35% of the total storage capacity. This indicates that 70% of the 'bottom' reservoir is filled with cold water at the end of the load shedding period. It is therefore expected that the 'top' reservoir should be filled with sufficient hot water due to the stratification effect achieved by the system.

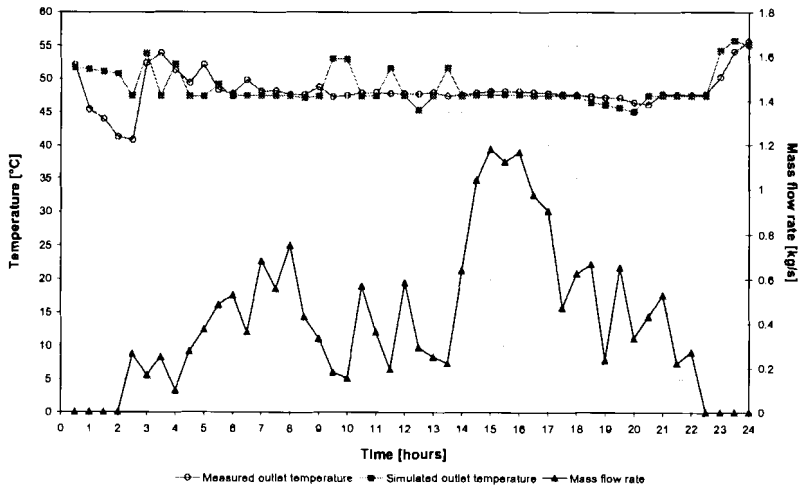

Figure B.21: Water consumption profile together with measured and simulated hot-water supply temperatures for the selected day.

Figure B.21 also indicates that the simulated outlet temperature compares well with the measured outlet temperature. A minimum outlet temperature of 46.4 °C is measured during the load shedding period compared to a minimum predicted temperature of 45.0 °C.

The measured and simulated temperatures near the top of the 'top' reservoir are shown in Figure B.22. The temperature near the top of this reservoir remains around 47 °C throughout the entire day. This can be expected since water is supplied to the top of this reservoir at 47 °C whenever the ILH is switched on.

The behaviour of the simulated top temperature compares well with the behaviour of the measured top temperature.

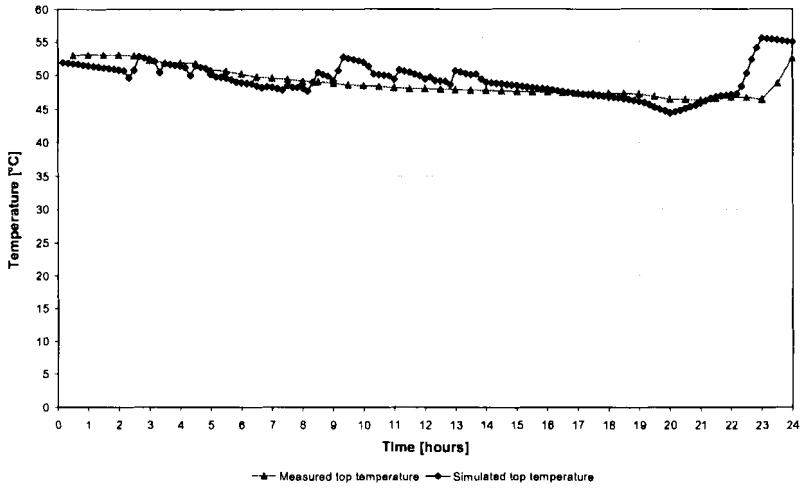

Figure B.22: Measured and simulated temperature at the top of the 'top' reservoir.

The middle temperature of the reservoir system is measured with the aid of the 'middle' PT-100 situated at the top of the 'bottom' reservoir. Figure B.23 shows the measured middle temperature together with the simulated middle temperature. It can be seen from the figure that middle temperature drops substantially during the peak demand period (18:00 to 20:00).

The middle temperature reaches a measured value of 17.8 °C at the end of the load shedding period compared to the top temperature reaching a value of 46.4 °C at the same time. This emphasises the high degree of stratification achieved by the ILH water heating system. The measured and simulated middle temperatures once again compare well with each other.

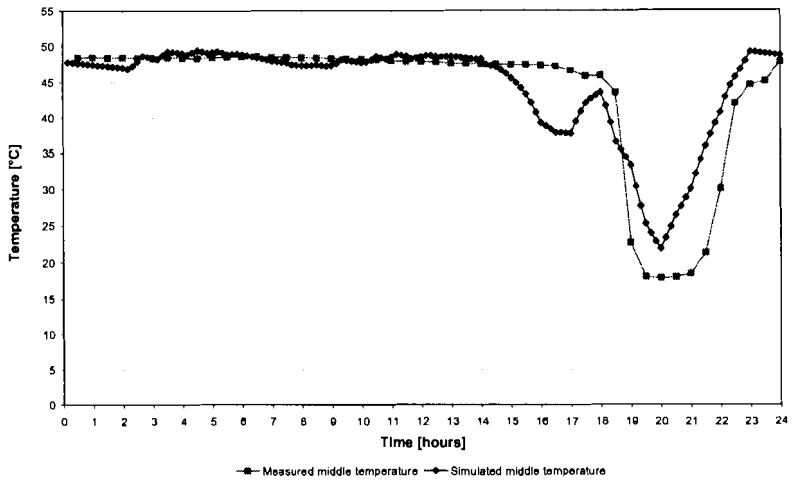

Figure B.23: Measured and simulated temperature at the top of the 'bottom' reservoir.

Figure B.24 compares the measured and simulated electricity demand profile for the selected day. It can be seen from the figure that the measured electricity demand compares very well with the simulated electricity demand. The full load is once again shed during the peak demand period for both the measured as well as the simulated electricity demand. The measured electricity consumption added up to 1 345 kWh during the entire day compared to 1 485 kWh predicted by the simulation model.

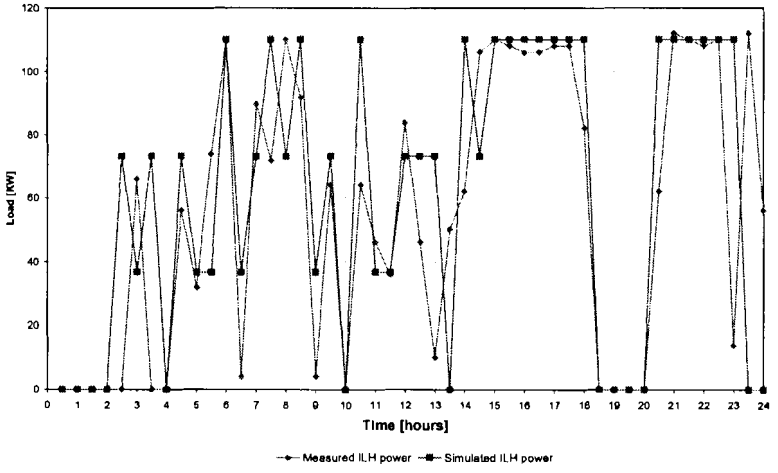

Figure B.24: Measured and simulated electricity demand profile for the selected day.

The performance number QD is found to be -0.05 indicating a 5.0% difference between the measured and simulated outlet temperatures over the entire day. QE is found to be 0.104 indicating a 10.4% difference between the measured and simulated electricity consumption.

Appendix C

STANDING HEAT LOSS SAMPLE CALCULATIONS

This section presents sample calculations for the calculation of the standing heat losses presented in Chapter 4.

Table C.1 provides an example of the results obtained for the calculation of the energy input to the system (E_{in}) via the measured electricity consumption as well as the energy withdrawn (E_{out}) from the system. The table only shows the results obtained for the first six and last five half-hours of one day. (Note that the data shown in the table is obtained from measured plant variables on a real-world water heating plant.)

Table C1: Example of results obtained for energy input and output.

Day	Time [hours]	Measured kWh	T_in [°C]	T_out [°C]	m_w [kg]	E_in [MJ]	E_out [MJ]
1	0.5	40	15.5	66.0	0	144	0.0
1	1	39	19.0	73.5	75	140.4	17.1
1	1.5	10	11.8	56.7	500	36	93.7
1	2	0	11.8	49.8	275	0	43.7
1	2.5	0	10.7	49.0	0	0	0.0
1	3	0	9.8	48.5	0	0	0.0
1	22	34	13.0	44.5	575	122.4	75.7
1	22.5	41	13.0	48.2	800	147.6	117.7
1	23	40	13.0	49.0	900	144	135.5
1	23.5	40	12.5	50.8	50	144	8.0
1	24	55	13.7	57.7	0	198	0.0
					Daily total [MJ]	6264.0	5636.5

The energy input is calculated according to equation 14 described in Chapter 4. The following sample calculations are based on the data shown in Table C.1 for the first half-hour:

$$E_{in} = 3.6E_{elec}$$

$$= (3.6)(40) = 144 \text{ MJ}$$

The energy output for the first half-hour is calculated via equation 15 described in Chapter 4 with c_p equal to 4.182 kJ/kg.K.

$$E_{out} = \frac{m_w c_p (T_{out} - T_{in})}{1000}$$

$$= \frac{(0)(4.182)(66.0 - 15.5)}{1000}$$

$$= 0 \text{ MJ}$$

The percentage of standing heat loss is calculated by adding up the energy input and energy output respectively for the entire day. The following sample calculation is based on the total energy output and input as shown in Table C.1:

$$\%Losses = \frac{\sum_{day} E_{in} - \sum_{day} E_{out}}{\sum_{day} E_{in}} (100)$$

$$= \frac{6264.0 - 5636.5}{6264.0} (100) = 10.0\%$$

This calculation can also be performed for the simulated plant variables in order to obtain the simulated heat losses.

Appendix D

PERFORMANCE NUMBER SAMPLE CALCULATIONS

This section presents sample calculations for the calculation of the various performance numbers employed to evaluate the accuracy of the water heating simulation model as discussed in Chapter 4.

The first of the performance numbers, QD, is calculated by employing equation 15 defined in Chapter 4. To be able to calculate $Q_{del,sim}$ and $Q_{del,exp}$ the mass flow rate together with the temperature of the water supplied to the occupants is required. Furthermore, the inlet temperature of the cold water which is supplied to the system as well as the length of the time-step over which the variables are measured/simulated is required. According to equation 15, QD can be calculated as:

$$QD = \frac{Q_{del,sim} - Q_{del,exp}}{Q_{del,exp}}$$

with $Q_{del,sim/exp}$ defined as

$$Q_{del} = \int_{day} \dot{m}_{del} c_p (t_s - t_c) dt.$$

Considering the values obtained via the empirical investigation shown in Table D.1, Q_{del} is determined by calculating the term $\dot{m}_{del} c_p (t_s - t_c) dt$ for each of the half-hours over the entire day. The value of c_p is taken as 4.182 kJ/kg.K and dt is 1 800 seconds. Theses results are added up in order to determine Q_{del}, which is used to calculate QD.

Table D1: Example of results.

Day	Time [hours]	t_c [°C]	t_s [°C]	m_del [kg/s]	$\dot{m}_{del} c_p (t_s - t_c) dt$
1	0.5	15.5	66.0	0.0000	0
1	1	19.0	73.5	0.0417	17093.925
1	1.5	11.8	56.7	0.2778	93746.5
1	2	11.8	49.8	0.1528	43701.9
1	23	13.0	49.0	0.5000	135496.8
1	23.5	12.5	50.8	0.0278	8015.5
1	24	13.7	57.7	0.0000	0
				Q_del,exp [kJ]	5636517.0

Considering the value obtained for $Q_{del,exp}$ in Table D.1 and assuming an arbitrary value of 5 697 400 kJ for $Q_{del,sim}$, QD can be calculated as:

$$QD = \frac{5697400 - 5636517}{5636517}$$

$$= 0.011$$

The second performance number QE, employed by Chapter 4, is calculated with the aid of equation 19:

$$QE = \frac{E_{in,sim} - E_{out,\exp}}{E_{in,\exp}}$$

with

$$E_{in} = \int_{day} P dt .$$

P is the power drawn from the electricity supply expressed as kW with dt the length of each time-step. In this case dt is taken as 1 800 seconds (30-minutes).

Table D2: Example of results.

Day	Time [hours]	Measured kW (P)
1	0.5	80
1	1	78
1	1.5	20
1	2	0
1	23	80
1	23.5	80
1	24	110

The following sample calculation calculates Pdt for the first half-hour of the data shown in Table D.2:

$$Pdt = (80)(1800)$$
$$= 144000 \text{ kJ}$$

In calculating Pdt for each of the time-intervals for the entire day and summating the results, E_{in} can be determined. Assuming that $E_{in,exp}$ is found to be 6 264 000 kJ with $E_{in,sim}$ 6 040 500 kJ, QE can be determined:

$$QE = \frac{6040500 - 6264000}{6264000}$$
$$= -0.036$$

Appendix E

BASELINE SAMPLE CALCULATIONS

This section provides sample calculations concerning the normalised baseline obtained for the conventional in-tank water heaters mentioned in Chapter 5. The sample calculations include examples for adjusting the baseline to reflect a certain amount of energy consumption as well as calculating the operating cost.

Table E.1 shows the normalised baseline for the first hour of the day, constructed for the conventional in-tank water heaters mentioned in Chapter 5. The table also contains results obtained by adjusting the baseline for a certain amount of energy use for a sample day, together with calculations for the cost according to the price of electricity for the specific time.

Table E1: Normalised baseline for conventional in-tank water heaters.

Time (5 min intervals)	Normalised baseline [kWh/kWh]	Adjusted baseline [kWh]	Price [c/kWh]	Cost [R]	Demand [kW]
5	0.001689	22.45	8.15	R 1.83	269.4
10	0.001688	22.44	8.15	R 1.83	269.2
15	0.001635	21.72	8.15	R 1.77	260.7
20	0.001612	21.42	8.15	R 1.75	257.0
25	0.001616	21.48	8.15	R 1.75	257.8
30	0.001526	20.27	8.15	R 1.65	243.3
35	0.001459	19.39	8.15	R 1.58	232.6
40	0.001445	19.21	8.15	R 1.57	230.5
45	0.001394	18.52	8.15	R 1.51	222.2
50	0.001358	18.05	8.15	R 1.47	216.6
55	0.001316	17.49	8.15	R 1.43	209.9
60	0.001223	16.25	8.15	R 1.32	195.0

In order to demonstrate the above-mentioned sample calculations, the data in Table E.1 is used, together with the assumption that 13 289 kWh of electricity is consumed by a sample plant. This makes it possible to determine the adjusted baseline for the sample plant as well as the cost for the first hour of the day.

The following sample calculation is based on the data obtained for the first five minutes shown in the table:

$$Baseline_{adj} = (Baseline_{norm})(E_{tot})$$
$$= (0.001689)(13289)$$
$$= 22.45 \text{ kWh}$$

By determining the sum of the calculated $Baseline_{adj}$-values over the first hour, the electricity cost can be calculated by using the cost of electricity shown in Table E.1.

Assuming that the $Baseline_{adj}$-values accumulate to 238.68 kWh over the first hour, the electricity cost is calculated as:

$$Cost_{hour} = (238.68)(8.15)/100$$
$$= \text{R } 19.45$$